FOREWORD

This final report was prepared for the United States Air Force by the Cornell Aeronautical Laboratory, Inc., Buffalo, New York, in fulfillment of Contracts AF33(616)-5823 and AF33(616)-7753.

The work reported herein was performed by the Flight Research Department under the sponsorship of the Control Criteria Branch, Air Force Flight Dynamics Laboratory, Research and Technology Division, Air Force Systems Command, Wright-Patterson Air Force Base, Dayton, Ohio, under Project No. 8219, Task No. 821905. The project was administered by Mr. R.J. Wasicko of the Control Criteria Branch of the Air Force Flight Dynamics Laboratory.

Significant contributions to the technical performance of this project have been made by the following members of the Flight Research Department: J.L. Beilman, R.P. Harper, Jr., N.L. Infanti, E.A. Kidd, P.A. Reynolds, J.C. Seal, W.H. Shed, and E.H. Smith.

This report is also being published as Cornell Aeronautical Laboratory Report No. TE-1516-F-1.

ABSTRACT

The results of a research investigation of longitudinal and lateral-directional flying qualities for the re-entry mission are reported. The research program utilized primarily a high-fidelity fixed-base ground simulator with evaluations made by three pilots. One of the three pilots also made in-flight evaluations of longitudinal flying qualities in the same vehicle, a three-axis variable stability airplane flown with a two-axis side controller and conventional rudder pedals.

The program results are reported and discussed. Control sensitivity evaluations were compared to center stick results of earlier work. The longitudinal flying qualities as evaluated both on the ground simulator and in flight are compared and related to earlier investigations. Pilot rating variability, both interpilot and intrapilot, are quantized and discussed for the ground and flight experiments. Performance measures are reported.

This report has been reviewed and is approved.

C. B. Westbrook

C. B. WESTBROOK

Chief, Control Criteria Branch
Air Force Flight Dynamics Laboratory

TABLE OF CONTENTS

Section			Page
1	INTRODUCTION		1
2	DESCRIPTION OF EXPERIMENT		3
	2.1	Equipment	3
	2.2	Evaluation Technique	5
	2.3	Test Procedure	7
3	EVALUATION OF LONGITUDINAL FLYING QUALITIES		10
	3.1	Gain of Pitch and Normal Acceleration Response to Elevator Stick Force, Fixed-Base Simulator	10
	3.2	Short Period Dynamics	12
	3.3	Steady State Normal Acceleration per Angle of Attack	15
4	EVALUATION OF LATERAL-DIRECTIONAL FLYING QUALITIES		20
	4.1	Gain of Roll Response to Aileron Stick Force Input	20
	4.2	Gain of Sideslip Response to Rudder Pedal Force Input	21
	4.3	Dutch Roll Dynamics	24
5	TRACKING PERFORMANCE MEASURES		28
6	PILOT RATING VARIABILITY		30
	6.1	Intrapilot Variability – Fixed-Base Simulation	30
	6.2	Intrapilot Variability – In-Flight Simulation	32
	6.3	Interpilot Variability – Longitudinal Evaluations	32
	6.4	Interpilot Variability – Lateral-Directional Evaluations	35
7	CONCLUSIONS		37
	References		40
APPENDIX			
A	STATISTICAL TESTS AND MEASURES		89
B	EQUATIONS OF MOTION AND PERTINENT TRANSFER FUNCTIONS		93

LIST OF ILLUSTRATIONS

Figure		Page
1	T-33 Variable Stability Airplane	43
2	Evaluation Pilot's Instrument Panel	44
3	Variable Stability T-33 Two-Axis Side Stick Controller	45
4	Block Diagram Representation of the Tracking Maneuver Including the Manner of Inserting the Noise Disturbance	46
5	Random Noise Filter Frequency Response	47
6	Pilot Rating Versus Gain of Pitch Response	48
7a	Pilot Ratings of Longitudinal Short Period Dynamics in Fixed-Base Simulator (Before Tracking)	49
7b	Pilot Ratings of Longitudinal Short Period Dynamics in Fixed-Base Simulator (After Tracking)	50
8	Fixed-Base Pilot Ratings Versus $2\zeta_{sp}\omega_{sp}$ and ω_{sp}^2	51
9	In-Flight and Simulator Ratings for Longitudinal Evaluations	52
10	Rating Boundary Comparisons	53
11	Summary of Rating Boundary Comparisons	54
12	Fixed-Base Simulator Pilot Rating Versus Lift Curve Slope Parameter	55
13	Effects of $1/\tau_\theta$ on Pitch Rate Frequency Response for Constant Short Period Dynamics	56
14	Effect of $1/\tau_\theta$ on Pitch Rate Response, $\dot{\theta}(t)$, to Elevator Stick Force Step Input, ΔF_{ES}	57
15	In-Flight Pilot Ratings Versus Lift Curve Slope Parameter	58
16	Pilot Rating Versus Gain of Roll Response	59
17	Pilot Rating Versus Gain of β/F_{RP}	60
18	Sideslip Response Gain Versus Dutch Roll Frequency	61
19	Dutch Roll Damping Versus Pilot Ratings (Before Tracking)	62
20	Standard Deviation Versus Pilot Rating (Longitudinal Evaluations)	63
21	Integral of Absolute Error Versus Pilot Rating (Longitudinal Evaluations)	64
22	Standard Deviation Versus Pilot Rating (Lateral-Directional Evaluations)	65
23	Integral of Absolute Error Versus Pilot Rating (Lateral-Directional Evaluations)	66

LIST OF ILLUSTRATIONS
(continued)

Figure		Page
24	Distributions of Control Inputs – Longitudinal Evaluations	67
25	Distributions of Control Inputs – Lateral-Directional Evaluations	71
26	Intrapilot Variability – Fixed Base Simulation	73
27	Intrapilot Variability – In-Flight Simulation	74
28	Interpilot Rating Comparisons – Longitudinal Evaluations	75
29	(After-Before) Tracking Differences as Function of Before Tracking Rating – Longitudinal Evaluations	76
30	Interpilot Rating Comparisons – Lateral-Directional Evaluations	77

LIST OF TABLES

Table		Page
1	Control and Display Element Characteristics	78
2	Pilot Comment Card	79
3	Pilot's Rating Scale	80
4	Pilot Experience	81
5a	Fixed-Base Evaluation – Longitudinal Characteristics	82
5b	Fixed-Base Evaluation – Lateral-Directional Characteristics	84
6	In-Flight Evaluation – Longitudinal Characteristics	86
7a	Performance Measures – Longitudinal Evaluations	87
7b	Performance Measures – Lateral-Directional Evaluations	88

LIST OF SYMBOLS

b	wing span, feet, or sample regression coefficient
c	mean aerodynamic chord of the wing, feet
C_{l_r}	rolling moment coefficient per non-dimensional yawing velocity, $= \partial C_l / \partial \left(\frac{rb}{2V}\right)$
C_{L_α}	lift force coefficient per angle of attack, positive upwards, $= \partial C_L / \partial \alpha$
$C_{m_{\delta_{ES}}}$	pitching moment coefficient per elevator control stick input
C_{m_q}	pitching moment coefficient per non-dimensional pitching velocity, $= \partial C_m / \partial \left(\frac{qc}{2V}\right)$
C_{n_r}	yawing moment coefficient per non-dimensional yawing velocity, $= \partial C_n / \partial \left(\frac{rb}{2V}\right)$
C_{y_β}	side force coefficient per angle of sideslip, $= \partial C_y / \partial \beta$

Note: other $C_{(i)}$ coefficients are similarly defined

F	force, pounds
I_x	moment of inertia about fuselage reference roll axis, slug-feet^2
I_y	moment of inertia about fuselage reference pitch axis, slug-feet^2
I_z	moment of inertia about fuselage reference yaw axis, slug-feet^2
I_{xz}	product of inertia about fuselage reference axis, slug-feet^2
$K_{\beta_{F_{RP}}}$	steady-state sideslip per rudder pedal force, deg/lb
$K_{\dot{\theta}_{F_{ES}}}$	steady-state pitch rate per elevator stick force, deg/sec-lb
$K'_{\dot{\theta}_{F_{ES}}}$	$= \omega_{sp}^2 K_{\dot{\theta}_{F_{ES}}}$, deg/sec^3-lb
$K_{\dot{\phi}_{F_{AS}}}$	steady-state roll rate per aileron stick force, deg/sec-lb
$K_{\dot{\theta}_{\delta_{ES}}}$	steady-state pitch rate per elevator stick deflection
$K_{n_{z_{F_{ES}}}}$	steady-state incremental normal acceleration per elevator stick force, g's/lb

$$L'_i = \frac{L_i + \frac{I_{xz}}{I_x} N_i}{1 - \frac{I_{xz}^2}{I_x I_z}}$$

$L_p = (q_o S b) \frac{b}{2V} \frac{C_{l_p}}{I_x}$, 1/sec

$L_r = (q_o S b) \frac{b}{2V} \frac{C_{l_r}}{I_x}$, 1/sec

$L_\alpha = (q_o S) \frac{C_{L_\alpha}}{mV}$, 1/sec

$L_\beta = (q_o S b) \frac{C_{l_\beta}}{I_x}$, 1/sec^2

$L_{\delta_{AS}} = (q_o S b) \frac{C_{l_{\delta_{AS}}}}{I_x}$, 1/sec^2

$L_{\delta_{ES}} = (q_o S) \frac{C_{L_{\delta_{ES}}}}{mV}$, 1/sec

$L_{\delta_{RP}} = (q_o S b) \frac{C_{l_{\delta_{RP}}}}{I_x}$, 1/in$_r$ sec^2

m mass, slugs

$M_q = (q_o S \bar{c}) \frac{\bar{c}}{2V} \frac{C_{m_q}}{I_y}$, 1/sec

$M_\alpha = (q_o S \bar{c}) \frac{C_{m_\alpha}}{I_y}$, 1/sec^2

$$M_{\dot{\alpha}} = (q_o S c) \frac{c}{2V} \frac{C_{m_{\dot{\alpha}}}}{I_Y} \quad , \ 1/\text{sec}$$

$$M_{\delta_{ES}} = (q_o S c) \frac{C_{m_{\delta_{ES}}}}{I_Y} \quad , \ 1/\text{sec}^2$$

$$N'_i = \frac{N_i + \frac{I_{xz}}{I_z} L_i}{1 - \frac{I_{xz}^2}{I_x I_z}}$$

$$N_p = (q_o S b) \frac{b}{2V} \frac{C_{n_p}}{I_z} \quad , \ 1/\text{sec}$$

$$N_r = (q_o S b) \frac{b}{2V} \frac{C_{n_r}}{I_z} \quad , \ 1/\text{sec}$$

$$N_\beta = (q_o S b) \frac{C_{n_\beta}}{I_z} \quad , \ 1/\text{sec}^2$$

$$N_{\delta_{AS}} = (q_o S b) \frac{C_{n_{\delta_{AS}}}}{I_z} \quad , \ 1/\text{sec}^2$$

$$N_{\delta_{RP}} = (q_o S b) \frac{C_{n_{\delta_{RP}}}}{I_z} \quad , \ 1/\text{in.-sec}^2$$

n_z normal acceleration, g's

Δn_z	incremental normal acceleration from 1 g level flight, g's
$\left\lvert \frac{n_z}{\alpha} \right\rvert_{ss}$	steady-state normal acceleration per angle of attack, g's/rad
p	rolling velocity, rad/sec
q	pitching velocity, rad/sec
q_o	dynamic pressure, lb/ft^2
r	sample correlation coefficient
r	yawing velocity, rad/sec
s	Laplace operator
S	wing area, ft^2
t	statistical test measure,
V	true airspeed, ft/sec
Y_β	$= (q_o S) C_{y_\beta} / mV$, 1/sec
$Y_{\delta_{RP}}$	$= (q_o S) C_{y_{\delta_{RP}}} / mV$, 1/in.-sec
α	angle of attack, rad or deg
β	angle of sideslip, rad or deg
γ	flight path angle, rad or deg
δ	control deflection, deg or in.
$\delta_e, \delta_a, \delta_r$	elevator, total aileron, and rudder control surface deflections, rad
δ_{ES}, δ_{AS}	elevator and aileron side controller deflections, rad
δ_{RP}	rudder pedal deflection, in.
ζ	damping ratio
ζ_d	Dutch roll damping ratio
ζ_{SP}	longitudinal short period damping ratio
ζ_ϕ	damping ratio of numerator quadratic in roll-to-aileron input transfer function

θ	pitch attitude, rad or deg
$\left\lvert \frac{\dot{\theta}}{F_{ES}} \right\rvert$	amplitude of pitch rate per elevator stick force frequency response, deg/sec per lb
τ	first order time constant, sec
τ_R	roll mode time constant, sec
τ_S	spiral mode time constant, sec
τ_θ	longitudinal short period lead time constant, sec
ϕ	bank angle, rad or deg
$\left\lvert \frac{\phi}{\beta} \right\rvert$	magnitude of roll-to-sideslip ratio at Dutch roll frequency
ω	undamped natural frequency, rad/sec
ω_d	Dutch roll undamped natural frequency, rad/sec
ω_{SP}	longitudinal short period undamped natural frequency, rad/sec
ω_ϕ	undamped natural frequency of numerator quadratic in roll-to-aileron input transfer function, rad/sec
$(\dot{})$	time derivative, $d(\,)/dt$
$\frac{1}{T}\int_0^T \lvert\varepsilon\rvert dt$	integral of absolute error, deg or in.

Subscripts

o	trim value
a	aileron
AS	aileron stick (right aileron stick displacement is positive)
e	elevator
ES	elevator stick (rearward elevator stick displacement is positive)
r	rudder
RP	rudder pedal (right rudder pedal forward is positive)

Axes and Sign Conventions

The airplane response sensors in the T-33 airplane are oriented with respect to the fuselage reference axes. These are the body axes with their

origin at the c.g., and defined by the leveling points in the airplane such that when the airplane is laterally and longitudinally level, the X and Y axes lie in the horizontal plane with the X axis in the plane of symmetry with its positive direction forward along the fuselage. The Y axis is normal to the plane of symmetry with its positive direction out the right wing. The Z axis lies in the plane of symmetry with its positive axis downward.

The moments and products of inertia, I_x , I_y , I_z , and I_{xz} are specified for this fuselage reference axis system. The equations of motion in Appendix B are written with respect to this axis system, and hence the stability derivatives (e.g., Y_β , N_β , L_β , C_{y_β} , C_{n_β} , C_{l_β} , etc.) are computed for this axis system.

The "primed" yawing and rolling moment derivatives, N'_β , L'_β , etc. are linear combinations of the fuselage reference axis derivatives, N_β , L_β , etc., and are defined in the List of Symbols.

SECTION 1
INTRODUCTION

The purpose of the investigation reported herein was to examine the effects of various longitudinal and lateral-directional handling quality parameters on the overall handling qualities of a lifting re-entry vehicle. Particular interest was centered in the area of minimum handling qualities in an effort to determine minimum-acceptable and minimum-flyable boundaries as a function of the individual handling quality parameters.

The need for this research is emphasized by the more recent trends in piloted vehicles toward increased use of stability augmentation because of the inherently poor flying qualities of the unaugmented vehicle. Since current and projected augmentation systems do not have extremely high reliability, it is necessary to determine the minimum flying qualities which a vehicle must possess for the pilot to maintain control in a failure mode. In addition, it is important to determine the effects of vehicle characteristics on flying qualities in the full range from minimum-controllable to good, since this information serves as design criteria for the augmentation system and permits trade-off compromises between system complexity and flying quality perfection.

Another problem area in handling quality research has been the determination of all the vehicle stability and control parameters which have a strong influence on the flying qualities of the airplane. In addition to obtaining quantitative data to assess the effects of known significant parameters, there is a continuing investigation of new parameters which have not in the past been critical for conventional airplane configurations but which may become important in future vehicles.

The evaluations reported herein were performed in a three-axis variable stability airplane, especially modified for use as a fixed-base ground simulator. The major portion of the reported data is from configurations evaluated in the fixed-base simulator, but selected configurations were also evaluated in flight for comparison purposes.

The complete experiment is described in Section 2 of this report. The equipment used, including the analog simulation of the aerodynamic characteristics of the T-33, the cockpit display employed, and the side stick configuration is reported. The orientation of the evaluation pilots, as regards the mission and flight tasks to be considered, is discussed. The specific maneuvers and rating scale which were used are presented. The detailed test program is outlined including the mechanics of the evaluations, techniques for determining vehicle characteristics, and the performance data measurements.

Original manuscript submitted August 1961; revised manuscript released by authors October 1963 for publication as an ASD Technical Documentary Report.

In Sections 3 through 6, the experimental results are reported. In Section 3, the longitudinal evaluations in the fixed-base simulator are discussed. The in-flight longitudinal evaluations are reported and the results compared to the fixed-base simulator evaluations. The lateral-directional evaluations in the fixed-base simulator are reported in Section 4. In Sections 3 and 4, comparisons are made with the results of other fixed-base, moving-base and in-flight simulations.

Tracking performance records were obtained for each configuration evaluated. This tracking performance data is reported in Section 5. In Section 6, the pilot rating variability is reported and discussed. Statistical analysis techniques are employed in the analysis of pilot rating variability, and a brief discussion of certain statistical parameters is given in Appendix A. In Appendix B, aircraft equations of motion and pertinent transfer functions are presented. Finally, in Section 7, conclusions are drawn based upon the discussion of the results.

SECTION 2
DESCRIPTION OF EXPERIMENT

2.1 EQUIPMENT

The vehicle used for this fixed-base and in-flight simulation was the three-axis variable stability T-33 airplane modified by the Cornell Aeronautical Laboratory for the Air Force Flight Dynamics Laboratory, Research and Technology Division, Air Force Systems Command. The variable stability equipment is described in References 3, 4, and 5. Details of the capabilities of this equipment as a fixed-base simulator are given in Reference 6. Figures 1, 2, and 3 picture the airplane, evaluation pilot's instrument panel, and the two-axis side controller.

Briefly, the vehicle is a standard T-33 which has been modified in such a way that the system manager, or rear seat pilot, may vary the handling characteristics about all three axes by simply changing the settings of gain controls located on the right console. The manner in which the handling characteristics are altered is such that the front seat pilot, or evaluation pilot, is completely unaware of what changes have been made. Realism is added to the evaluation and any chance of bias as a result of knowledge of the characteristics to be evaluated is eliminated.

All evaluations in this investigation were conducted in simulated instrument flight. During the fixed-base simulation, the canopy was covered with a white cloth. In flight, a white hood inside the canopy excluded the outside view of the evaluation pilot.

The fixed-base simulator utilizing the variable stability T-33 provides an environment essentially identical with that of instrument flight with the exception of the proprioceptive cues resulting from translational and angular accelerations. The cockpit instrument displays and controls operate just as they do in flight. The variable stability system is used to vary the stability and control characteristics just as it is in flight. The only essential difference is that an analog computer is used to solve modified linear six-degree-of-freedom equations of motion of the normal T-33 to replace the aerodynamic and mass effects of flight. The following block diagram illustrates the mechanization of the fixed-base simulation:

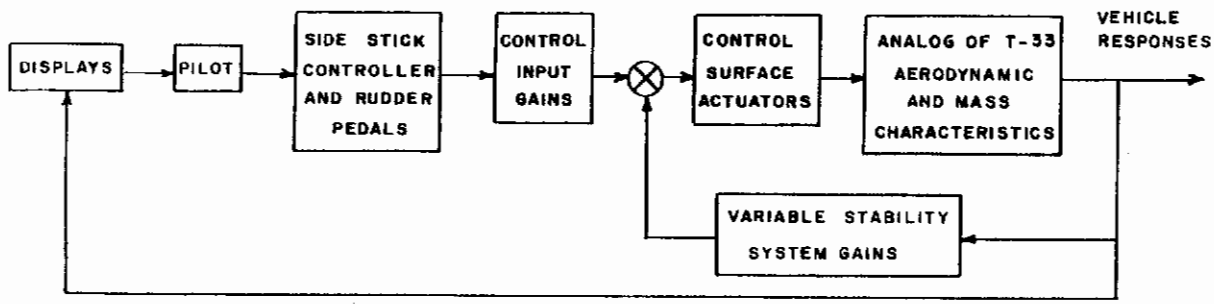

In the in-flight simulation, the analog of the aerodynamic and mass characteristics was replaced by the airplane itself.

The cockpit display instruments activated for this investigation were as follows:

1. Lear remote attitude-director indicator, type ARU-2-A. This instrument presents pitch attitude as the rotation of a sphere which appears as a vertical translation of a horizontal white line with respect to the instrument case. Roll angle is presented as the rotation of this same sphere which appears as a rotation in the vertical plane of the horizontal white line. Sideslip is presented as the horizontal translation of a vertical bar. A horizontal bar which is a part of this instrument was not utilized, and was electrically displaced from the pilot's view. A rate-of-turn indicator is also provided. Side acceleration, as indicated by a ball, is provided for flight use but was not activated for the fixed-base simulation.

2. Airspeed – Trim was at 250 knots IAS with a range of 190 to 310 knots allowed.

3. Altitude – Trim was at 25,000 feet with a range of 22,500 to 27,500 feet allowed.

4. Rate of climb or descent – Standard nonlinear scale with ±6000 feet per minute range.

5. Normal acceleration.

6. Heading angle as presented by a radio magnetic indicator (RMI)— range of ψ = ±120 degrees from North.

7. Angle of attack.

Dynamics of the Lear attitude displays (θ , ϕ , and β) are described in Table 1.

The side stick installation has been designed to allow attachment of various types of primary controllers. The two-axis side stick utilized in this investigation had axis locations and moment arms as presented in Figure 3. Breakout forces were approximately one pound for both the pitch and roll axes. These values of breakout force are the result of inherent friction and of force added to provide positive centering. Inductive type pick-offs were used on each of the axes to measure stick position and served as inputs to the respective control surface servos. Calculated values of the frequency and damping of the side stick and its spring rates about each axis are indicated in Table 1.

Yaw inputs were applied by the pilot through conventional rudder pedals. Pedal forces were provided by an electro-hydraulic servo which

opposed pedal deflection as a linear spring. Breakout forces for this pedal force servo were approximately 15 pounds. Pedal position served as the pilot control input to the rudder surface servo. The frequency and damping of the rudder pedal servo and its spring gradient are given in Table 1.

Characteristics of the controlled element – the simulated airplane – were varied in both the fixed-base and in-flight simulations through the control input and variable stability system gains. The dynamics of the control surface actuators, through which pilot control inputs and variable stability system inputs were applied, are given in Table 1.

A source of random disturbances was used in the investigation to provide a piloting task. The manner in which these disturbances were displayed to the pilots is shown in Figure 4. The random inputs were injected directly into the cockpit displays of bank angle and sideslip angle, and were also fed as command inputs to the elevator servo. The disturbances were not injected directly into the pitch attitude display since preliminary investigation showed that undesirably large changes in aircraft altitude and airspeed would result from tracking the displayed lower frequency pitch attitude disturbances. Therefore, it was decided to disturb the airplane (and simulator) in pitch through inputs to the elevator servo, and thus provide a tracking task about trim pitch attitude.

The random inputs were obtained from a gas tube white noise source and passed through a band pass filter. The filter had break points at 0.1 rad/sec and 1.0 rad/sec as shown in Figure 5, with a 6 db per octave rising asymptote to the lower break point and a 12 db per octave rolloff from the higher break point. The magnitude of the random disturbances was maintained constant throughout the evaluation program.

2.2 EVALUATION TECHNIQUE

Prior to the actual test program each pilot was informed of the general mission characteristics for which the evaluations were to be done. The overall mission was described as the re-entry, descent and landing of a re-entry vehicle. In particular, each pilot was told that this mission did not require high maneuverability but did require fairly precise control of attitude. Each configuration was to be evaluated in light of the entire required mission, except that low L_α configurations were not penalized for their inherently low available n_z. The following maneuvers were selected as representative of the piloting task:

1. Straight flight, including small turns, pitch corrections, and pilot-induced disturbances about level flight.

2. Turning flight. Shallow and steeply banked turns involving heading changes of at least 90° and bank angles up to 60°, with particular attention to the control of pitch angle, bank angle, and sideslip angle as required.

3. Tracking task. Track roll and sideslip random inputs and minimize pitch disturbances (two minutes).

The third maneuver was included to provide the pilot with a flying task not induced by his own disturbances. It was also included in order that performance measures of pilot tracking could be obtained.

Pilot comments on each configuration were recorded at the completion of the first two maneuvers, and again following the tracking maneuver. A comment card (Table 2) was provided with suggested items to be covered. Two ratings were assigned to each configuration. The first rating was given along with the comments at the completion of the first two maneuvers. A second rating was given at the completion of the third maneuver. The pilot was asked to assign each rating on the basis of the suitability of the configuration for the mission. The second rating should then reflect the influence of the tracking maneuver (and possibly some influence of the additional evaluation time) on the pilot's evaluation of the configuration.

A ten-point rating scale (Table 3) was used by the pilots. The procedure followed by the pilot in arriving at a summary rating was to first categorize the configuration as satisfactory, unsatisfactory but acceptable, unacceptable, or unflyable. Within the first three categories, a word description was selected which further categorized the configuration to a numerical rating.

The rating scale appears similar to the Cooper rating scale of Reference 17 but important differences do exist. First, the CAL rating scale does not allow for the existence of an alternate mission since re-entry is a "one-way street". That is, once re-entry has commenced, it must be continued. Each configuration is thus evaluated regarding its suitability for the mission. The CAL scale differs, secondly, from the Cooper scale in the unacceptable region. Expanded definitions of the unacceptable ratings (7, 8, and 9) are shown in Table 3.

It should be noted that a rating of 10 was used by each pilot in certain instances where the particular configuration could be controlled in the ground simulator for some period of time in straight and level flight. However, the pilot commented that the configuration was so bad that he could control it only under the optimum circumstances represented by the simulation program. That is, it would be unflyable if the configuration was encountered:

1. suddenly, as with augmentation system failure,
2. when not in a trimmed condition or with non-zero initial conditions, or
3. in a time of physical or mental stress, such as in the real environment of re-entry.

Another rating category could be devised which would define the worst configuration which the pilot could control under optimum conditions for a predetermined period. It was the opinion of the pilots, however, that such a rating would be of academic interest only – when they say it is unflyable for the mission, they want absolutely no part of it, ever!

2.3 TEST PROCEDURE

A. Fixed-Base Simulator

The fixed-base ground simulator evaluations were performed by three pilots, herein referred to as pilots A, B, and C. Each pilot's flying experience is presented in Table 4. Pilots A and C had previous experience in variable stability airplane evaluations. Pilot B, while an experienced engineering test pilot, had no such prior experience.

The pilots were informed as to whether lateral-directional or longitudinal handling qualities were being altered. No information was given to them as to what actual parameters were being varied. The configurations were presented in a random order except that control sensitivity evaluations were conducted separately from dynamic parameter evaluations.

The pilots were scheduled according to availability. Thus pilot B completed the longitudinal short period dynamics investigations, and the control sensitivity investigations about all three axes without hiatus. Pilot A then accomplished these same phases. These two pilots next alternated from day to day, or on a half-day basis, in accomplishing the evaluation of Dutch roll dynamics and lateral-directional control coupling. Pilot B then completed the investigation of various lateral parameters at one other longitudinal configuration while alternating with pilot C, who accomplished the longitudinal investigation and the effects of control sensitivities about all three axes.

The investigations accomplished by each pilot are summarized below:

Flying Qualities Parameters	Evaluation Pilots
1. Longitudinal Flying Qualities	
a. Elevator Control Sensitivity	A, B, C
b. Short Period Dynamics	A, B, C
c. Lift Curve Slope	A
2. Lateral-Directional Flying Qualities	
a. Aileron Control Sensitivity	A, B, C
b. Rudder Control Sensitivity	A, B
c. Dutch roll dynamics plus effects of the magnitude of roll-to-sideslip ratio and yaw-to-aileron coupling	A, B

Initially, each pilot was given three configurations to familiarize him with the simulator and the evaluation procedure. These configurations were selected to provide a wide range of control characteristics as follows:

1. Normal T-33
2. Poor lateral-directional, good longitudinal characteristics
3. Poor longitudinal, good lateral-directional characteristics.

These evaluations were run just as the remainder of the program, but were not used as test data. The configuration characteristics as evaluated in the ground simulator are listed in Tables 5a and 5b.

In general, test periods of approximately one and one-half hours to two hours were accomplished with brief rest periods in between. Each pilot was allowed as much time per configuration as he required. The mean time required for all configurations was: pilot A, 28 minutes; pilot B, 19 minutes; and pilot C, 23 minutes.

The test program was run in the same manner as previous flight programs. The configurations were presented to the pilots in random fashion. The configurations were set up via the rear cockpit system controls by a test monitor. A second test monitor was required in the analog computer room for initial setup and balancing procedures and to monitor for possible amplifier overloading. Pilot comments and ratings on each configuration were recorded and transcribed. The two-minute tracking maneuver was recorded for each configuration. In addition, the pilot was required to accomplish calibration maneuvers (such as rudder kicks and elevator steps) to provide time histories of control inputs and simulated vehicle motion responses from which stability and control parameters could be determined.

B. In-Flight Simulation

The in-flight simulations were principally directed toward replication of portions of the ground simulator investigation of longitudinal flying qualities, short period dynamics (item 1 b in the table above). In addition, a brief examination was made of the effects of different values of normal acceleration per angle of attack, $(n_z/\alpha)_{ss}$, on the short period evaluations.

The in-flight evaluations were made only by Pilot A. A white instrument flying hood was used to obscure the outside view, and the in-flight evaluations were conducted in simulated instrument flight. The same evaluation maneuvers, comment card, and rating scale were used as for the ground evaluations (Section 2.2, and Tables 2 and 3). The flight evaluation program consisted of fifteen flights during which twenty-six configurations were evaluated. The pilot was not restricted in his evaluation time, but averaged twenty-seven minutes per configuration.

Pilot comments were recorded at the end of the maneuvering portion of the evaluation, and again after completion of the tracking task. The evaluation pilot assigned a rating to the configuration following the maneuvering evaluation, and again following the tracking task. For the tracking task, the random noise signals were injected into the bank angle and sideslip displays, and as commands to the elevator servo in the same manner as the ground evaluations. However, due to a malfunction this signal was not available on all flights. Hence, the pilot ratings after the random noise maneuver are omitted in Table 6 for certain configurations. Fortunately, the ground simulator work showed that Pilot A's ratings following the noise maneuvers were not significantly different from his smooth air ratings, and hence it is assumed that the dearth of noise ratings is not a serious deficiency.

The instructions to the pilot as to the mission of the vehicle under evaluation were the same as in the ground simulation program. The

configurations were presented in random order, except that evaluations of variations of $(n_z/\alpha)_{ss}$ were conducted separately, following the short period evaluations. Repeat configurations were assigned different numbers ("fifty" series) from the original evaluations.

The in-flight evaluations of short period dynamics were flown at 25,000 feet pressure altitude, 0.6 Mach number, and 250 knots indicated airspeed. Variations in $(n_z/\alpha)_{ss}$ were achieved by altering airspeed (indicated airspeeds of 250, 205, and 160 knots) at 25,000 feet. Adjustments were made to the variable stability system gains in order to achieve as nearly the same short period characteristics as possible at each airspeed. The cockpit controls were the same side controller and rudder pedals as used in the ground experiments. The throttle was the standard T-33 throttle control. The cockpit display instruments were the same as used on the ground, with the following exceptions:

a. The altimeter, rate-of-climb, and airspeed indicators were conventional pressure sensing instruments, located on the left side of the instrument panel shown in Figure 2.

b. The ball on the attitude display instrument was operative.

Calibrations maneuvers were performed for each configuration to provide airplane response time histories to control inputs. The analysis results of this data are the basis of the parameter values listed in Table 6 for each configuration. The data for configurations of moderate stability and/or with an oscillatory response were extracted from the response time histories using conventional curve-fitting techniques. Those configurations for which such analysis is not suitable (unstable or not-well-separated modes) were examined by using an equations-of-motion digital computation (Reference 19). With this technique, the coefficients of the equations of motion of unstable vehicles can be measured in flight with the pilot acting as a stabilizing, and disturbing, element. It should be emphasized that the mode characteristics of Table 6 are actually measured values.

SECTION 3

EVALUATION OF LONGITUDINAL FLYING QUALITIES

3.1 GAIN OF PITCH AND NORMAL ACCELERATION RESPONSE TO ELEVATOR STICK FORCE, FIXED-BASE SIMULATOR

The transfer functions of pitch rate and normal acceleration response to elevator stick force may be defined as follows for the short period response at constant airspeed with lift due to elevator control input, $L_{\delta_{ES}}$, assumed zero (see Appendix B for derivatives):

$$\frac{\dot{\theta}}{F_{ES}} = K'_{\dot{\theta}_{F_{ES}}} \frac{(\tau_\theta s+1)}{s^2+2\zeta_{sp}\omega_{sp}s+\omega_{sp}^2} \tag{3.1}$$

$$\frac{n_z}{F_{ES}} = \frac{K_{n_{z_{F_{ES}}}}\omega_{sp}^2}{s^2+2\zeta_{sp}\omega_{sp}s+\omega_{sp}^2} = \frac{K'_{\dot{\theta}_{F_{ES}}}\frac{V}{(57.3)(32.2)}}{s^2+2\zeta_{sp}\omega_{sp}s+\omega_{sp}^2} \tag{3.2}$$

where

$$K'_{\dot{\theta}_{F_{ES}}} = L_\alpha M_{\delta_{ES}} \frac{\delta_{ES}}{F_{ES}} \quad \text{in units of deg/sec}^3\text{-lb} \tag{3.3}$$

and $K_{n_{z_{F_{ES}}}}$ is in units of g's/lb.

The gain, $K'_{\dot{\theta}_{F_{ES}}}$, was evaluated in the fixed-base simulator to determine its effect on pilot rating for three different values of longitudinal short period dynamics, ω_{sp}^2 and $2\zeta_{sp}\omega_{sp}$. The results are presented in Figure 6. These evaluations were done with the inherent lateral-directional characteristics of the T-33 for the test airspeed and altitude. The configurations which present the characteristics evaluated in this study of the gain $K'_{\dot{\theta}_{F_{ES}}}$ are 1 - 4a and 78 - 85 as presented in Table 5. The variations in $K'_{\dot{\theta}_{F_{ES}}}$ were made by altering the gear ratio, δ_e/δ_{ES}, with constant M_{δ_e} and L_{δ_e} at values representative of the T-33 at this flight condition. Thus the variations in $M_{\delta_{ES}} = M_{\delta_e}(\delta_e/\delta_{ES})$ and $L_{\delta_{ES}} = L_{\delta_e}(\delta_e/\delta_{ES})$ were proportional to the changes in $K'_{\dot{\theta}_{F_{ES}}}$. The elevator side-control deflection per force input was maintained at a constant value of one degree per pound.

A. $\omega_{sp}^2 = 10.6$ 1/sec^2 and $2\zeta_{sp}\omega_{sp} = 2.15$ 1/sec

With longitudinal short period dynamics of $\omega_{sp}^2 = 10.6$ and $2\zeta_{sp}\omega_{sp} = 2.15$, pilots A and C downgraded configurations on either side of the optimum value of $K'_{\dot{\theta}_{F_{ES}}}$ as a result of sensitivity to control inputs. Their optimum value of $K'_{\dot{\theta}_{F_{ES}}}$ was 5 deg/sec^3-lb. For lower values, insensitivity in pitch response was commented upon. For $K'_{\dot{\theta}_{F_{ES}}}$ above the optimum, pitch control was too sensitive, and there were numerous instances when the placarded 4 g normal acceleration limit was exceeded. Pilot B was less sensitive to the value of $K'_{\dot{\theta}_{F_{ES}}} = 10$ deg/sec^3-lb; it was still felt to be quite a good configuration and was not regarded as too sensitive. His comments indicated that his optimum would occur between $K'_{\dot{\theta}_{F_{ES}}} = 5$ and 10. At $K'_{\dot{\theta}_{F_{ES}}} = 5$, Pilot B commented on the slow pitch response, and at $K'_{\dot{\theta}_{F_{ES}}} = 10$, he noted some difficulty in maintaining pitch attitude in trim. For $K'_{\dot{\theta}_{F_{ES}}} = 30$ deg/sec^3-lb, all three pilots commented that the response in pitch was too sensitive.

Two sets of ratings (before and after-tracking) differ markedly from the other ratings at the same configuration: pilot B's initial ratings at $K'_{\dot{\theta}_{F_{ES}}}$ = 30 deg/sec^3-lb and pilot C's initial ratings at $K'_{\dot{\theta}_{F_{ES}}}$ = 10 deg/sec^3-lb. In each case the respective configuration was the first evaluated after the three familiarization configurations. The repeat rating by pilot B was done six configurations later and agreed quite well with the ratings of the other pilots. It seems likely that the three practice configurations were inadequate for pilots B and C to establish the necessary familiarization with the simulator. However, the results indicate that after four configurations (three practice plus one evaluation for data), these two pilots were well oriented.

B. ω_{sp}^2 = 3.58 1/sec^2 and $2\zeta_{sp}\omega_{sp}$ = 1.00 1/sec

With longitudinal short period dynamics of ω_{sp}^2 = 3.5 and $2\zeta_{sp}\omega_{sp}$ = 1.00, pilots A and C apparently realized their optimum value of $K'_{\dot{\theta}_{F_{ES}}}$ at the tested value of 1.68 deg/sec^3-lb. Based upon the recorded comments, pilot B preferred a gain somewhere between this value and the next higher one tested, $K'_{\dot{\theta}_{F_{ES}}}$ = 5. All pilots commented on the slow, sluggish pitch response for all values of gain tested. Configurations with $K'_{\dot{\theta}_{F_{ES}}}$ above the optimum value were downrated due to oversensitivity. Pilot C was even more critical of this shortcoming than the other two pilots. At the highest value of gain tested, all pilots reported that pilot-induced oscillations resulted.

C. ω_{sp}^2 = -0.38 1/sec^2 and $2\zeta_{sp}\omega_{sp}$ = 1.62 1/sec

The effects of variations in $K'_{\dot{\theta}_{F_{ES}}}$ were investigated with only one pilot for longitudinal short period dynamics of ω_{sp}^2 = -0.38 and $2\zeta_{sp}\omega_{sp}$ = 1.62. The results, shown in Figure 6, indicate only a small effect of gain due to the inherently poor over-all characteristics with these short period dynamics. Based upon the pilot comments, the gain value of 1.68 was best for these longitudinal dynamics. The configuration with $K'_{\dot{\theta}_{F_{ES}}}$ = 5.0 was considered somewhat too sensitive although this configuration was given the same rating as the one with lower gain. Apparently the difference which existed between the two configurations was not sufficiently great to warrant a rating change. It seems safe to conclude that the optimum gain for this configuration is either 1.68 or somewhere between 1.68 and 5.0 deg/sec^3-lb.

Pilot comments on the configurations with gains of 10 and 30 deg per sec^3-lb were quite similar to each other. In both cases, the pilot was oscillating between ratings of 9 and 10. The tracking maneuver resolved the dilemma for each configuration and resulted in ratings of 10.

For all values of gain at these longitudinal dynamics, the configurations were unacceptable for entry. They could be flown for a short time with no distractions beyond scanning the instrument panel. Even a quick check of airspeed was sufficient distraction from the attitude display to cause great difficulty. If the lateral-directional characteristics had not been good, it was the pilots' opinion that these configurations could not have been flown.

D. Summary and Discussion

Although the gain, $K'_{\dot{\theta}_{F_{ES}}}$, was the test variable in this phase of the investigation, the results may be considered in terms of other gains of the

pitch and normal acceleration transfer functions. The optimum values as obtained from the data of Figure 6 are presented in the following table for $K'_{\dot{\theta}_{F_{es}}}$, $K_{\dot{\theta}_{F_{es}}}$ (steady state pitching velocity per elevator control force) and for $1/K_{n_z F_{es}}$ (steady state stick force per normal acceleration):

ω_{sp}^2	Optimum $K'_{\dot{\theta}_{F_{es}}} \sim$	Optimum $K_{\dot{\theta}_{F_{es}}} \sim$	Optimum $1/K_{n_z F_{es}} \sim$
$1/sec^2$	deg/sec^3-lb	deg/sec-lb	lb/g
10.6	5.0 - 8.0	.47 - .75	6.4 - 4.0
3.58	1.7 - 3.0	.47 - .84	6.4 - 3.6

The values listed first for each gain are the optimums for pilots A and C; the second values are the optimums for pilot B.

For this range of short period natural frequency, the pilots preferred constant steady state pitching velocity and/or normal acceleration per stick force. In the in-flight simulation of Reference 11 with a center-stick control, the optimum value of stick force per normal acceleration was 6 lb/g. The close agreement with the above fixed-base simulator results with a side-stick control is attributed to the similarity in the use of the two types of control. A pilot using a center-stick normally rests his forearm on his thigh. For small control displacements, he applies pitch control force by rotation of his hand about the vertical wrist pivot. With the side-stick control and the forearm supported as in Figure 3, pitch control force is applied in a similar manner although the wrist pivot axis employed is 90 degrees from that used with the center-stick. Based upon the results of Reference 15, it might be concluded that desirable pitch force levels would be higher with the side-stick (about the pitch axis of Figure 3) than with the center-stick which in effect is utilizing the yaw axis of Figure 3. It was shown in Reference 15 that desired operational torque levels with a side-controller were higher for the pitch axis than the yaw axis. However, the center-stick optimum force levels are undoubtedly influenced by the ability to use the entire arm, shoulder and back musculature if needed.

An investigation with a simple pitch mode tracking simulation (Reference 7) obtained, at a value of $\omega_{sp}^2 = 9.85$, an optimum range of $K'_{\dot{\theta}_{F_{es}}} = 5.9$ to 11.8 with a center-stick control. This is in good agreement with the data at $\omega_{sp}^2 = 10.6$ in Figure 6 and further indicates the correlation of optimum gains determined for side-stick controls with those determined for center-stick controls.

3.2 SHORT PERIOD DYNAMICS

An investigation of the effects of longitudinal short period dynamics on pilot ratings was conducted using the T-33 both as a fixed-base simulator and as an in-flight simulator. The emphasis of this phase of the program was on the minimum flyable region. During this evaluation of short period dynamics, the lateral-directional characteristics were those of the normal T-33 airplane. The short period gain, $K'_{\dot{\theta}_{F_{es}}}$, was maintained constant at the optimum value as determined for each pilot at $\omega_{sp}^2 = 10.6$ and $2\zeta_{sp}\omega_{sp} = 2.15$ (Section 3.1.A).

This gain, $K'_{\dot{\theta}_{FES}}$, was maintained constant rather than stick force per normal acceleration as the latter gain is not definable for values of $\omega_{sp}^2 < 0$.

A. Fixed-Base Rating Boundaries

The pilot rating data are presented in Figure 7 for the fixed-base simulator evaluations. Configurations 57 through 77 of Table 5 comprise the basic investigation by three pilots as supplemented by configuration 2 (pilots A and C) and configurations 86, 89 and 92 (pilot A). Faired boundaries are drawn in Figure 7 as based upon the pilot ratings and recorded comments. For the range of dynamics tested the boundaries for both before and after-tracking ratings demonstrate a predominant influence of total damping, $2\zeta_{sp}\omega_{sp}$, for values of ω_{sp}^2 above 2.0 1/sec^2. Below this value of ω_{sp}^2 the minimum acceptable (6.5) and minimum controllable (9.0) boundaries are determined essentially by ω_{sp}^2. In this region there is little effect of total damping in pilot rating boundaries for the range of $2\zeta_{sp}\omega_{sp}$ tested. In general, the boundaries drawn through the after-tracking data indicate a requirement for slightly greater damping than that indicated for the before-tracking data at values of ω_{sp}^2 above 2.0 1/sec^2.

These boundaries were constructed with the assistance of the data plots of Figure 8. In this figure the pilot rating data are presented as functions of $2\zeta_{sp}\omega_{sp}$ for approximately constant values of ω_{sp}^2 and as functions of ω_{sp}^2 for approximately constant values of $2\zeta_{sp}\omega_{sp}$.

B. In-Flight Versus Fixed-Base Ratings

Figure 9 presents the before-tracking ratings of longitudinal short period dynamics by pilot A in the fixed-base and in-flight evaluations. As the before-tracking and after-tracking ratings by pilot A were not significantly different, only the one set of ratings is discussed. The in-flight configurations used in Figure 9 are the first sixteen configurations listed in Table 6, i.e., those configurations evaluated at the largest $(n_z/\alpha)_{ss}$.

Although an inadequate amount of data was obtained to draw boundaries from the in-flight ratings, it is evident that the in-flight ratings for ω_{sp}^2 of 7.0 and higher are considerably better than the fixed-base ratings. At lower values of ω_{sp}^2 this difference is not apparent.

For $\omega_{sp}^2 \approx 2$ and $2\zeta_{sp}\omega_{sp} \approx 0.5$, the in-flight ratings were worse than the fixed-base ratings. However, the two fixed-base ratings of 5 for this configuration were considerably better than would be expected from the data obtained in this region by all three pilots (Figure 7). This configuration, number 89, was evaluated along with configurations 86 and 92 as part of the evaluation that is discussed later. There is no explanation for the apparently better ratings for this particular configuration 89.

All other ratings obtained in the region of $\omega_{sp}^2 < 5.0$ and $2\zeta_{sp}\omega_{sp} < 1.5$ indicate little difference in the fixed-base and in-flight ratings of pilot A. The in-flight ratings would result in minimum acceptable and minimum controllable boundaries that would be shifted toward somewhat lower damping and lower frequency than the fixed-base boundaries of Figure 7. However, the fixed-base boundaries are based upon mean ratings by all three pilots,

and pilot A tended to rate poor configurations somewhat better than the mean of the other two pilots. (Interpilot comparisons are made in Section 6.) Therefore, the only valid comparison is that of Figure 9.

Minimum controllable boundaries (pilot rating of 9.0) have been estimated in Figure 9 for the ratings by pilot A in both the in-flight and fixed-base simulations. The in-flight boundary can be defined only at the two extremes of ω_{sp}^2 tested; however, there is evidence for the shape of the boundary as drawn between these defined areas. These boundaries are presented only to give an indication of the differences in ratings for one pilot between in-flight and fixed-base evaluations. The more general boundaries are presented in Figure 7.

C. Rating Boundary Comparisons

The fixed-base, after-tracking rating boundaries are compared in Figure 10 with results from in-flight mirror landing evaluations using a variable stability airplane (Reference 9), single-axis centrifuge evaluations (Reference 10), and in-flight evaluations in maneuvering flight using a variable stability airplane (Reference 11).

The minimum flyable boundary established for mirror landing approaches in rough air (Reference 9) is a "safe to fly" boundary although it includes configurations that are sufficiently difficult to fly that a successful landing approach is not guaranteed on every trial. However, these configurations could be flown safely in accomplishing missed approach procedures – activation of landing gear and flaps and power application for wave-off. The shaded area shows the approximate variation in this minimum flyable boundary for the two pilots who evaluated in rough air. These results from Reference 9 agree with the fixed-base minimum controllable boundary at values for ω_{sp}^2 of 2.0 and 0 $1/sec^2$. However, this in-flight boundary tends to continue for values of $\omega_{sp}^2 < 0$ while the fixed-base boundary does not allow for values of $\omega_{sp}^2 < 0$. It is possible that motion cues, proprioceptive and visual, can account for this difference. The aperiodic divergent configurations were not adequately investigated in flight with the T-33 (Figure 9) to determine directly the difference between fixed-base and flight simulations in this region of $\omega_{sp}^2 < 0$. It can only be assumed that the additional cues available in flight would be particularly beneficial for aperiodic divergent configurations.

The centrifuge program of Reference 10 obtained rating data for six pilots and involved only a pitch-axis control task. Stick force per normal acceleration was maintained constant for $\omega_{sp}^2 > 0$, while in the fixed-base simulation constant elevator motion per stick force was maintained. The discussion in Section 3.1 points out the preference for constant stick force per normal acceleration at least for a range of ω_{sp}^2 from 3.6 to 10.6 $1/sec^2$. Therefore, some portion of the difference between the fixed-base and centrifuge simulations may be attributable to the off-optimum gain of the fixed-base simulation. The major difference in the evaluation programs was the piloting task. The fixed-base simulator task was considerably more complex in that the pilot was required to maintain airspeed, altitude and normal acceleration limits while in a rather complete simulation of instrument flight in six degrees of freedom. The centrifuge evaluation was only a two-degree-of-freedom simulation of the pitching motion. Thus, the centrifuge rating

boundaries of Reference 10 would be expected to be less restrictive than the fixed-base boundaries.

Pilot rating boundaries as reported in Reference 11 by Chalk were established from in-flight evaluations in a variable stability airplane by three pilots for a fighter mission. Although a rating scale was used which differs from that of Table 3 herein, the boundaries shown in Figure 10 are believed to correspond to the minimum acceptable (6.5) boundaries of the present rating scale. Two boundaries from Reference 11 are shown to indicate the interpilot variability in that evaluation,* and the region between the boundaries is shaded. When the Reference 11 results are compared to the fixed-base simulation of the re-entry mission, it is apparent that the need for maneuverability and precise tracking controllability is greater for the fighter mission. The fighter mission would appear even more restrictive if the in-flight re-entry boundary could be shown instead of the simulator boundary.

The minimum flyable boundary drawn in Figure 10 from the data of Reference 11 was obtained from the ratings by one pilot – Pilot C of the T-33 fixed-base simulation. The additional cues afforded the pilot by visual flight resulted in less damping requirements for $\omega_{sp}^2 > 2.0$ than the fixed-base boundary. Somewhat higher values for the minimum value of ω_{sp}^2 are indicated, although the configurations evaluated in this region were less well defined as per Reference 11.

A summary curve including all of the boundaries discussed above is presented in Figure 11. The only area of unexplainable disagreement between the boundaries established with the fixed-base simulation and those of References 9 and 10 is for $2\zeta_{sp}\omega_{sp} > 0.75$. The flight data of Reference 11 and the fixed-base data tend to agree that there is a minimum value of ω_{sp}^2. The flight data of Reference 9 and the centrifuge data of Reference 10 allow increasingly greater values of $\omega_{sp}^2 < 0$ as damping is increased. The boundaries in this area need to be better defined through fixed-base and in-flight simulation.

3.3 STEADY STATE NORMAL ACCELERATION PER ANGLE OF ATTACK

A. Fixed-Base Simulation

During the evaluations of short period dynamics, there was evidence in the pilot comment data that the pilot ratings would be affected by the value of the lift curve slope parameter, L_α, particularly in the region of zero stiffness (ω_{sp}^2), zero damping ($2\zeta_{sp}\omega_{sp}$). It had been considered originally beyond the scope of this experiment to include evaluations of the effect of L_α. However, a brief examination of the effects of L_α at low ω_{sp}^2 and $2\zeta_{sp}\omega_{sp}$ was included at the end of the fixed-base simulator program. The configurations were rated only by pilot A.

The nominal longitudinal characteristics were:

Configuration Number	ω_{sp}^2	$2\zeta_{sp}\omega_{sp}$	L_α
86 - 88	0	0	0.8, 1.0, 1.2
89 - 91	2	.6	0.8, 1.0, 1.2
92 - 94	4	.8	0.8, 1.0, 1.2

*Some of the interpilot variability of Reference 11 was attributable to variability between pilots in interpretation of the rating scale definitions.

The actual values of ω_{sp}^2, $2\zeta_{sp}\omega_{sp}$ and L_α are listed in Table 5a. Each configuration was evaluated twice, and the order of presentation was randomly selected.

It should be noted that the variations in L_α were achieved by alteration of the lift curve slope, C_{L_α}, in the fixed-base simulation. No compensation was made for the effects of C_{L_α} on $K'_{\dot\theta_{F_{ES}}}$ and hence since:

$$K'_{\dot\theta_{F_{ES}}} = L_\alpha M_{\delta_e}\left(\frac{\delta_e}{\delta_{ES}}\right)\left(\frac{\delta_{ES}}{F_{ES}}\right) \text{ for } L_{\delta_e} = 0 \text{ at constant speed}$$

it is seen that the variations in $K'_{\dot\theta_{F_{ES}}}$ were nearly proportional to the variations in L_α. And, of course, since the speed was held constant, the stick force per g varied inversely with $K'_{\dot\theta_{F_{ES}}}$.

The drag forces in the longitudinal force equation were also unchanged between configurations. Since normal acceleration per angle of attack $[(n_z/\alpha)_{ss}]$ decreased in magnitude with decreasing L_α, the drag forces are correspondingly larger in the low L_α configurations for similar accelerated maneuvers.

The pilot rating results in the fixed-base simulation are shown in Figure 12. Perhaps as interesting as the specific ratings are the pilot comments themselves since the latter show how really complex are the effects of L_α, at least when the variations are made in the manner reported here. Five separate factors are evidenced in the pilot comments:

1. Tendency to bobble in pitch,
2. Tendency to overshoot g and concern over structural integrity,
3. Effects of variations in elevator control sensitivity,
4. Separation of pitch attitude from flight path angle, and
5. Increased use of throttle to maintain airspeed.

The tendency to bobble in pitch is due partly to the short period dynamics, but is considerably influenced by the magnitude of L_α. Since at constant speed,

$$\frac{\dot\theta}{F_{ES}} = \frac{K'_{\dot\theta_{F_{ES}}}(\tau_\theta s + 1)}{s^2 + 2\zeta_{sp}\omega_{sp}s + \omega_{sp}^2}$$

it can be seen that the location of the numerator break point, $\omega_{b.p.}{}_{NUM} = 1/\tau_\theta$

with respect to the denominator break point, $\omega_{b.p.}{}_{DEN.} = \omega_{sp}$

determines the influence of the first-order numerator term on the pitch response to elevator force inputs. Amplitude frequency response plots are shown in Figure 13 to illustrate this influence. Since

$$\tau_\theta = \frac{M_{\delta_e} - M_{\dot\alpha} L_{\delta_e}}{L_\alpha M_{\delta_e} - M_\alpha L_{\delta_e}}$$

$$\cong \frac{1}{L_\alpha} \text{ for } L_{\delta_e} \cong 0 \quad ,$$

$$\omega_{\substack{s.p. \\ NUM.}} = \frac{1}{\tau_\theta} \cong L_\alpha$$

It can be seen in Figure 13 that if $1/\tau_\theta < \omega_{sp}$ the amplitude ratio, $\left|\frac{\dot\theta}{F_{es}}\right| \Big/ K'_{\dot\theta_{F_{es}}}$, will be larger than unity over a larger band of frequencies than if $1/\tau_\theta \geq \omega_{sp}$. The effect of $1/\tau_\theta$ on the transient pitch rate response to an elevator step input is shown in Figure 14. From consideration of the bobble tendency, pilot rating would be expected to degrade with decreasing L_α.

The second general comment on g-overshoot and structural integrity is influenced by the bobble tendency due to the short period dynamics and to τ_θ as discussed above. However, the pilot is also talking about the consequences of his pitch oscillations in terms of the structural loads which they produce. Since these loads are proportional to L_α, pilot rating would be expected to improve with decreasing L_α from this consideration.

The variations in elevator control sensitivity,

$$K'_{\dot\theta_{F_{es}}} = L_\alpha M_{\delta_e} \left(\frac{\delta_e}{\delta_{es}}\right)\left(\frac{\delta_{es}}{F_{es}}\right) \quad \text{for } L_{\delta_e} \cong 0 \text{ at constant speed}$$

which attended the variations in L_α evoked certain pilot comments. For example, at $\omega_{sp}^2 \cong 2$, the pilot complained that the pitch control was too sensitive for $L_\alpha \cong 1.2$, a little too sensitive at $L_\alpha \cong 1.0$, and better (not oversensitive) at $L_\alpha \cong .8$. These values of L_α correspond to values of $K'_{\dot\theta_{F_{es}}} \cong 5, 4$, and 3 deg/sec^3-lb respectively, and the comments concur with those of the $K'_{\dot\theta_{F_{es}}}$ investigation discussed in Section 1.1. Thus it would appear that the $K'_{\dot\theta_{F_{es}}}$ variations caused by L_α would be such that pilot rating would tend to be improved by decreasing L_α.

The next pilot comment, the separation of pitch attitude from flight path angle, is an interesting one. The pilot in an instrument flying task principally maneuvers using his attitude (Θ) presentation, cross-checking rate of climb ($\dot h$) to correlate Θ with γ. If L_α is large, then the $\Delta\alpha$ required to maneuver is correspondingly small and Θ control is adequate γ control. For example, in a steady turn the attitude for zero rate of climb ($\gamma = 0$) appears only slightly different than for $\gamma = 0$ in wings-level flight. As L_α is reduced, larger angle-of-attack changes are required to produce the added lift to maintain zero rate of climb in banked flight. In the turn with low L_α, the required Θ to maintain $\gamma = 0$ is noticeably larger, and it is thus necessary to significantly modify Θ whenever the bank angle is changed. Similarly, in a pull-up to level flight from a dive, the pilot must continued the nose on above the horizon by an amount dependent upon the normal acceleration and L_α until the rate of climb is zero, then reduce the pitch attitude

to maintain level flight. Thus, flight path and pitch attitude are separated, and pilot rating would be expected to degrade from this consideration as L_{α} is reduced.

The variations in L_{α} also caused changes in the use of the throttle by the pilot. These changes were due in part to the fact that the variation in drag force with angle of attack was held constant as L_{α} was reduced. Hence, for the same maneuvering requirements as L_{α} was reduced, larger angle-of-attack changes were required and the pilot had to make greater use of the throttle in order to balance the X-force equation and keep the airspeed constant. This effort would be expected to cause the pilot's rating to degrade as L_{α} is reduced.

When the various effects of L_{α} (or $1/\tau_{\theta}$) are examined as above, some insight is obtained into the difficulty of predicting the shape of pilot rating versus L_{α} . Three of the factors tend to cause a degradation in pilot rating, and two factors tend to cause pilot rating to improve as L_{α} decreases. The relative importance of each factor is related to the quality of the short period dynamic parameters, ω_{sp}^2 and $2\zeta_{sp}\omega_{sp}$, so that, for example, a larger effect of L_{α} on the tendency to bobble would be expected with a low $2\zeta_{sp}\omega_{sp}$ configuration than on a high one.

The pilot rating data of Figure 12 is evidence of the complex nature of L_{α} as a handling quality parameter. At $\omega_{sp}^2 \cong 4$ $1/sec^2$, L_{α} has no apparent effect on the over-all rating of the configurations. This does not say that all configurations are alike; it merely says they are of approximately equal over-all quality for the assumed mission.

At $\omega_{sp}^2 \cong 2$ $1/sec^2$, an effect of L_{α} on pilot rating is apparent and, at first glance, somewhat surprising in its trend. Higher ratings are exhibited at the high and low extreme values of L_{α} . The intermediate value of L_{α} is rated poorest. Based upon the preceding discussion of the individual effects of L_{α} , one would expect that the improved rating of the lowest value of L_{α} was influenced by the reduced concern for structural integrity and by the now-nearly-optimum value of $K'_{\dot{\theta}_{FCS}}$. The improvement in over-all flying quality which resulted from these factors outweighed any degradation from the other three factors. At the highest value of L_{α} , the improved pilot rating would be expected from the lessened tendency to bobble, the improved correspondence of θ with γ , and a reduction in the need for precise throttle control to maintain airspeed while maneuvering. A review of the pilot's comment data supports these conclusions.

It is difficult to draw conclusions regarding the effect of L_{α} at the near-zero values of ω_{sp}^2 for two reasons. First, the short period dynamics were so basically objectionable that little spread in ratings is evident. Second, as may be noted in Table 5a, there was some variation in short period dynamics that attended the L_{α} variations and may account for the rating trends. However, after examination of the comment data, it is believed that the slight – but repeatable – improvement in pilot rating at the lowest L_{α} is valid and due primarily to the reduced concern over exceeding the structural limits of the airplane. This improvement of rating at reduced L_{α} is consistent with the known controllability of a zero-stiffness, zero-damped, non-lifting vehicle such as a piloted space capsule in orbit.

B. In-Flight Simulation

The ground simulator evaluations of the effects of L_α on flying qualities were heavily weighted by the pilot's comments regarding normal acceleration (g's) and structural integrity. No vehicle acceleration or motion feel is present in the fixed-base simulation and so an in-flight evaluation seemed necessary. Unfortunately, the in-flight simulation could not replicate the ground experiment of altering $|n_z/\alpha|_{ss}$ with C_{L_α} since no independent lift control is available in the T-33 variable stability airplane. The in-flight variations in L_α were achieved by altering speed at constant altitude. The variable stability system was used to provide the desired short period dynamics at each speed. The lateral-directional handling characteristics were not held constant but were allowed to vary with speed in a normal manner.

The data to define each configuration is shown in Table 6, and the pertinent rating results are shown plotted in Figure 15. Before and after tracking results are presented although no significant difference is believed to exist for pilot A.

A preference is shown for the intermediate value of $|n_z/\alpha|_{ss}$ at the two larger values of short period stiffness. The pilot comments indicate that the highest $|n_z/\alpha|_{ss}$ brings problems which include over-sensitive elevator control and concern over structural integrity in the ensuing pitch oscillations. Both of these objections are quite serious and cause the rather large decrease in rating from the intermediate value of $|n_z/\alpha|_{ss}$.

The lowest values of $|n_z/\alpha|_{ss}$ at the two higher values of short period stiffness, ω_{sp}^2 , show a reduction in pilot rating from the peak value. This reduction in rating arises from objections to the "looseness in pitch", pitch overshoot, and lack of precise flight path control.

At the lowest ω_{sp}^2 , a small preference is shown for the two lower values of $|n_z/\alpha|_{ss}$ although the general quality of the short period dynamics is in the unacceptable region for the generalized mission. With the largest value of $|n_z/\alpha|_{ss}$, the pilot commented that constant closed-loop control was required. Even when flying the aircraft tightly, the normal acceleration oscillated from 0 to 2 g, and this made him apprehensive about overstressing the airplane. With the lowest value of $|n_z/\alpha|_{ss}$, the pilot commented that "g" and pitch control were improved, and that it was apparent to him that the handling qualities with these poor dynamics were improved as $|n_z/\alpha|_{ss}$ was reduced.

SECTION 4

EVALUATION OF LATERAL-DIRECTIONAL FLYING QUALITIES

4.1 GAIN OF ROLL RESPONSE TO AILERON STICK FORCE INPUT

The transfer function of roll response to aileron stick force may be defined as follows (See Appendix E) for rudder fixed and for a neutrally stable spiral mode:

$$\frac{\phi}{F_{AS}} = \frac{K_{\dot{\phi}F_{AS}} \left(\frac{s^2}{\omega_\phi^2} + \frac{2\zeta_\phi}{\omega_\phi} s + 1 \right)}{s \left(\tau_R s + 1 \right) \left(\frac{s^2}{\omega_d^2} + \frac{2\zeta_d}{\omega_d} s + 1 \right)} \qquad (4.1)$$

Pilot rating versus the gain, $K_{\dot{\phi}F_{AS}}$, is presented in Figure 16 for each of the three pilots for the fixed-base simulations. Data from an in-flight evaluation by pilot A in the T-33 (Reference 8) are also included. These evaluations were done with the inherent longitudinal and other lateral-directional characteristics of the T-33 for the test airspeed and altitude. The characteristics evaluated in the fixed-base program are configurations 5 through 8, and configuration 2 for Pilot A, as presented in Table 5. The parameters of the above transfer function are described in terms of the stability derivatives in Appendix B. For this investigation of $K_{\dot{\phi}F_{AS}}$, and the investigation of $K_{\beta F_{RP}}$ (Section 4.2), the parameter ω_ϕ/ω_d was held constant. The importance of ω_ϕ/ω_d was indicated in Reference 16 and verified in the in-flight simulation reported in Reference 8. An approximate expression for this parameter is presented in Appendix B.

Agreement between the in-flight center-stick and fixed-base side-stick results of pilot A is excellent. As discussed with regard to pitch control in Section 3.1.D, pilots apply force to a center stick in much the same manner as a side stick. Thus the optimum control force levels as selected by pilot A would be expected to be much the same for the two types of control.

There were interpilot differences in the fixed-base evaluations. In commenting on the configurations evaluated, pilot A indicated that a gain value, $K_{\dot{\phi}F_{AS}}$ = 4.9 deg/sec-lb, was a little insensitive and $K_{\dot{\phi}F_{AS}}$ = 20.0 was a little too sensitive. He also commented that the $K_{\dot{\phi}F_{AS}}$ = 10.0 deg per sec-lb was better than either of these two but these differences did not warrant rating changes. Pilot B in his before-tracking ratings was less critical of the value of $K_{\dot{\phi}F_{AS}}$. His poorer ratings after tracking in three out of four of the configurations were attributed to yawing oscillations due to aileron inputs which were difficult to damp through use of the rudder. He did feel that a value of $K_{\dot{\phi}F_{AS}}$ = 1.9 was somewhat too insensitive. Pilot A also commented that for insensitive gear ratios, when large aileron control inputs were required, it became difficult to apply appropriate pitch control inputs.

The preference of pilot C for a less sensitive roll response to control input may possibly be attributed to his requirements as regards "harmonization" of the pitch and roll controls. As reported in Reference 15,

the following operational force preferences were obtained for each of these pilots with a side stick control:

Operational Force Range - Pounds

	Pitch	Roll
Pilot A	±20	±10
Pilot B	±15	± 5 to 10
Pilot C	±15	±15

These values of force ranges indicate that pilots A and B preferred a 2 to 1 ratio of pitch to roll while pilot C preferred a 1 to 1 ratio. As all three pilots selected approximately the same optimum value for pitch control gain (Section 3.1), it could be expected that pilot C would select a roll response gain one-half that selected by the other two pilots. This difference in optimum gains is indicated in Figure 16.

4.2 GAIN OF SIDESLIP RESPONSE TO RUDDER PEDAL FORCE INPUT

The transfer function of sideslip response to rudder pedal force input may be defined as follows (see Appendix B) for aileron fixed and for the spiral mode removed by the assumption of $g/V_o = 0$:

$$\frac{\beta}{F_{RP}} = \frac{K_{\beta F_{RP}} \left(\frac{s^2}{\omega_{\beta_R}^2} + \frac{2\zeta_{\beta_R}}{\omega_{\beta_R}} s + 1 \right)}{\left(\tau_R s + 1 \right) \left(\frac{s^2}{\omega_d^2} + \frac{2\zeta_d}{\omega_d} s + 1 \right)} \qquad (4.2)$$

The numerator of Equation 4.2 usually factors into two first-order zeros, and hence ζ_{β_R} is usually greater than unity.

The effects of the gain, $K_{\beta F_{RP}}$, on pilot rating were determined by pilots A and B in the fixed-base simulator for three values of Dutch roll damping and frequency, ζ_d and ω_d. Figure 17 presents the pilot ratings obtained. Configurations 45 - 56 of Table 5b present the characteristics evaluated. Values for ζ_d and ω_d are given in Figure 17. $K_{\beta_{F_{RP}}}$ was varied through changes in $N'_{\delta_{RP}}$. At the three values of ω_d for which $K_{\beta_{F_{RP}}}$ was examined, the attempt was made to keep ω_ϕ/ω_d constant with small, slightly adverse, aileron yaw, and $|\phi/\beta|$ constant at a value of 2. As may be seen in Table 5b, this objective was fairly well achieved. The values were selected such as to give the pilot basic configurations which required use of the rudder pedals for rolling maneuvers. Both ζ_{β_R} and ω_{β_R} were held constant throughout this investigation of $K_{\beta F_{RP}}$ as is evident from the approximate expressions of Appendix B and the parameter values of Table 5b. These evaluations were done with the inherent longitudinal short period characteristics of the T-33. The value of $K'_{\theta_{FES}}$ was maintained constant at the optimum value for each pilot. $K_{\dot{\phi}_{FAS}}$ was approximately constant at a value ($K_{\dot{\phi}_{FAS}}$ = 3.5 to 3.8 deg/sec-lb) less than optimum, which would result in a pilot rating reduction of approximately 0.5 rating as per Figure 16.

During the evaluation at the Dutch roll frequency of approximately 1.0 rad/sec (Figure 17A), the damping ratio was not maintained constant.

Examination of the pilot comment data indicated that, despite the low value of ζ_d for the configuration with $K_{\beta F_{RP}} = -.066$ deg/lb, this gain was preferred among the specific values evaluated. Based upon the comment data, the optimum gain value would occur somewhat higher than -.066 deg/lb. At the gain value of -.122 deg/lb, there was no direct comment by either pilot regarding rudder effectiveness. The major complaint regarding the configuration was that whenever aileron input was applied and sideslip resulted, considerable difficulty was experienced in damping the resulting oscillation in sideslip. There were some indications, although not specifically stated, that this particular gain may have been too high and was resulting in overcontrol of sideslip. At the two lowest values of gain tested, $K_{\beta F_{RP}} = -.038$ and -.016 deg/lb, the ailerons were too effective in producing sideslip and the rudder pedals were too ineffective in controlling sideslip. At $K_{\beta F_{RP}} = -.016$ both pilots developed a special technique for flying this configuration. Ailerons were applied in small amplitude pulses to approach gingerly the desired bank angle. Rudder inputs could then be used to control the resulting sideslip. Pilot A did two tracking maneuvers on his first evaluation of this value of gain – one using rudder pedals and one not. In his opinion his tracking performance may perhaps have been better when rudder pedals were not employed. Upon evaluation of this particular configuration later in the program, this tracking technique without use of rudder was not discovered. At the low values of gain it was felt that ratings based only upon the tracking maneuver could lead to wrong conclusions regarding the configuration – a better rating might be given. It was primarily in maneuvering flight that the mismatch in yaw-producing capabilities of the aileron and rudder controls was recognized.

For the Dutch roll characteristics of $\omega_d \cong 2.0$ rad/sec and $\zeta_d \cong .036$ (Figure 17B), a general comment by each pilot was related to the moderate to large adverse yaw due to ailerons. The severity of this comment increased as $K_{\beta F_{RP}}$ was decreased. At the highest gain evaluated, $K_{\beta F_{RP}} = -.131$ deg/lb, the yaw resulting from aileron inputs was not disturbing. However, both pilots felt this configuration should be flown with only elevator and ailerons; the use of rudder inputs resulted in Dutch roll oscillations difficult or impossible to damp. At $K_{\beta F_{RP}} = -.069$, pilot A felt this gain to be good for tracking although a little too sensitive. It did allow coordination of the adverse yaw due to aileron inputs. Pilot B had most success in controlling the airplane if rudder inputs were not used and any ensuing oscillation damped with aileron inputs only. With the two lowest values of gain, $K_{\beta F_{RP}} = -.036$ and -.018 deg/lb, all three controls were used to fly the airplane. At a gain value of -.018, pilot A commented that this low sensitivity resulted in less excitation of the Dutch roll when rudder inputs were required as a result of roll maneuvers.

In the evaluations at $\omega_d \cong 4.3$ rad/sec, there was again some variability in Dutch roll damping as shown in Figure 17C. One important factor not shown, however, was the variation in ζ_d with amplitude of β. Both pilots reported (and this was also observed in the response time histories) that a small (one-degree) limit cycle in β persisted following a disturbance even though for larger amplitudes, the response exhibited positive damping. The disagreement between pilots A and B regarding the over-all suitability of these basic characteristics for the re-entry mission is, in large measure, attributed to their individual interpretation of the effects of this limit cycle.

The major difficulty experienced by the pilots for all of the values of $K_{\beta_{F_{RP}}}$ at ω_d = 4.3 rad/sec was with the low damping. For this value of Dutch roll frequency (ω_d = 4.3 rad/sec), pilot rating is very sensitive to ζ_d as indicated in Section 4.3. However, the pilot comments delineate the preferred value of $K_{\beta_{F_{RP}}}$ as -.032 deg/lb regardless of the absolute level of rating given. The low values of ζ_d resulted in the need for rudder inputs to augment the damping, and the pilots were able to determine the value of $K_{\beta_{F_{RP}}}$ that allowed this augmentation.

The adverse yaw due to ailerons was not as bothersome for the configurations with ω_d = 4.3 rad/sec as for those with ω_d = 1.0 and 2.0 rad/sec. Although $N'_{\delta_{AS}}$ was increasingly larger, in order to maintain ω_ϕ/ω_d and $|\phi/\beta|$ each approximately constant as ω_d was increased, the actual sideslip and yaw per aileron input were smaller, as may be seen from the values of $K_{\beta_{F_{AS}}}$ tabulated below (and in Table 5b).

In the pilot comments, the amount of rudder pedal force needed for coordination as a result of aileron stick force inputs seemed to be a possible criterion for the suitability of particular values of $K_{\beta_{F_{RP}}}$. Thus it might be inferred that the pilots would select $(K_{\beta_{F_{RP}}})_{OPT}$ such as to have constant rudder pedal forces per aileron stick force for the condition of zero sideslip. Let us examine the possibility.

An approximate expression as developed in Appendix B for β/F_{AS} is as follows:

$$\frac{\beta}{F_{AS}} \cong \frac{K_{\beta_{F_{AS}}} \left| \tau_{\beta_A} s + 1 \right|}{\left| \tau_R s + 1 \right| \left| \frac{s^2}{\omega_d^2} + \frac{2\zeta_d}{\omega_d} s + 1 \right|} \qquad (4.3)$$

The parameters of transfer functions (4.2) and (4.3) are presented in the following table for the configurations at which the optimum gain, $K_{\beta_{F_{RP}}}$, was realized. In calculating these gains for the evaluation at $\omega_d \cong$ 1.0 rad/sec, the δ_r/δ_{RP} gain and consequently the values of $N'_{\delta_{RP}}$, $L'_{\delta_{RP}}$ and $Y_{\delta_{RP}}$ were adjusted to the faired optimum value of $K_{\beta_{F_{RP}}}$ of Figure 17A. For the calculations at $\omega_d \cong$ 2.0 and 4.3 rad/sec, the optimum was achieved approximately at one of the tested gains (Figures 17B and 17C).

ω_d	ζ_d	$(K_{\beta_{F_{RP}}})_{OPT.}$	$K_{\beta_{F_{AS}}}$	ω_{β_R}	ζ_{β_R}	τ_{β_A}	τ_R	$\left.\frac{F_{RP}}{F_{AS}}\right\|_{\beta_{ss}=0}$	$\left.\frac{F_{RP}}{F_{AS}}\right\|_{\substack{\beta=0 \\ \omega=\omega_d}}$
1/sec		deg/lb	deg/lb	1/sec		sec	sec		
1	.20	-.08	1.50	14.2	2.9	.21	.40	18.8	17.8
2	.04	-.07	.56	14.2	2.9	.26	.40	8.00	7.09
4.3	.02	-.032	.15	14.2	2.9	.28	.40	4.68	3.74

With the basic test variations in ω_d, $K_{\beta_{F_{AS}}}$ varied as indicated above in keeping ω_ϕ/ω_d approximately constant. The value of rudder pedal force required to produce sideslip (β_{RP}) to counteract the sideslip (β_{AS}) produced by use of the ailerons is as follows:

$$\beta = \beta_{AS} + \beta_{RP} = 0$$

$$\frac{\beta}{F_{AS}} F_{AS} + \frac{\beta}{F_{RP}} F_{RP} = 0$$

$$\left.\frac{F_{RP}}{F_{AS}}\right|_{\beta=0} = -\frac{\beta/F_{AS}}{\beta/F_{RP}}$$

$$\left.\frac{F_{RP}}{F_{AS}}\right|_{\beta=0} \cong -\frac{K_{\beta_{F_{AS}}}\left(\tau_{\beta_A} s+1\right)}{K_{\beta_{F_{RP}}}\left(\frac{s^2}{\omega_{\beta_R}^2} + \frac{2\zeta_{\beta_R}}{\omega_{\beta_R}} s+1\right)} \qquad (4.4)$$

For zero steady state sideslip, $\beta_{ss} = 0$,

$$\left.\frac{F_{RP}}{F_{AS}}\right|_{\beta_{ss}=0} = -\frac{K_{\beta_{F_{AS}}}}{K_{\beta_{F_{RP}}}} \qquad (4.5)$$

As may be seen in the above tabulation, the pilot does not select $(K_{\beta_{F_{RP}}})_{OPT}$ such that $(F_{RP}/F_{AS})_{\beta_{ss}=0}$ is constant. Another possibility is that the pilot selects $(K_{\beta_{F_{RP}}})_{OPT}$ such that $(F_{RP}/F_{AS})_{\beta=0}$ evaluated at ω_d is constant. But this is not true either, as may be seen in the table above.

The optimum values of $K_{\beta_{F_{RP}}}$ are plotted in Figure 18 versus ω_d. A straight line fits the three points well, but is not believed to be a valid expression for the optimum $K_{\beta_{F_{RP}}}$ above or below the tested values of ω_d.

How rudder control is used by the pilot is a major factor in the understanding of lateral-directional handling qualities. The results of this investigation indicate the need for a more extensive investigation to establish optimum values of the gains of responses to rudder control inputs for ranges of ω_d, ζ_d, ω_ϕ/ω_d, and $|\phi/\beta|$.

4.3 DUTCH ROLL DYNAMICS

An investigation of Dutch roll natural frequency, ω_d, and damping ratio, ζ_d, at selected values of $|\phi/\beta|$ and favorable and adverse yaw due to ailerons was conducted with pilots A and B. The parameters that describe the test configurations are presented in Table 5, configurations 9 through 44. The program planning for this fixed-base ground simulator evaluation was done subsequent to the flight evaluations of Reference 8. At that time, the analysis of the Reference 8 data indicated that pilot opinion was more strongly a function of $N'_{\delta_{AS}}$ than ω_ϕ/ω_d. Hence it was planned to investigate a range of values of ω_d and ζ_d at selected values of $N'_{\delta_{AS}}$ and $|\phi/\beta|$, rather than at selected values of ω_ϕ/ω_d and $|\phi/\beta|$ as in Reference 8. For the convenience

of the reader, an approximate relationship between $N'_{\delta_{AS}}$ and ω_ϕ/ω_d as developed in Appendix B is

$$\left(\frac{\omega_\phi}{\omega_d}\right)^2 \cong 1 - \frac{N'_{\delta_{AS}}}{L'_{\delta_{AS}}} \frac{L'_\beta}{N'_\beta} \tag{4.6}$$

An approximate expression for $|\phi/\beta|$ is (for $\tau_R^2 \omega_d^2 >> 1$):

$$\left|\frac{\phi}{\beta}\right| \cong -\frac{L'_\beta}{N'_\beta} \tag{4.7}$$

Combining Equations (4.6) and (4.7),

$$\left(\frac{\omega_\phi}{\omega_d}\right)^2 \cong 1 + \frac{N'_{\delta_{AS}}}{L'_{\delta_{AS}}} \left|\frac{\phi}{\beta}\right| \tag{4.8}$$

and

$$\left[\left(\frac{\omega_\phi}{\omega_d}\right)^2 - 1\right] \Big/ \left|\frac{\phi}{\beta}\right| \cong \frac{N'_{\delta_{AS}}}{L'_{\delta_{AS}}} \tag{4.9}$$

Thus, if $L'_{\delta_{AS}}$ is constant and the above relationship is in fact correct, then $N'_{\delta_{AS}}$ is a function of the lumped parameter $\dfrac{\left[\left(\frac{\omega_\phi}{\omega_d}\right)^2 - 1\right]}{\left|\frac{\phi}{\beta}\right|}$. It was hypothesized that if this lumped parameter were maintained constant, then pilot rating would be only a function of Dutch roll damping, ζ_d. Two values of this lumped parameter were programmed: (1) a positive value (called favorable aileron yaw) and (2) a negative value (called adverse yaw). Some difficulties were experienced in maintaining the desired values due to system gain variations. Also, due to a system gain calibration change, the values of $|N'_{\delta_{AS}}|$ actually tested were much less than desired. In addition, $(-L'_\beta / N'_\beta)$ was found not to be a good approximation for $|\phi/\beta|$. This resulted in an additional variation in $N'_{\delta_{AS}}$.

Evaluation results are presented in Figure 19 for the before-tracking ratings. As discussed in Section 6, there was no significant difference between pilots A or B in their before- or after-tracking ratings. However, if pilot B's after-tracking ratings were plotted on this figure, they would be increased by slightly greater than .5 rating points on the average. This would

not change significantly the conclusions drawn from these data. Due to inability to realize precisely the values of damping desired in these relatively low ranges, the values of damping obtained for each value of $|\phi/\beta|$ and ω_ϕ/ω_d did not cover quite the same ranges. This was less of a problem at the two higher frequencies.

There was an additional difficulty in the analysis of these data in that the desired values of the roll to aileron stick force gain, $K_{\dot{\phi}_{FAS}}$, were not realized. These gains were generally considerably below the optimum values previously determined for pilots A and B. It is questionable whether correction of the pilot ratings for the difference in $K_{\dot{\phi}_{FAS}}$ from optimum, using the curves in Figure 16, would be valid, for it is not known whether the variations in pilot rating with $K_{\dot{\phi}_{FAS}}$ would apply over wide ranges of various other lateral-directional parameters. Such a correction has not been made to the data in Figure 19.

In general, at the medium and high frequency configurations the lumped-parameter hypothesis was borne out for the range of $|\omega_\phi/\omega_d|$ tested. That is, if the parameter $[(\omega_\phi/\omega_d)^2 - 1] / |\phi/\beta|$ is held constant then pilot rating is definitely a function of Dutch roll damping. However, at a given value of ζ_d, there still remains considerable variation in ratings. The range of variation in pilot rating at constant ζ_d is difficult to interpret due to the design of the experiment. By attempting to hold the lumped-parameter constant for a range of ζ_d, there resulted no significant variations in ω_ϕ/ω_d or $|\phi/\beta|$ at constant values of ζ_d (or ω_d). Thus, the best that can be done is present pilot rating as a function of ζ_d. The variations in rating at constant ζ_d can be ascribed to the independent effects of ω_ϕ/ω_d, $|\phi/\beta|$, and ω_d which have been studied in previous work such as that reported in Reference 8. The pilot comments are discussed and compared as follows.

A. Favorable Yaw Due to Ailerons ($\omega_\phi/\omega_d > 1.0$)

For the low frequency case, ω_d = .95 to 1.36 1/sec, two different curves are indicated – one for the lowest value of $|\phi/\beta|$ and one for the two highest values. For low $|\phi/\beta|$ the ratings are much more critical of Dutch roll damping. The pilot comments with $|\phi/\beta|$ = 1.61 to 2.13 and ζ_d = .10 were very critical of the favorable yaw and the difficulties in damping with rudder pedals any oscillations resulting from aileron inputs. With $|\phi/\beta|$ = 4.02 to 5.11 and ζ_d = .06 to .09, favorable yaw was noticeable but not particularly bothersome. In fact, pilot B commented that the configuration with $|\phi/\beta|$ = 4.02 and ζ_d = .09 was much like the configuration with $|\phi/\beta|$ = 2.13 and ζ_d = .20 which he had evaluated immediately before. With low $|\phi/\beta|$ aileron inputs result in relatively large yawing disturbances, particularly at low ζ_d, that are difficult for the pilot to damp out.

With high stiffness (ω_d = 4.27 to 4.52 1/sec) and any value of damping greater than zero, adequate control could be maintained without the use of rudder pedal inputs. In those configurations with high roll-to-sideslip ratios, this two-control operation was generally mandatory, as use of rudder pedals to damp any induced oscillations only aggravated the situation. Damping of the Dutch roll motion was even more important at the higher Dutch roll

frequencies than the low, particularly with moderate to high roll-to-sideslip ratio.

Consider the high $|\phi/\beta|$ configurations at $\zeta_d = -.025$ as plotted on Figure 19 for all three values of ω_d. With $\omega_d \cong 4.3$ 1/sec, pilot A found it impossible to use rudder pedals to damp any induced oscillations; however, he could fly this particular configuration by applying aileron input as a function of sideslip. Pilot B gave up on this configuration due to the fact that he could not damp the Dutch roll with rudder pedals. At the value of $\omega_d \cong 2.11$ 1/sec, pilot A considered the best technique to be the same as previously mentioned – use only ailerons to damp oscillations. However, he could use rudder pedals to damp sideslip when large values were realized. Pilot B utilized a somewhat different technique. He first zeroed sideslip as well as possible with rudder control and then used ailerons to achieve the desired bank angle. With low ω_d, pilot A still considered using the ailerons to damp out sideslip as the best technique although use of rudder pedals was possible. The primary reason for the improvement in rating at this value of $|\phi/\beta|$ as ω_d decreased was the improved ability to move the ailerons at the Dutch roll frequency for damping purposes. The inadvertent low $K_{\dot{\phi}_{F_{AS}}}$ did nothing to improve control of these configurations.

At low $|\phi/\beta|$ the influence of ω_d is also felt. With ζ_d values of approximately 0.10, the pilots noted the favorable yaw due to ailerons in all cases but only with low ω_d was it much of a problem. At high ω_d, aileron inputs resulted in little yaw disturbance and the necessity for "cross controls" was not as disturbing as at a low value of ω_d.

B. Adverse Yaw Due to Ailerons ($\omega_\phi/\omega_d < 1.0$)

At the two highest values of ω_d, the adverse yaw configurations were grouped with the favorable yaw configurations generally as a function of ζ_d. For those high $|\phi/\beta|$ configurations with near-zero ζ_d, the pilots were able to use rudder inputs to damp oscillations and found no need to develop the technique of aileron inputs with sideslip as they did with favorable yaw configurations. This is attributed to the increase in closed-loop damping with normal use of the ailerons when adverse yaw is present. This added damping was apparently just enough that normal use of the rudder pedals was possible to supply the total damping required. With low $|\phi/\beta|$ at values of ζ_d between .05 and .085, the adverse yaw present had to be coordinated at the medium value of ω_d but was not even commented on at the high ω_d.

With low ω_d the pilots commented on low rudder effectiveness. The values of $K_{\beta_{F_{RP}}}$ were essentially the same as for the other values of ω_d. However, the values of $K_{\beta_{F_{AS}}}$ were considerably higher; so the comments are easily understood.

SECTION 5
TRACKING PERFORMANCE MEASURES

A two-minute tracking maneuver was accomplished as part of the evaluation procedure for each configuration. The tracking input for this task has been described in Section 2. The quantities $\Theta_{DISPLAY}$, $\Phi_{DISPLAY}$, $\beta_{DISPLAY}$, δ_{AS}, δ_{ES} and δ_{RP} were recorded on an oscillograph. Integrated absolute error, IAE, and standard deviation for each quantity were calculated from these time histories for selected configurations via an IBM 704 digital computer. The integral of the absolute error was calculated about zero error, while the standard deviation was calculated about the mean. The integral of the absolute error was calculated about zero error to include the effect of mean values of error different from zero. The recorded quantities were sampled every 0.5 seconds, so that for the two-minute tracking maneuver a total of 240 values was obtained for each quantity. The integral of the absolute error about zero and the standard deviation were calculated as follows:

$$IAE = \sum_{i=1}^{N} |\varepsilon| = \sum_{i=1}^{N} |X - \bar{X}| \tag{5.1}$$

$$s = \left[\frac{\sum_{i=1}^{N} (X - \bar{X})^2}{N-1} \right]^{1/2} \tag{5.2}$$

where N = number of measures of the quantity X

$$\bar{X} = \frac{1}{N} \sum_{i=1}^{N} (X) \tag{5.3}$$

Performance measures were determined for configurations receiving ratings covering the complete scale with particular attention to those near and beyond the boundary of unflyable for the mission (ratings 9, 9.5, and 10). Table 7 presents separately the calculated data obtained for the longitudinal and lateral-directional evaluations. The ratings listed are those given after tracking. Rudder pedal deflection in the longitudinal evaluations with good lateral-directional characteristics was within only ±0.1 inch. Therefore in the longitudinal analysis of the performance measure, it is not included.

The two performance measures of each of the recorded variables are presented in Figures 20 and 21 for the selected longitudinal evaluations and in Figures 22 and 23 for the selected lateral-directional evaluations. These measures are plotted versus the after-tracking ratings.

There is no apparent correlation of these performance measures with pilot rating. In general, both the standard deviation and the integrated absolute error remain relatively constant, at least to a rating of 10. In the longitudinal evaluations (Figures 20 and 21) the standard deviation of Θ and δ_{ES} and the integrated absolute error of Θ indicate a definite increase for a rating of 10. However, as there is no significant trend of increasing errors

at lower ratings, this increase in error measures is of no use in predicting pilot rating.

A similar result for in-flight tracking was obtained in the investigation of Reference 18 and for the centrifuge evaluations of Reference 10. The adaptability of the human pilot is such that relatively constant tracking performance can be maintained as handling qualities become poorer almost up to the point of uncontrollability.

The IBM 704 was programmed to print the content of δ_{ES} , δ_{AS} , and δ_{RP} in intervals of 2 degrees for each of the side stick deflections and 0.2 inches for the rudder pedal deflection. Distributions for the selected configurations are presented in Figures 24 and 25.

SECTION 6
PILOT RATING VARIABILITY

There are two major concerns regarding pilot rating variability: 1) how consistent individual pilots are (intrapilot variability), and 2) how well pilots agree among themselves (interpilot variability). In this investigation two of the pilots, A and B, repeated a sufficient number of configurations that a measure of their individual repeatability could be obtained. Comparisons of all three pilots' ratings provide indications of magnitude and type of variability among pilots.

Each pilot rated each configuration twice – before accomplishing the tracking maneuver and after. The first rating considered only the straight and turning flight maneuvers (page 5), while the second rating considered all three maneuvers. This second rating differed from the first only if the pilot changed his overall evaluation of the particular configuration as a result of flying it in the presence of disturbances other than his own inputs. The intra- and interpilot variability were examined for each set of rating data. The intrapilot variability was determined from all repeat runs throughout all phases of the investigation. For differences among pilots, the longitudinal evaluations and lateral-directional evaluations were examined separately. This separation was necessary as three pilots accomplished the former evaluations while only two pilots accomplished the latter.

In the analyses of pilot variability, the ratings were compared for the same configuration. The differences between these ratings were then analyzed to determine if these differences were statistically significant. The test of significance employed was the Student's "t" test. Although this test assumes a normal distribution of the data (in this case, distribution of differences), the investigation reported in Reference 14 demonstrates the validity of its use even for rather extreme violations of this assumption. A description of the "t" test is presented in Appendix A.

6.1 INTRAPILOT VARIABILITY – FIXED-BASE SIMULATION

A number of configurations were repeated by each pilot throughout the fixed-base simulator investigation. Pilot C accomplished only a small number of these repeat configurations as his total number of configurations evaluated was considerably less than the other two pilots. Therefore, it is not practical to test his variability in this experiment. The repeat ratings of pilots A and B have been statistically analyzed. Configurations which the pilot rated 10 on each occasion were not included – there was no possibility for differences. One configuration was included for which ratings of 9 and 10 were given on the assumption that this is a valid comparison not yet affected by the rating scale bounds. Also, those configurations that were ostensibly repeats but were known to be different from the analysis of the simulated responses were not included (e.g., configurations 9 and 11 in Table 5).

The results of the analysis of the difference in ratings for the configurations repeated by pilots A and B are as follows:

Type of Rating	Pilot	Number of Configurations Evaluated Twice	Mean Difference in Ratings	"t" Value
Before Tracking	A	15	.03	.12
	B	11	.56	1.21
After Tracking	A	15	.17	.65
	B	11	.32	.49

None of the mean differences are significantly different from zero. Thus, based upon this statistical analysis, there were no significant differences in repeat ratings by either pilot for this fixed-base evaluation of various configurations rated from good to dangerous.

In addition to the above test of significance, it is important to know what the actual intrapilot rating variation is. This is indicated graphically in Figure 26 in which each pilot's first and second ratings are compared. The dashed line drawn for each comparison is the line for perfect agreement. There are two statistics which provide measures of the variability: 1) sample correlation coefficient, and 2) standard deviation about the line for perfect agreement. The sample correlation coefficient is a measure of the mutual relationship between two variables (for perfect correlation, $r = 1.0$). A discussion of this coefficient and the "t" test of its differences from a value of zero are presented in Appendix A. Standard deviation about the line for perfect agreement is an estimate of each pilot's variability as if he were repeating the valuation of a single configuration. It is assumed that the standard deviation is not a function of the numerical rating. The line of perfect agreement, for which the mean error between first and second ratings is zero, is the best estimate for the population and is the reference about which such standard deviations should be measured. The orthogonal standard deviation is the measure used here. That is, the variability is assumed to exist equally in both the first and second ratings. In calculating the standard deviation, the perpendicular distance from each point to the line of perfect agreement was used.

These measures of intrapilot variability are as follows:

Type of Rating	Pilot	Standard Deviation in Ratings	Sample Correlation Coefficient
Before Tracking	A	0.8	.85**
	B	1.1	.74**
After Tracking	A	0.7	.88**
	B	1.5	.44

**Significantly different from zero at the 1% probability level.

The standard deviations of pilot B's ratings are somewhat greater than those for pilot A. However, the effect of one point on a sample of this small size can be quite important. For example, there is some reason for neglecting the configuration which resulted in the greatest deviation in the ratings of pilot B. In the first evaluation of this configuration it was rated 3 and 4, before and after tracking, respectively, while in the repeat evaluation it was rated 6.5 and 8. This configuration was the first evaluated by pilot B after completing the three familiarization configurations described in Section II and was repeated during the second day of simulation. If the familiarization time was inadequate for this pilot, then this particular configuration could reasonably be omitted in this analysis. Such omission would result in a standard deviation for pilot B of 0.9 for before-tracking ratings and 1.3 for after-tracking ratings.

The sample correlation coefficients are all significant except the after-tracking ratings of pilot B. Elimination of the configuration discussed above from the data would increase the coefficient from 0.44 to 0.58, which is still not statistically significantly different from zero.

This latter measure of intrapilot variability, sample correlation coefficient, is more definitive than the "t" test of differences for this type of data. If there is a large variation in the differences between first and second ratings, then the "t" test tends to show no significant difference between ratings, but of itself it is no measure of variability. On the other hand, the correlation coefficient is directly reduced by large differences and is a direct indication of the variability in the data – the larger the coefficient, the less variability is present.

6.2 INTRAPILOT VARIABILITY – IN-FLIGHT SIMULATION

During the in-flight evaluations, pilot A repeated six configurations which had measured characteristics sufficiently close to the original configurations to be classified as true repeats. The first and second ratings for these configurations are compared in Figure 27.

Although insufficient data points are available for a significant statistical analysis, the variability is approximately that obtained in the fixed-base simulation as presented in the previous section.

6.3 INTERPILOT VARIABILITY – LONGITUDINAL EVALUATIONS

In the longitudinal flying qualities evaluation in the fixed-base simulator, pilot ratings were compared for those configurations rated by more than one pilot. Only those configurations known to be alike were included in the comparison, and configurations with ratings of 10 by more than one pilot were excluded as in the analysis of intrapilot variability.

The differences between the ratings of pilots A, B and C were examined for significant differences by means of the "t" test. It was assumed that each of the three possible comparisons was a separate experiment and therefore that the probability of error in the statement of significance was as stated. The results of this analysis of differences are as follows:

Type of Rating	Pilot Comparison	Number of Comparisons	Mean Difference in Ratings	"t" Value
Before Tracking	A-B	19	.01	.49
	A-C	13	-1.08	3.38**
	B-C	13	-0.81	2.30*
After Tracking	A-B	17	-1.15	2.36*
	A-C	13	-1.61	4.61**
	B-C	12	-.04	.07

* Significant difference at 5% probability level
** Significant difference at 1% probability level

No significant difference is indicated between the ratings of pilot A and pilot B as given before tracking, but there is a significant difference in these ratings after tracking. Pilots A and C demonstrate significant differences for both the before-tracking and after-tracking ratings. When pilots B and C are compared, a significant difference is noted in the before-tracking ratings, but no significant difference in the after-tracking ratings.

Although the significance test of differences does indicate the existence of interpilot variability, it does not provide a measure of variability, as discussed earlier in this section. The measure previously employed for intra-pilot variability, standard deviation about the line of perfect agreement, cannot be applied as a measure of interpilot variability. There is no basis, in this instance, for the assumption that the line of perfect agreement is the best estimate for the population. Rather, this is part of the information that is desired – the manner in which the data vary from the line of perfect agreement.

A method for investigating this aspect of the data is the use of sample regression lines or lines about which the summation of the squares of the deviations is the least (least squares fit). As indicated in Appendix A there are two regression lines that may be drawn for these comparisons of pilot ratings. These two regression lines are drawn in the comparison of all three pilots presented in Figure 28. Normally, a sample regression line is determined as a measure of the dependence of one variable on another, the independent variable. All variability is assumed to be in the dependent variable. For this comparison of pilot ratings, there is no independent variable. However, if each pilot's ratings are assumed in turn to be the independent variable, then two regression lines are obtained. These two possible linear fits to the data give an indication of the trend of one pilot's ratings with another. Use of the orthogonal least squares fit would provide a single line for indicating the trend of one pilot's ratings with another. However, the determination of this line requires knowledge of assumptions regarding the ratio of the standard

deviations in the two sets of data being compared. As estimates of intrapilot variability are available for only pilots A and B, the orthogonal least squares fit could be determined only for the two A vs. B comparisons of Figure 28. In any case, the orthogonal fit will be between the two least squares fits shown and generally will have a slope value near the mean of these two.

Each of the slopes of the regression lines (see Appendix A for definition) may be tested, via the "t" test, for its significant difference from the line of perfect agreement or a slope of 1.0. This test provides information as to how significant an indicated trend may be. The two sample regression line slopes are also directly related to the sample correlation coefficient – the correlation coefficient is the geometric mean of the two slopes as indicated in Appendix A. Thus, the more divergent the two sample regression lines, the smaller the sample correlation coefficient will be.

The results of the analysis of the comparison of the rating data from the three pilots are as follows:

Type of Rating	Pilot Comparison	Sample Correlation Coefficient	Sample Regression Lines: Slopes		"t" Value for Test of Significant Difference from Slope of 1.0	
			b_{yx}	b_{xy}	t_{yx}	t_{xy}
Before Tracking	A-B	.89**	1.001	.960	.96	1.02
	A-C	.94**	.771	1.266	4.88**	2.38**
	B-C	.84**	.822	1.170	3.20**	1.02
After Tracking	A-B	.70**	.814	1.124	1.77	1.52
	A-C	.87**	.712	1.353	3.55**	1.05
	B-C	.65*	.935	.969	1.66	1.26

* Significant at 5% probability level
** Significant at 1% probability level

Regression lines (solid) are drawn on Figure 28 for each comparison along with the line of perfect agreement (dashed). From this figure and the above table, several inferences may be drawn as to the rating differences between these pilots. In the before-tracking ratings, there are strong indications that pilot C is rating poor configurations worse than either pilots A or B. This is indicated by the reduction from 1.0 in the slopes of the regression lines in the comparisons A vs. C and B vs. C of Figure 28. It is also indicated in the "t" test of these slopes in the above table. In both of these comparisons the regression lines are on either side of the line for perfect agreement at a pilot rating of 2, but are well below this line at poorer ratings. This trend is less definite in the comparison of pilots B and C, both from inspection of the plotted data and from the test of the slopes of the two least squares fit lines. Only one of the two values of slope is significantly different from 1.0.

In the after-tracking ratings, an increase in variability of the data of pilot B is evident from the scatter of the plotted ratings in the comparisons of pilot B with pilots A and C. There is a resulting marked decrease in the sample correlation coefficients for these two comparisons. On the other hand, the after-tracking rating comparison of pilots A and C indicates little increase in scatter and correspondingly little change in correlation coefficient. There is still some indication that pilot C is rating poor configurations worse than pilot A, but no similar trend is apparent in comparing pilot C with pilot B. Additional evidence of differences between pilots in the after-tracking ratings is the translation of the ratings away from the line of perfect agreement when pilots B and C are compared with pilot A. That is, pilots B and C were apparently rating all configurations worse, on the average, after tracking.

An analysis was performed to determine directly the effect of the tracking maneuver on pilot ratings for the longitudinal configurations considered in the interpilot comparisons. The mean differences in before- and after-tracking ratings were determined and these differences were tested for significance. These differences were also examined to determine if they were correlated with before-tracking ratings. The results of this analysis of the before- and after-tracking differences are as follows:

Pilot	Number of Configurations	Mean Difference in Ratings (After-Tracking) minus (Before-Tracking)	"t" Values for Mean Differences	Sample Correlation Coefficient – Difference versus Before-Tracking Rating
A	24	.10	1.49	-.09
B	17	1.29	3.64**	-.06
C	15	.87	3.78**	-.07

** Significantly different from zero at the 1% probability level

Pilots B and C increased (worsened) their ratings significantly while pilot A made no significant change in ratings as a result of the tracking maneuver. The sample correlation coefficients, although not significant, are consistent in that each has a negative sign indicating some tendency for a decrease in difference with increasing before-tracking rating. This tendency is apparent in Figure 29. The tracking task may serve as a more useful additional task for the better configurations. These configurations may possess more subtle discrepancies in control characteristics that are not evident to these pilots in their self-induced maneuvers. On the other hand, configurations approaching the unflyable category have sufficiently gross discrepancies that are readily apparent even in the pilot-induced maneuvers.

6.4 INTERPILOT VARIABILITY – LATERAL-DIRECTIONAL EVALUATIONS

In the lateral-directional flying qualities evaluation in the fixed-base simulator, only pilots A and B were used. The differences between these pilots were analyzed as in the longitudinal evaluations with the following results:

Type of Rating	Pilot Comparison	Number of Comparisons	Mean Difference in Ratings	"t" Value
Before Tracking	A-B	32	.31	1.29
After Tracking	A-B	32	-.22	.91

The indicated differences between these two pilots are not significant. The mean difference is somewhat larger for before-tracking and somewhat smaller for after-tracking ratings as compared with the longitudinal evaluations.

Rating data for these two pilots are compared in Figure 30. The results of the analysis of this comparison are as follows:

Type of Rating	Pilot Comparison	Sample Correlation Coefficient	Sample Regression Lines Slopes		"t" Value for Test of Significant Difference from slope = 1.0	
			b_{yx}	b_{xy}	t_{yx}	t_{xy}
Before Tracking	A-B	.80**	.817	.793	1.71	1.94
After Tracking	A-B	.84**	.760	.932	2.93**	.62

** Significant at 1% probability level.

Regression lines (solid) are drawn on Figure 30 for each comparison along with the line of perfect agreement (dashed). In this figure and the above analysis of the comparison of pilots A and B, there is little indication of any consistent differences. In the after-tracking ratings, there is a slight tendency for pilot B to rate poor configurations worse than pilot A. This is indicated by the significant difference from 1.0 of one of the least squares line slopes and the location of the lines of least squares with respect to the line of perfect agreement. Even this slight tendency is not apparent in the before-tracking ratings.

SECTION 7
CONCLUSIONS

The conclusive results of the ground and flight simulation programs reported herein may be summarized in the items listed below.

A. Ground Simulator Evaluation

1. For the particular two-axis side controller used in this experiment, the pilot-selected control sensitivities in terms of applied aileron and elevator stick force agree closely to values previously obtained during in-flight evaluations with a center stick. The pilots were quite tolerant of a wide range of rudder pedal control sensitivities. Sensitivities higher than optimum evoked a sharper reduction in rating than did insensitive rudder pedals.

2. The pilot is quite tolerant of off-optimum control sensitivites for the re-entry mission, but the desired control sensitivities agree well with control sensitivities selected in other experiments for the fighter mission.

3. The pilot requirements of longitudinal short period dynamics for re-entry are less stringent than for the fighter mission.

4. For $\omega_{sp}^2 > 4$ 1/sec^2, and with $(n_z/\alpha)_{ss} = 22$ g/rad, positive longitudinal short period damping ($2\zeta_{sp}\omega_{sp}$) was required in the ground simulator for minimum controllable handling characteristics when the lateral-directional handling characteristics were good. In the most desirable range of ω_{sp}^2 ($10 < \omega_{sp}^2 < 22$ 1/sec^2) the pilots considered zero damping ($2\zeta_{sp}\omega_{sp}$) to be controllable; but above and below this range of ω_{sp}^2, they required positive damping.

5. For $2\zeta_{sp}\omega_{sp} > 0.5$ 1/sec, and with $(n_z/\alpha)_{ss} = 22$ g/rad, a positive maneuver margin (positive ω_{sp}^2) was required for controllability when the lateral-directional handling characteristics were good. This result conflicts with the results of earlier investigations for different missions than re-entry.

6. In the region of short period dynamics where $\omega_{sp}^2 < 4$ 1/sec^2 and $2\zeta_{sp}\omega_{sp} < 0.5$ 1/sec, the pilot's requirements for controllability are more restrictive in terms of ω_{sp}^2 and $2\zeta_{sp}\omega_{sp}$. The scope of the simulation experiment was not sufficient to establish a definite boundary in this region, but for $(n_z/\alpha)_{ss} = 22$ g/rad, a straight-line boundary:

$$\omega_{sp}^2 + 8(2\zeta_{sp}\omega_{sp}) = 4$$

is proposed for consideration.

7. An investigation by one pilot of the effects of $(n_z/\alpha)_{ss}$ on the short period evaluations showed a definite, though not large, effect over the limited range of $(n_z/\alpha)_{ss}$ examined. A trend of improved rating of low ω_{sp}^2, low $2\zeta_{sp}\omega_{sp}$ configurations was

noted at the smallest value of $(n_z/\alpha)_{ss}$ tested. Thus it has been shown that rating boundaries are functions of $(n_z/\alpha)_{ss}$, or L_α, as well as of ω_{sp}^2 and $2\zeta_{sp}\omega_{sp}$ for any one mission. The reported investigation was not of sufficient scope to establish the minimum controllable boundaries as a function of $(n_z/\alpha)_{ss}$.

8. Pilot evaluations of re-entry flying qualities for a range of lateral-directional handling characteristics were somewhat inconclusive. For relatively constant values of a lumped parameter, $\frac{(\omega_\phi/\omega_d)^2-1}{|\phi/\beta|}$, pilot rating is shown to be a strong function of Dutch roll damping ratio, ζ_d. The importance of ζ_d has been firmly established by many prior investigations, and is confirmed here. There remains, at any one value of ζ_d, a significant range of variation in pilot rating which cannot be attributed to its individual causative effects due to the nature of the reported experiment.

9. Analysis of the repeatability of two pilots in rating configurations which had a range of ratings throughout the rating scale showed no significant differences in repeat ratings by either pilot.

10. In the interpilot comparisons, the agreement is excellent as to effects of specific parameters on the over-all suitability for performance of the specified mission, although statistically significant differences in ratings did exist between pilots.

B. In-Flight Evaluations

1. In the evaluations of short period dynamics for the re-entry mission, the pilot tended to rate similar handling characteristics the same or better in flight than in the fixed-base ground simulator. In one region, $\omega_{sp}^2 = 2\ 1/sec^2$, $2\zeta_{sp}\omega_{sp} = 0.5\ 1/sec$, the opposite was true: the pilot consistently rated configurations better in the fixed-base simulator than in flight.

2. Variations in $(n_z/\alpha)_{ss}$ were made in flight in a different manner than in the ground simulator, and produced somewhat different results. The major difference was again in the region of short period dynamics, $\omega_{sp}^2 = 2\ 1/sec^2$, $2\zeta_{sp}\omega_{sp} = 0.5\ 1/sec$, and amounted to a distinctly different trend of pilot rating with $(n_z/\alpha)_{ss}$. Additional evaluations are needed in this area of flying qualities, which is related to many missions such as re-entry, re-fueling, high-altitude reconnaissance, landing, take-off, etc. It appears from this study that, in this region of short period dynamics, ground simulator evaluation data is subject to significant errors and may lead to erroneous conclusions if not verified by flight evaluation.

3. Evaluation and rating of minimum longitudinal handling characteristics are strongly dependent upon:

a. The conditions under which the pilot encounters the poor characteristics. A configuration encountered without

initial transients presents less difficulty.

b. The amount of training which the pilot has had in the subject characteristics – his preparedness for them.

c. The external disturbances which are present to excite the configuration.

d. The amount of concentration required for other piloting or management tasks.

e. The length of time which the condition must be controlled.

f. The task which must be performed, including the control precision required.

g. The state of anxiety of the pilot.

4. Pilot comment data suggests that proprioceptive cues of flight may not account for all the differences between flight and ground simulator results. Some difference may be due to the acute awareness in flight of the structural limitations of the aircraft, and the consequential change in control characteristics of the pilot.

5. A high-fidelity fixed-base ground simulator is a useful device in handling qualities research for defining the problem through preliminary examination of handling qualities under consideration, for bounding the areas of principal interest, and for generation of pilot comment and rating data to aid in the design of subsequent flight verification experiments.

REFERENCES

1. Snedecor, G. W.: Statistical Methods. The Iowa State College Press, Ames, Iowa. 1959.

2. Dixon, W. J. and Massey, F. J., Jr.: Introduction to Statistical Analysis. McGraw-Hill Book Company, Inc., New York, N.Y., 1957.

3. Flight Research Department: Installation of An Automatic Control System in a T-33 Airplane for Variable Stability Flight Research – Part I - Preliminary Investigation and Design Studies: Wright Air Development Center Technical Report 55-156, Part I. April 1955. (Also published as Cornell Aeronautical Laboratory Report No. TB-936-F-1.)

4. Flight Research Department: Installation of An Automatic Control System in a T-33 Airplane for Variable Stability Flight Research – Part II - Detail Design, Fabrication and Installation. Wright Air Development Center Technical Report 55-156, Part II. September 1956. (Also published as Cornell Aeronautical Laboratory Report No. TB-936-F-2)

5. Beilman, J. L. and Harper, R. P., Jr.: Installation of An Automatic Control System in a T-33 Airplane for Variable Stability Flight Research – Part III - Ground and Flight Checkout. Wright Air Development Center Technical Report 55-156, Part III. August 1957. (Also published as Cornell Aeronautical Laboratory Report No. TB-936-F-3.)

6. Infanti, N. L.: Augmented Capabilities of the Variable Stability T-33 Airplane for Ground and Flight Handling Qualities Evaluations. Cornell Aeronautical Laboratory Report No. TE-1234-F-1. November 1960.

7. Jex, H. R. and Cromwell, C. H., III: Theoretical and Experimental Investigation of Some New Longitudinal Handling Qualities Parameters. Aeronautical Systems Division Technical Documentary Report No. 61-26, June 1962.

8. Harper, R. P., Jr.: In-Flight Simulation of the Lateral-Directional Handling Qualities of Entry Vehicles. Wright Air Development Division Technical Report No. 61-147. February 1961. (Also published as Cornell Aeronautical Laboratory Report No. TE-1234-F-2.)

9. Bull, Gifford: Minimum Flyable Longitudinal Handling Qualities of Airplanes. Cornell Aeronautical Laboratory Report No. TB-1313-F-1. December 1959.

10. Sadoff, M.; McFadden, N. M.; and Heinle, D. R.: A Study of Longitudinal Control Problems at Low and Negative Damping and Stability with Emphasis on Effects of Motion Cues. NASA TN D-348. January 1961.

11. Chalk, C. R.: Additional Flight Evaluations of Various Longitudinal Handling Qualities in a Variable-Stability Jet Fighter, Part II. Wright Air Development Center Technical Report 57-719, Part II. July 1958. (Also published as Cornell Aeronautical Laboratory Report No. TB-1141-F-2.)

12. McFadden, N. M.; Vomaske, R. P.; and Heinle, D. R.: Flight Investigation Using Variable-Stability Airplanes of Minimum Stability Requirements for High-Speed, High-Altitude Vehicles. NASA Technical Note D-779. April 1961.

13. Taylor, L. W., Jr. and Day, R. E.: Flight Controllability Limits and Related Human Transfer Functions as Determined from Simulator and Flight Tests. NASA Technical Note D-746. May 1961.

14. Boneau, C. Alan: The Effects of Violations of Assumptions Underlying the "t" Test. Psychological Bulletin, Volume 97, No. 1. 1960.

15. Reynolds, P. A.: Ground Measurements of Torques Applied to a Three-Axis Side Located Aircraft Controller. Cornell Aeronautical Laboratory Report FDM No. 298. 31 July 1959.

16. Ashkenas, I. L. and McRuer, D. T.: The Determination of Lateral Handling Quality Requirements from Airframe-Human Pilot System Studies. Wright Air Development Center Technical Report 59-135. June 1959.

17. Cooper, George B.: Understanding and Interpreting Pilot Opinion. Aero Engineering Review. Vol. 16, No. 3, March 1957.

18. Harper, Robert P., Jr.: Flight Evaluations in Variable-Stability Airplanes of Elevator Control Motion Gradients for High Speed Bombers. Wright Air Development Center Technical Report 56-258. November 1956. (Also was published as Cornell Aeronautical Laboratory Report No. TB-969-F-2.)

19. Gowin, N.E.: Lateral Stability Investigation of an F-100A Airplane. Wright Air Development Center Technical Report 57-563, November 1957. (Also published as Cornell Aeronautical Laboratory Report No. TB-593-F-5).

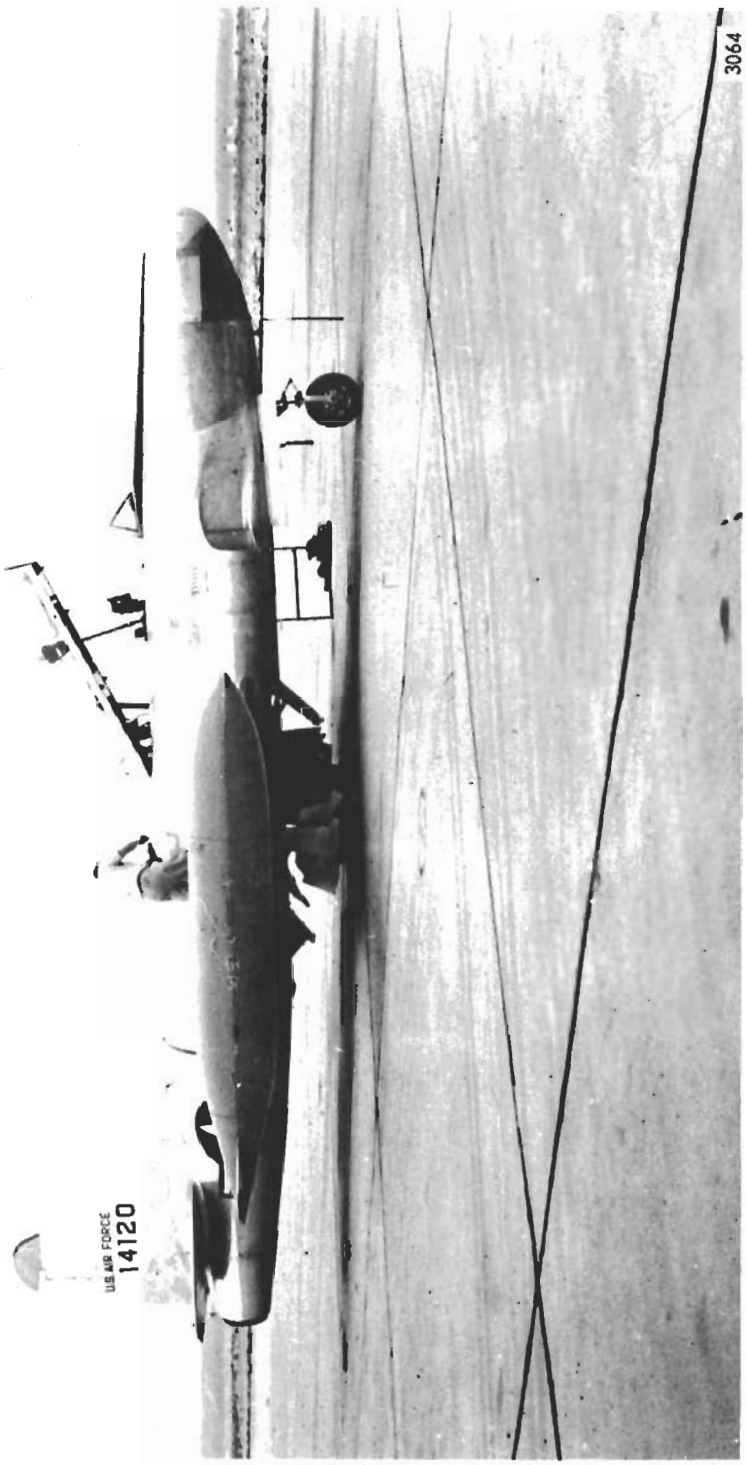

FIGURE 1 T-33 VARIABLE STABILITY AIRPLANE

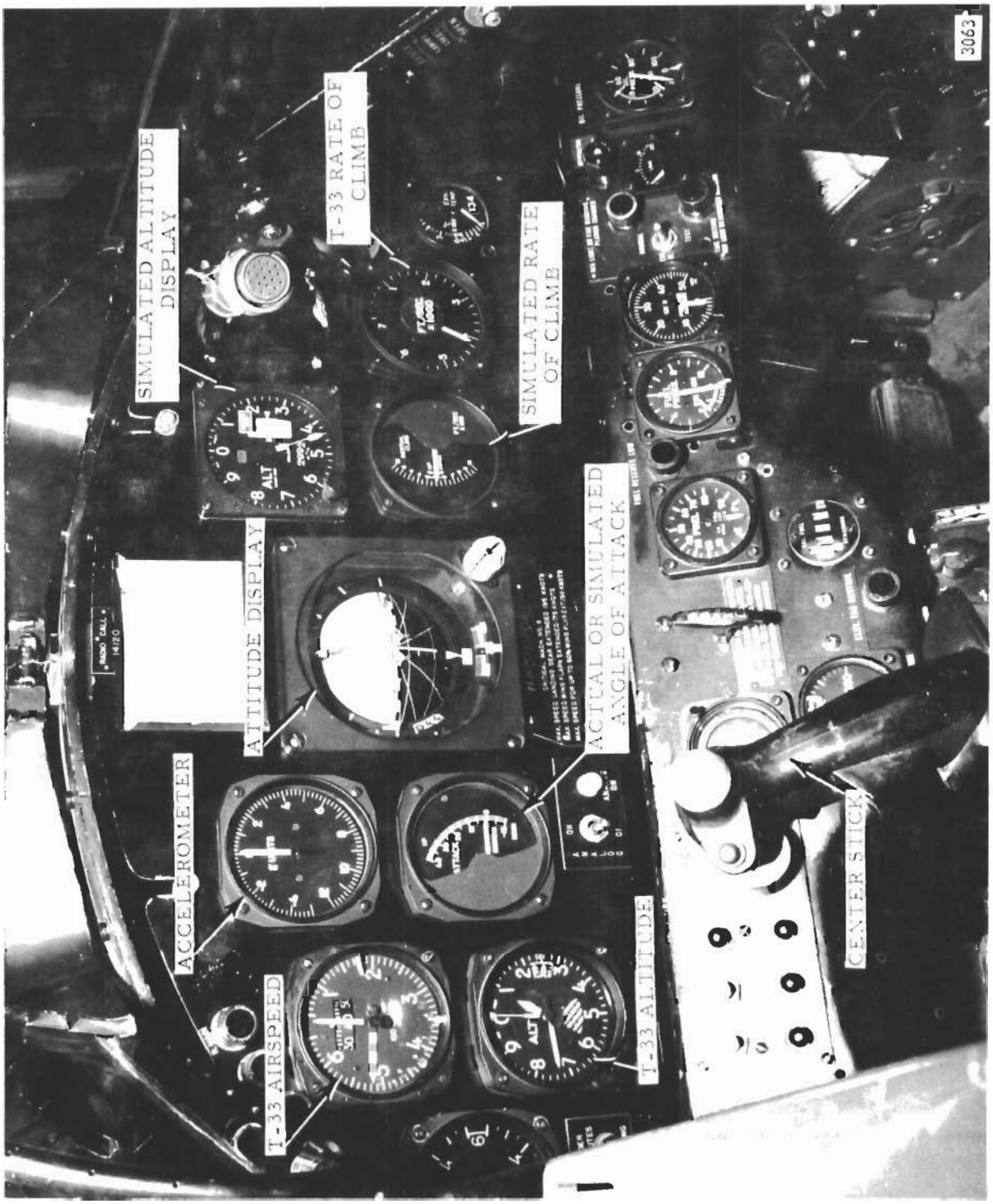

FIGURE 2 EVALUATION PILOT'S INSTRUMENT PANEL

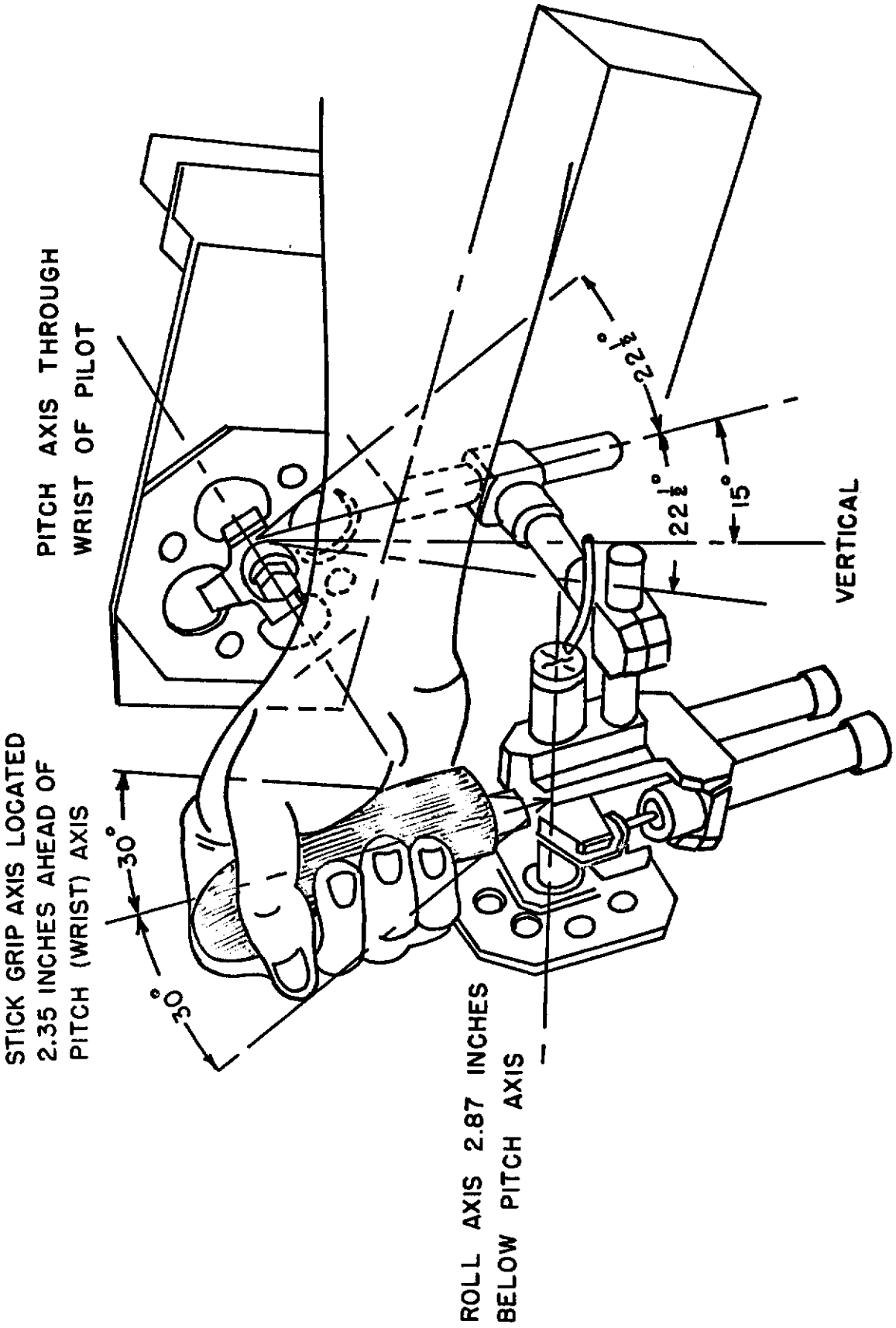

FIGURE 3 VARIABLE STABILITY T-33 TWO-AXIS SIDE STICK CONTROLLER

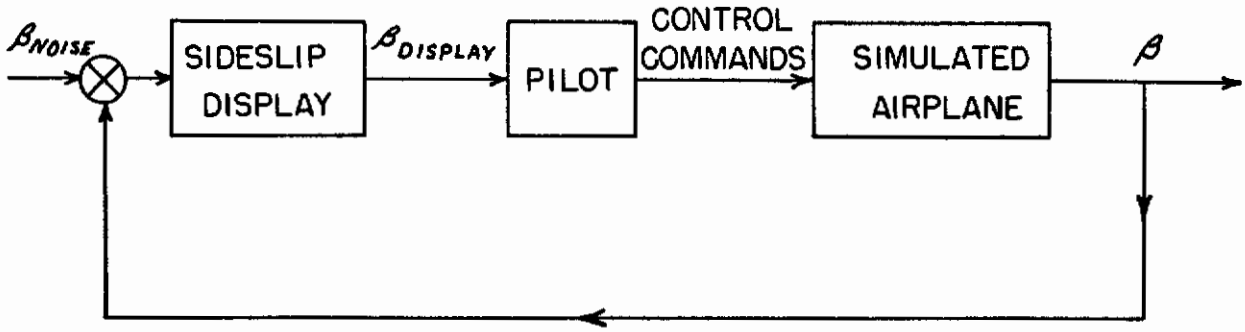

a) Sideslip Display Tracking Loop

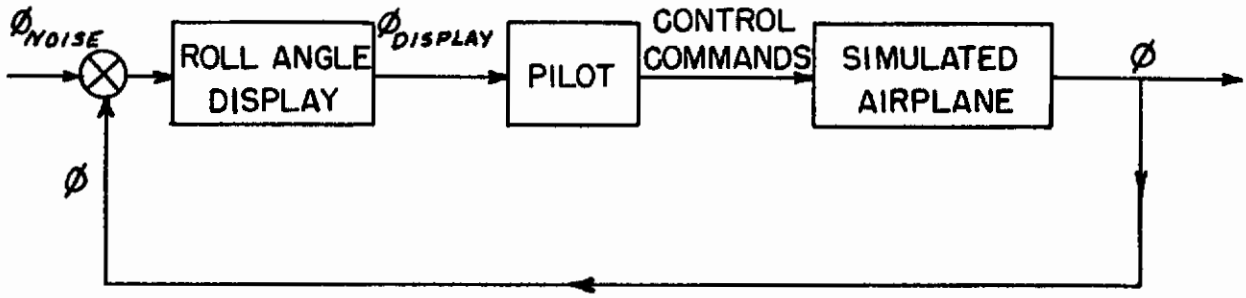

b) Bank Angle Display Tracking Loop

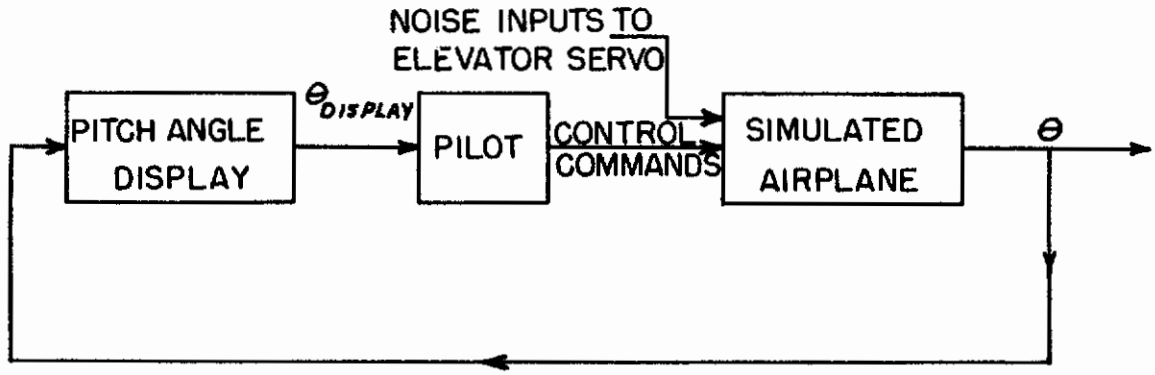

c) Pitch Attitude Display Tracking Loop

FIGURE 4 BLOCK DIAGRAM REPRESENTATION OF THE TRACKING MANEUVER INCLUDING THE MANNER OF INSERTING THE NOISE DISTURBANCE

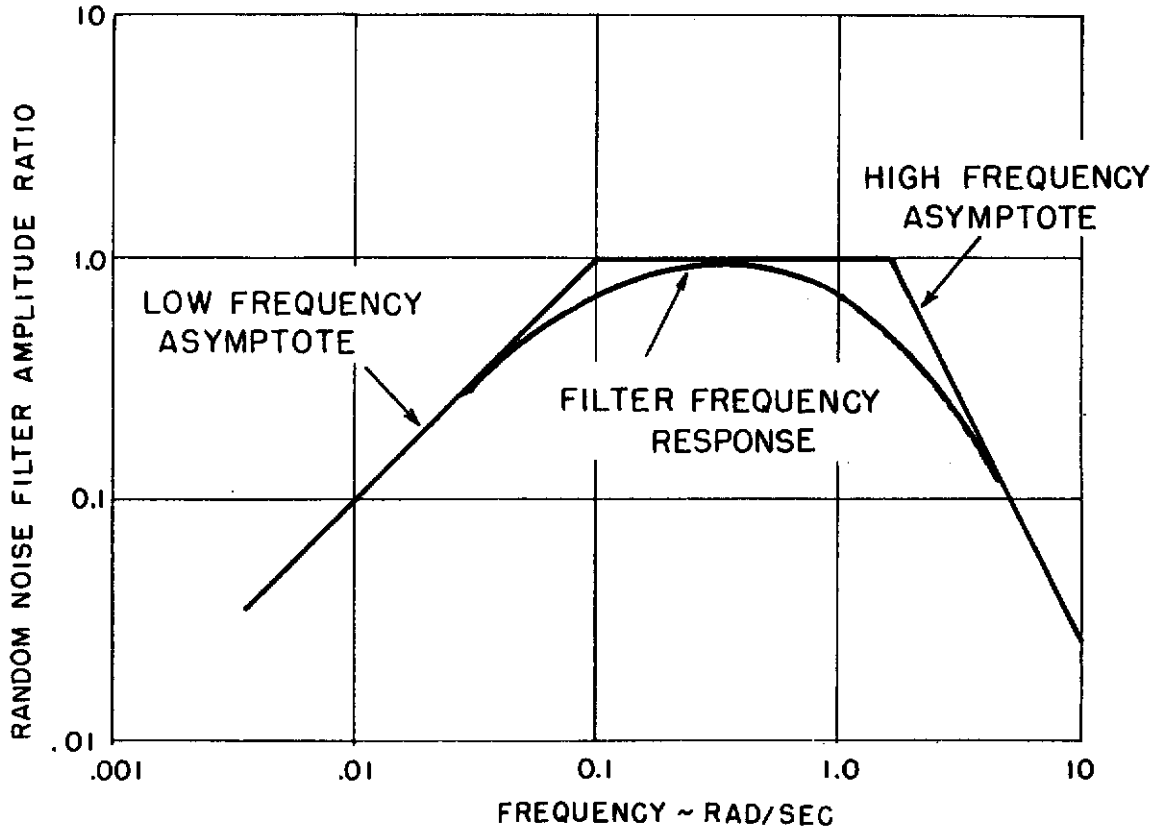

FIGURE 5 RANDOM NOISE FILTER FREQUENCY RESPONSE

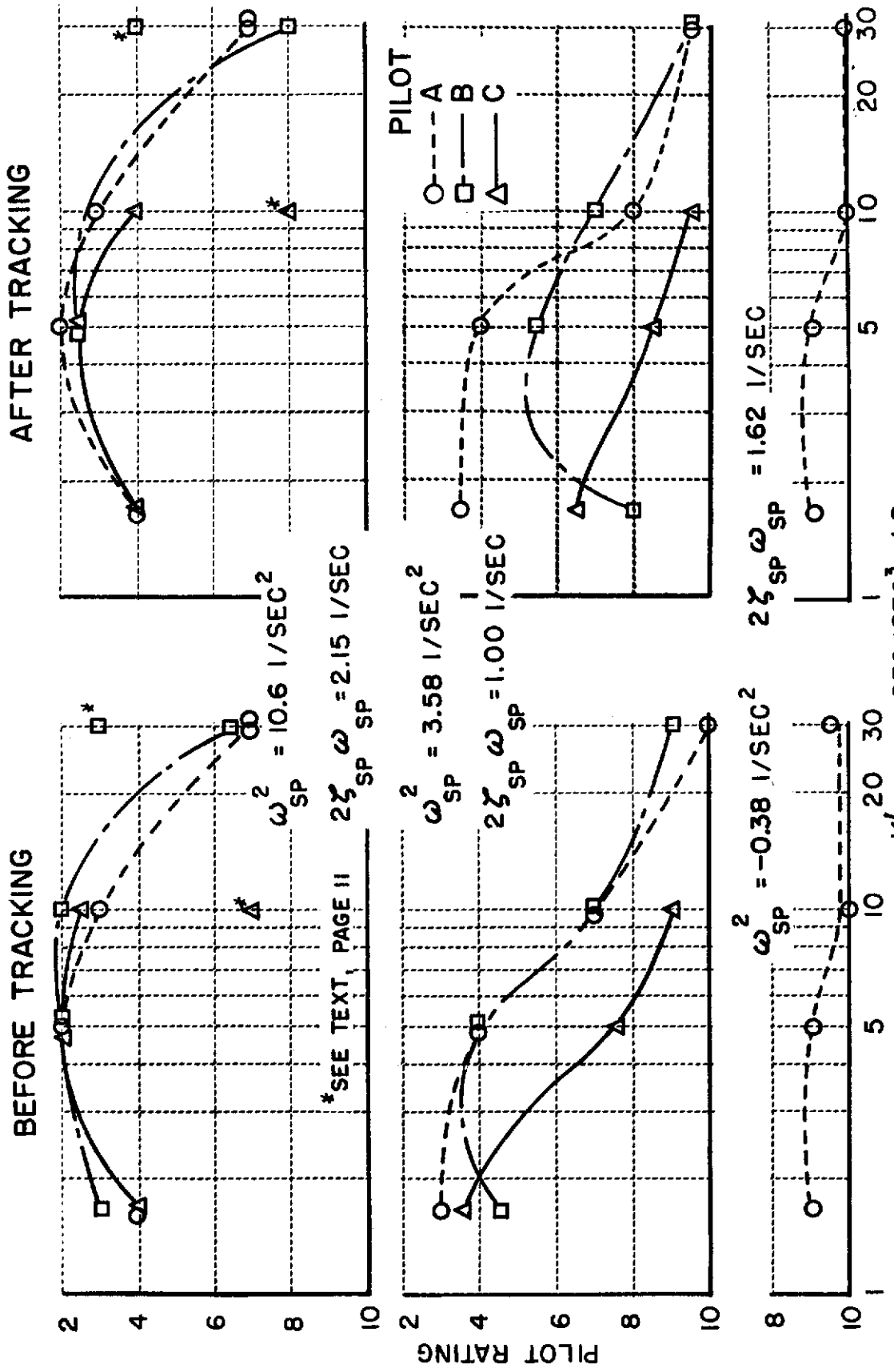

FIGURE 6 PILOT RATING VERSUS GAIN OF PITCH RESPONSE

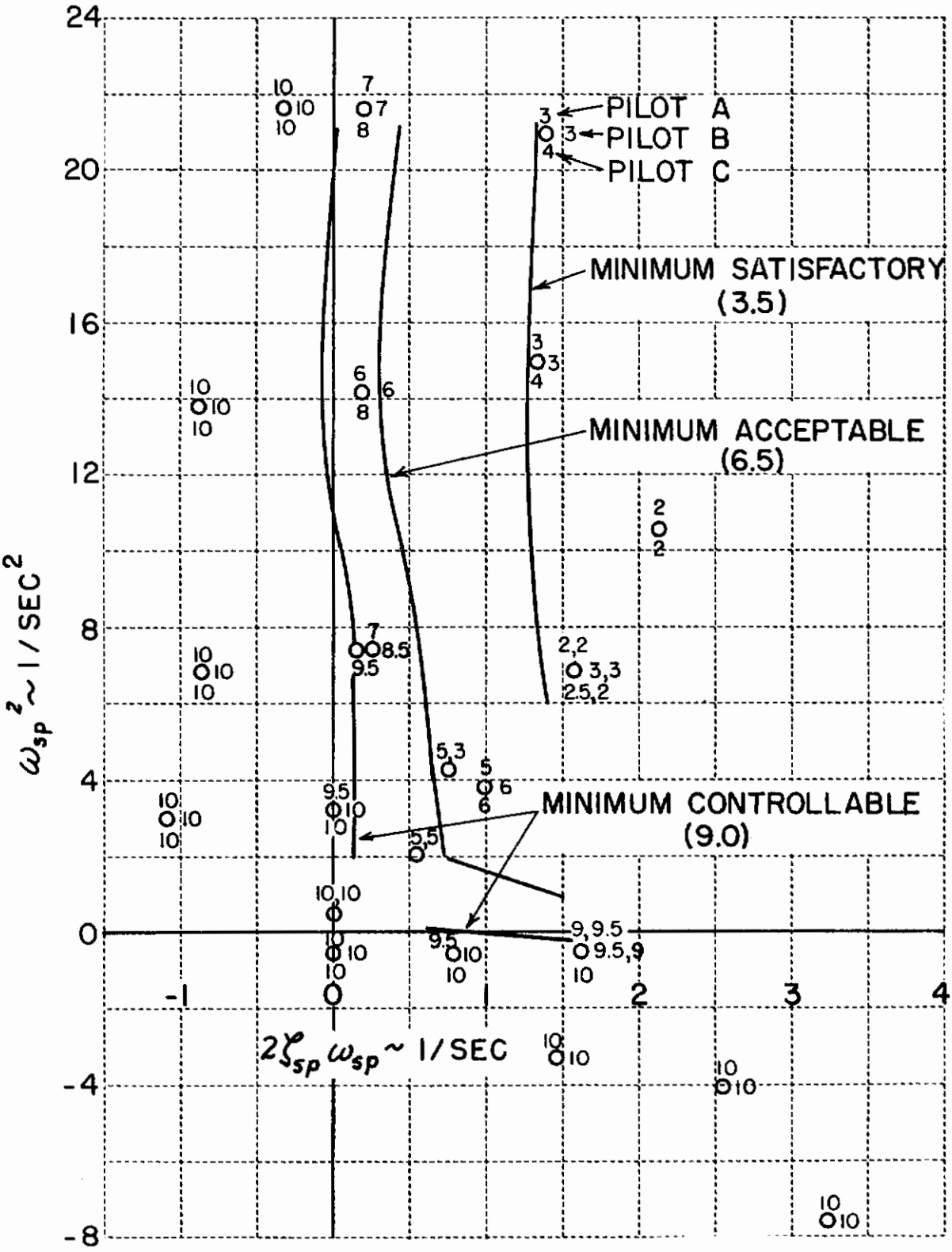

FIGURE 7 PILOT RATINGS OF LONGITUDINAL SHORT PERIOD DYNAMICS IN FIXED-BASE SIMULATOR
(a) Before Tracking

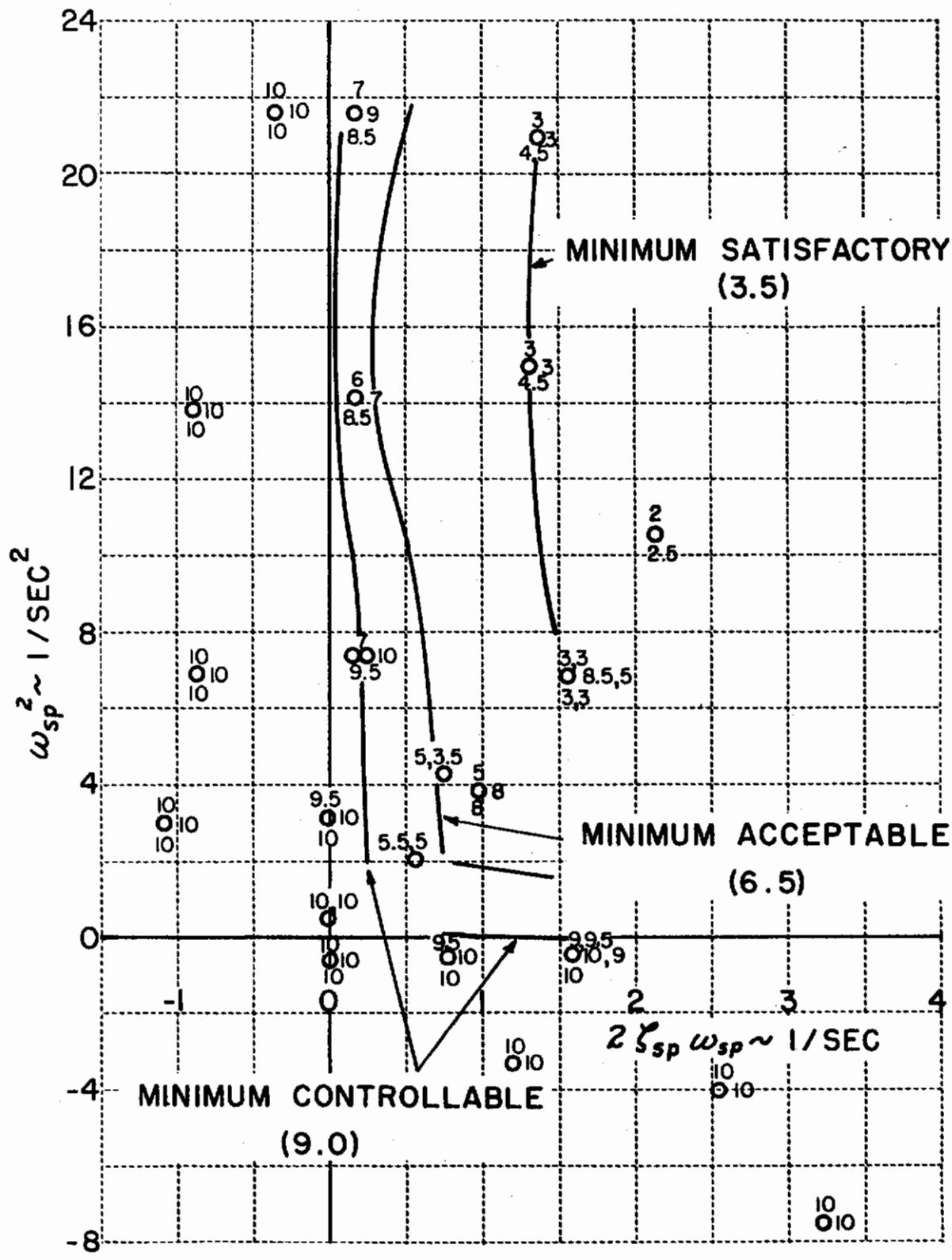

FIGURE 7 PILOT RATINGS OF LONGITUDINAL SHORT PERIOD DYNAMICS IN FIXED-BASE SIMULATOR
(b) After Tracking

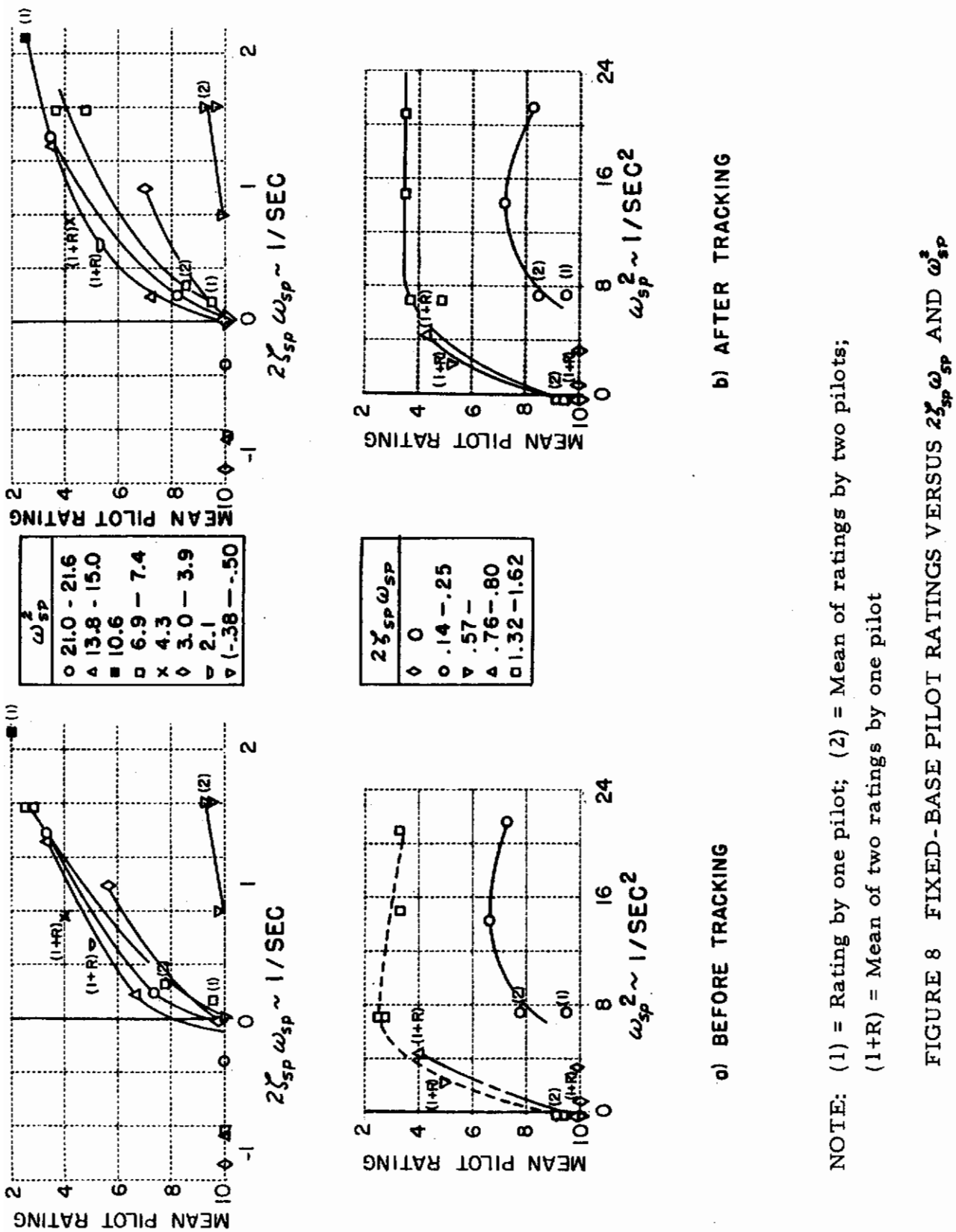

NOTE: (1) = Rating by one pilot; (2) = Mean of ratings by two pilots;
(1+R) = Mean of two ratings by one pilot

FIGURE 8 FIXED-BASE PILOT RATINGS VERSUS $2\zeta_{sp}\omega_{sp}$ AND ω_{sp}^2

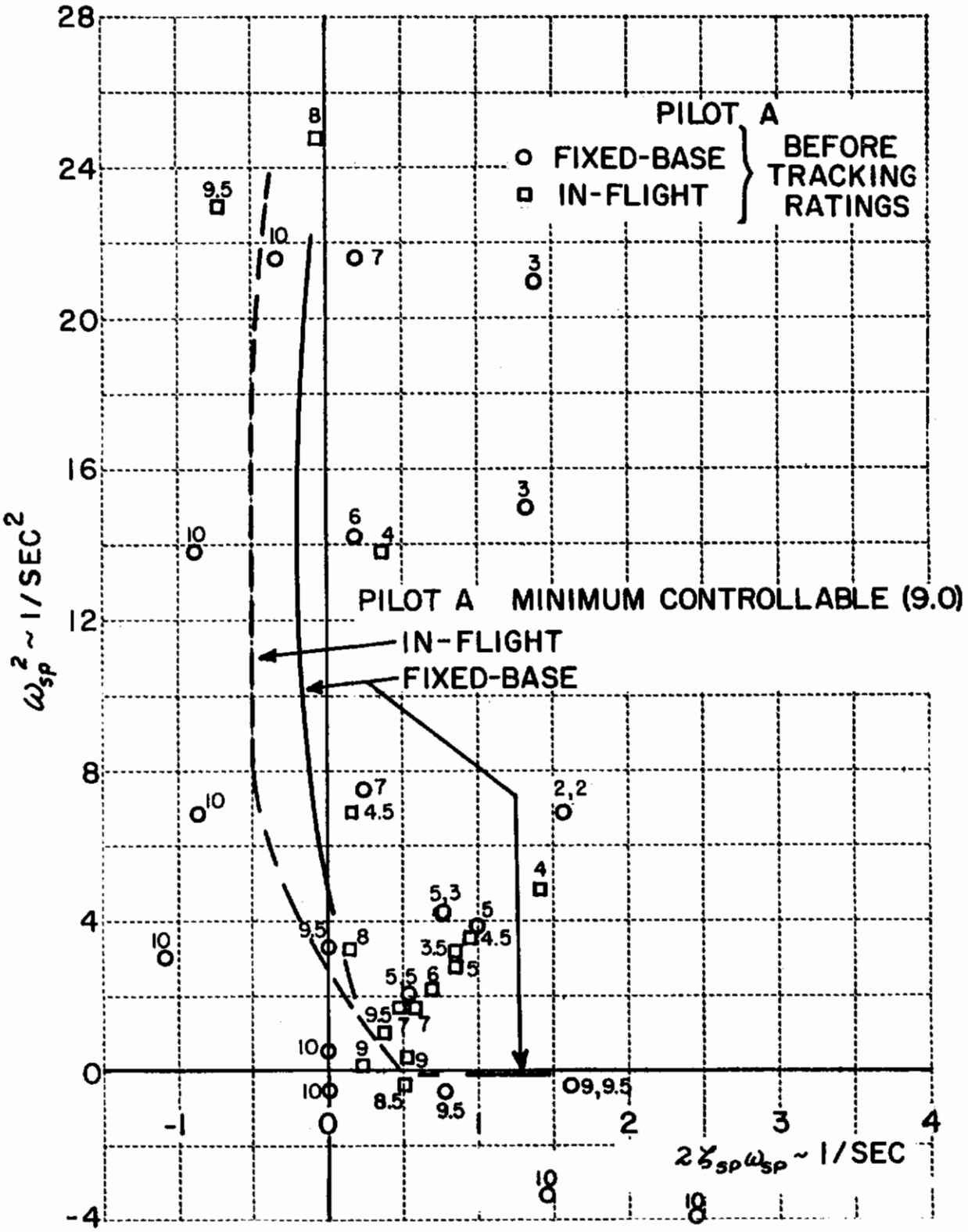

FIGURE 9 IN-FLIGHT AND SIMULATOR RATINGS FOR LONGITUDINAL EVALUATIONS

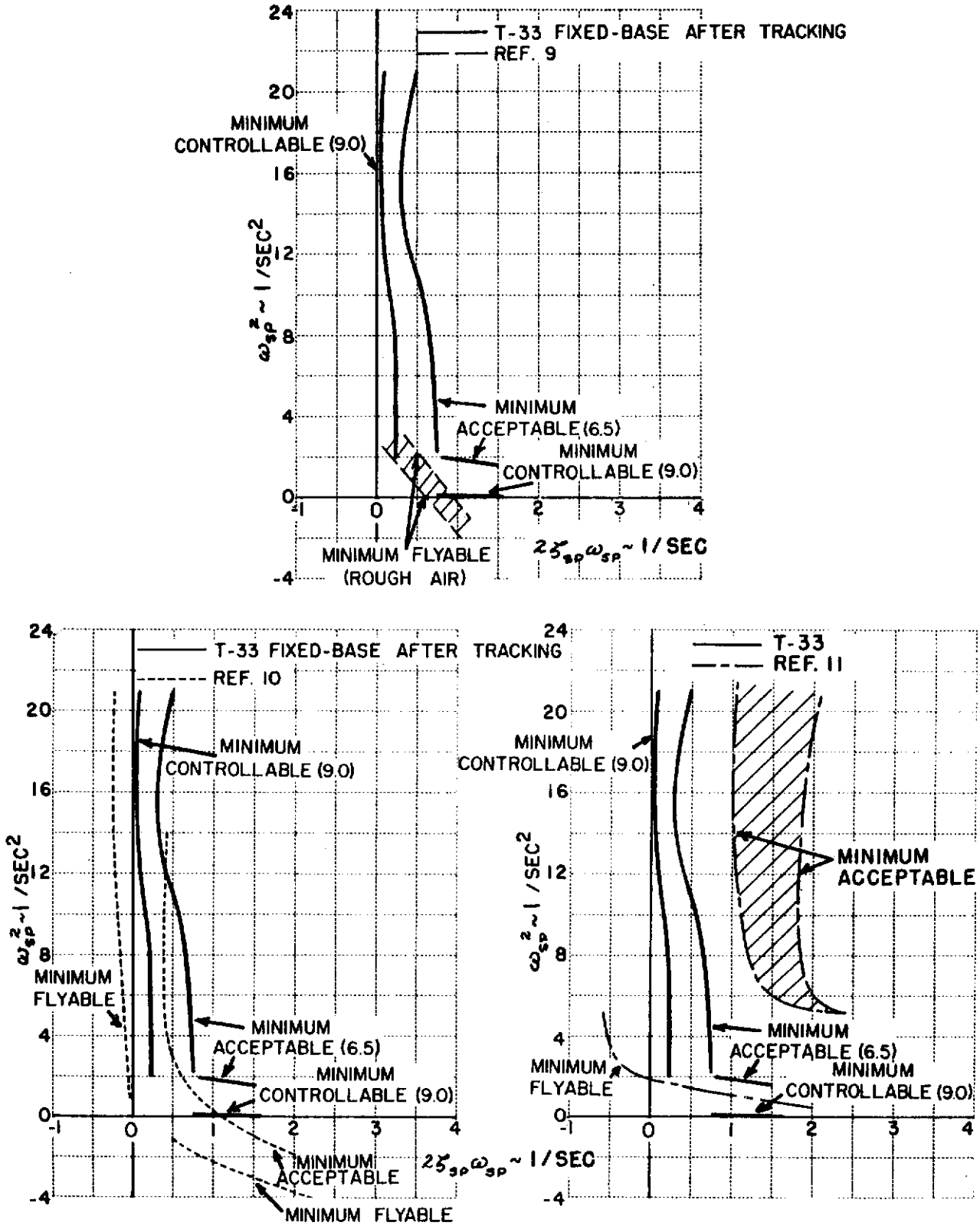

FIGURE 10 RATING BOUNDARY COMPARISONS

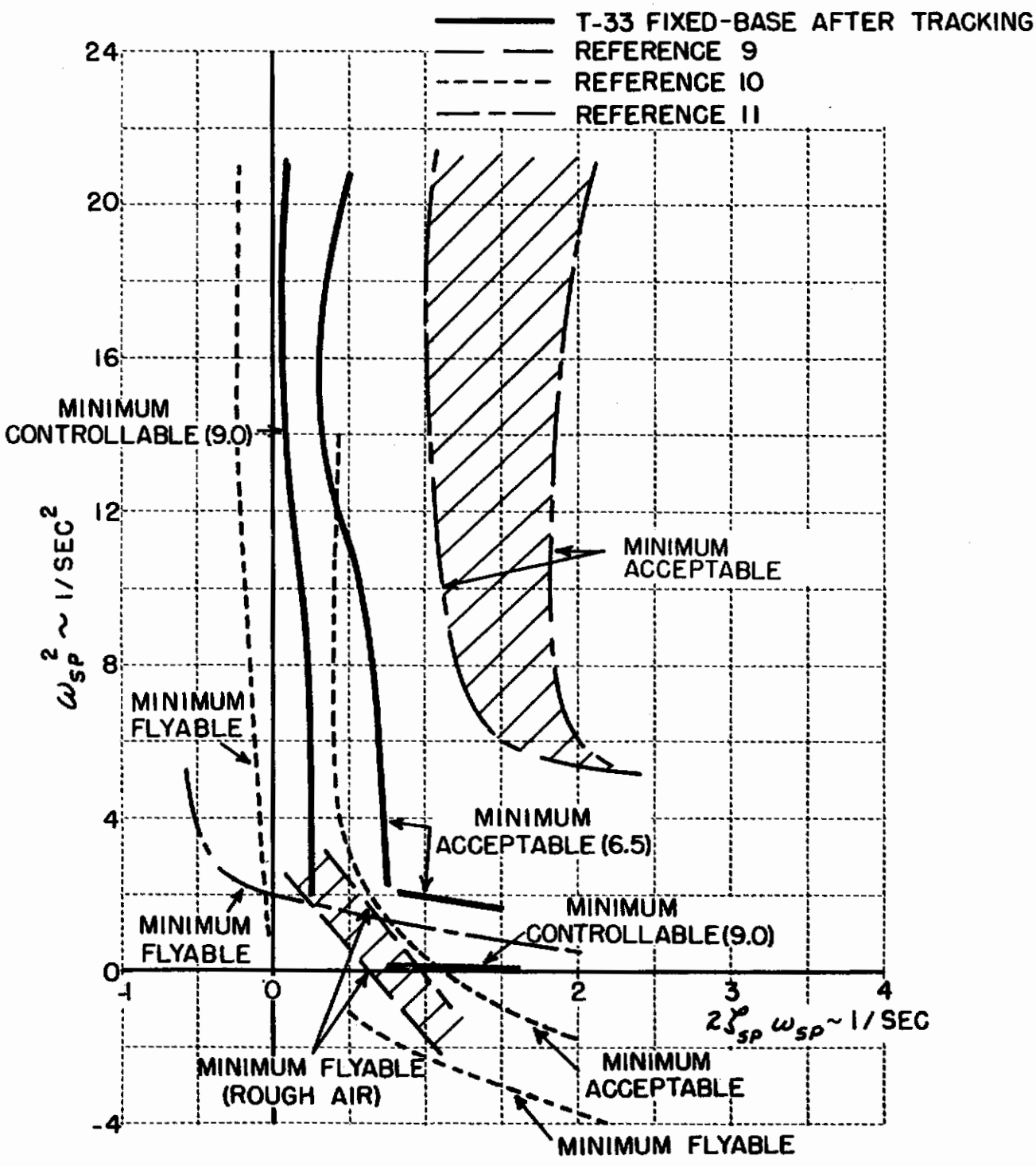

FIGURE 11 SUMMARY OF RATING BOUNDARY COMPARISONS

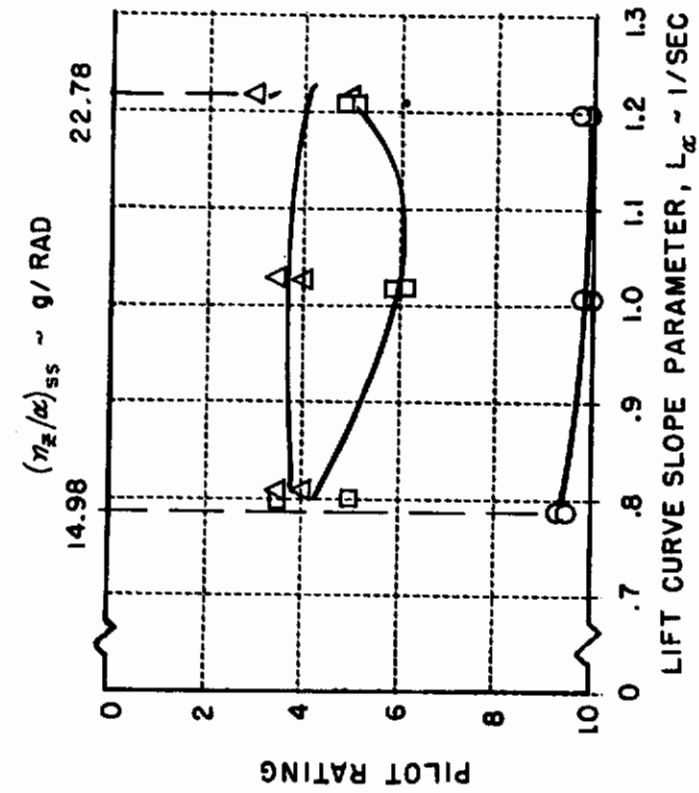

(a) Before Tracking

(b) After Tracking

SYMBOL	CONFIGURATIONS	ω_{sp}^2 ~ 1/SEC^2	$2\zeta_{sp}\omega_{sp}$ ~ 1/SEC
○	86, 86a, 87, 87a, 88, 88a	-.36 TO 1.12	0 TO .15
□	89, 89a, 90, 90a, 91, 91a	2.11	.57
△	92, 92a, 93, 93a, 94, 94a	4.33	.76

FIGURE 12 FIXED-BASE SIMULATOR PILOT RATINGS VERSUS LIFT CURVE SLOPE PARAMETER

$\omega_{sp}^2 = 3.61 \ 1/SEC^2$

$2\zeta_{sp}\omega_{sp} = 1.04 \ 1/SEC$

$\omega_{sp} = 1.90 \ 1/SEC$

$\zeta_{sp} = .30$

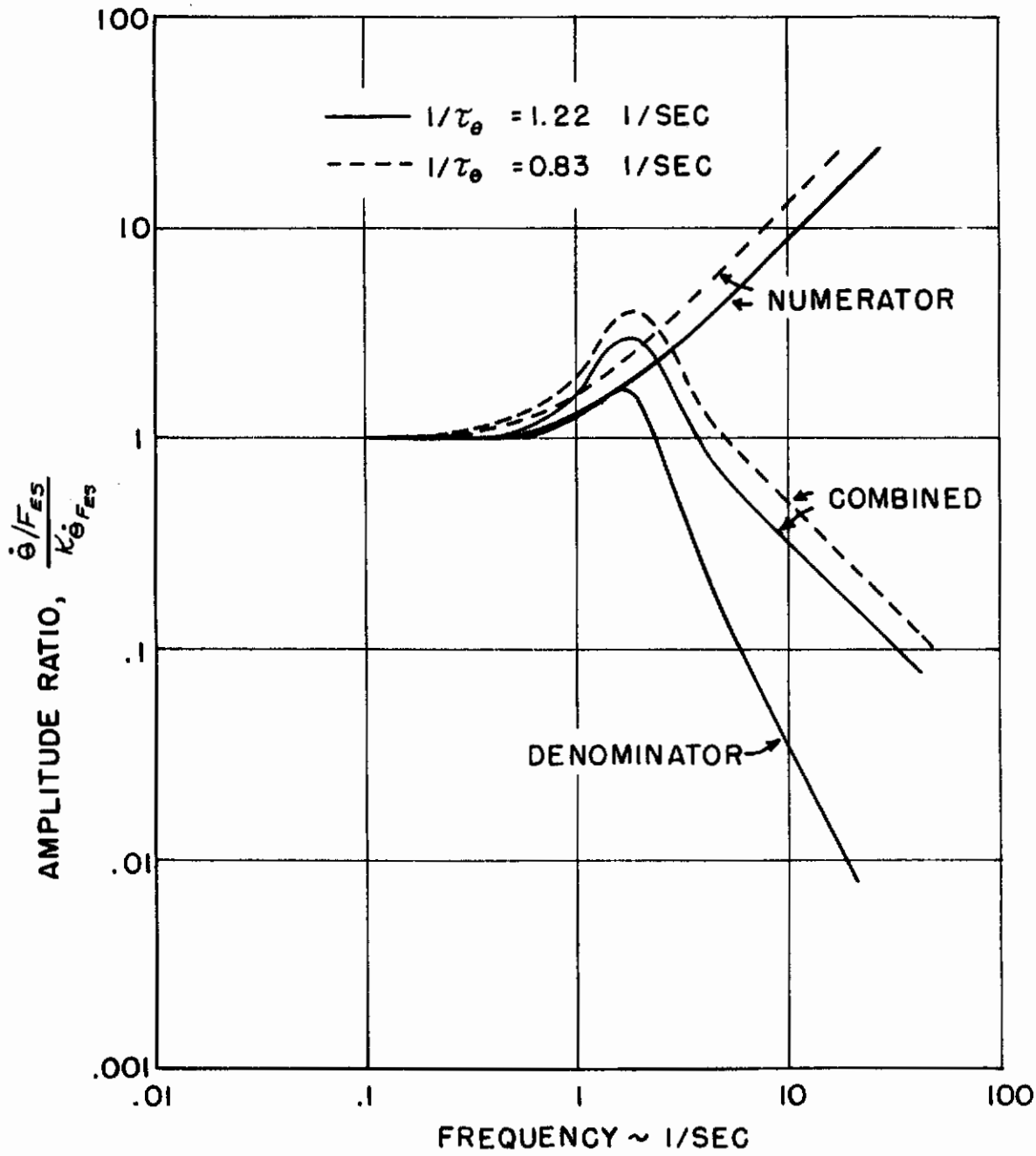

FIGURE 13 EFFECTS OF $1/\tau_\theta$ ON PITCH RATE FREQUENCY RESPONSE FOR CONSTANT SHORT PERIOD DYNAMICS

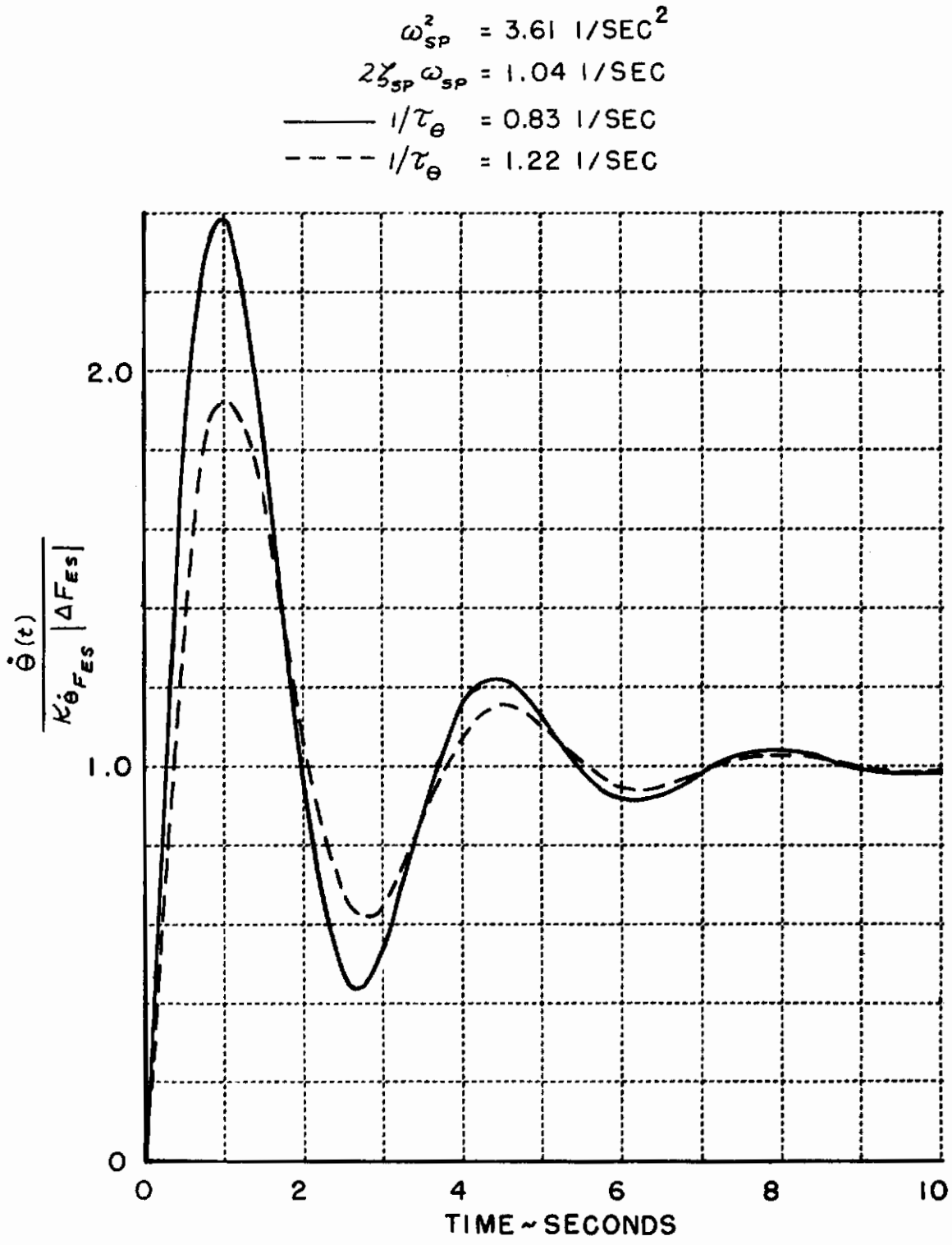

FIGURE 14 EFFECT OF $1/\tau_\theta$ ON PITCH RATE RESPONSE, $\dot{\theta}(t)$, TO ELEVATOR STICK FORCE STEP INPUT, ΔF_{ES}

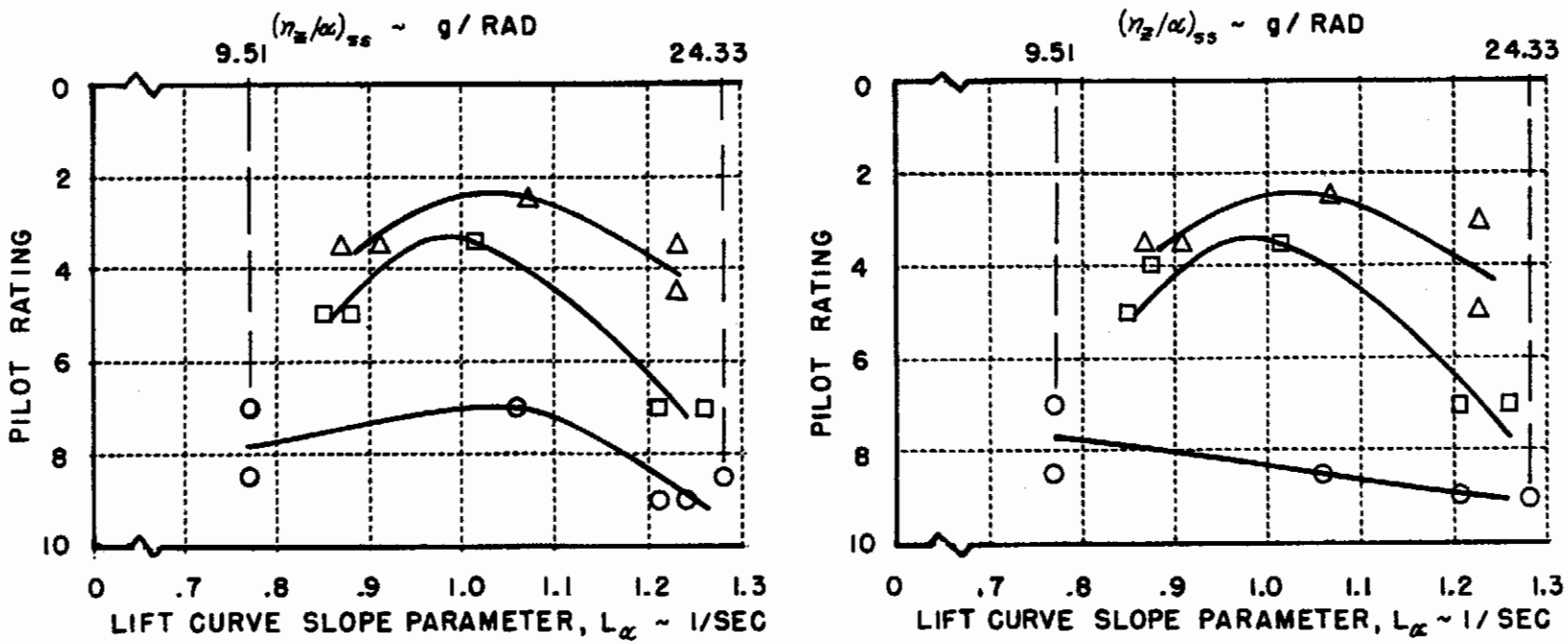

(a) Before Tracking

(b) After Tracking

SYMBOL	CONFIGURATIONS	ω_{sp}^2 ~ 1/SEC^2	$2\zeta_{sp}\omega_{sp}$ ~ 1/SEC
O	F2, F15, F55, F12, F9, F54	-.334 TO .413	.22 TO .62
□	F16, F58, F13, F10, F56	1.69 TO 1.99	.48 TO .80
△	F17, F59, F14, F11, F51	3.17 TO 4.00	.85 TO 1.20

FIGURE 15 IN-FLIGHT PILOT RATINGS VERSUS LIFT CURVE SLOPE PARAMETER

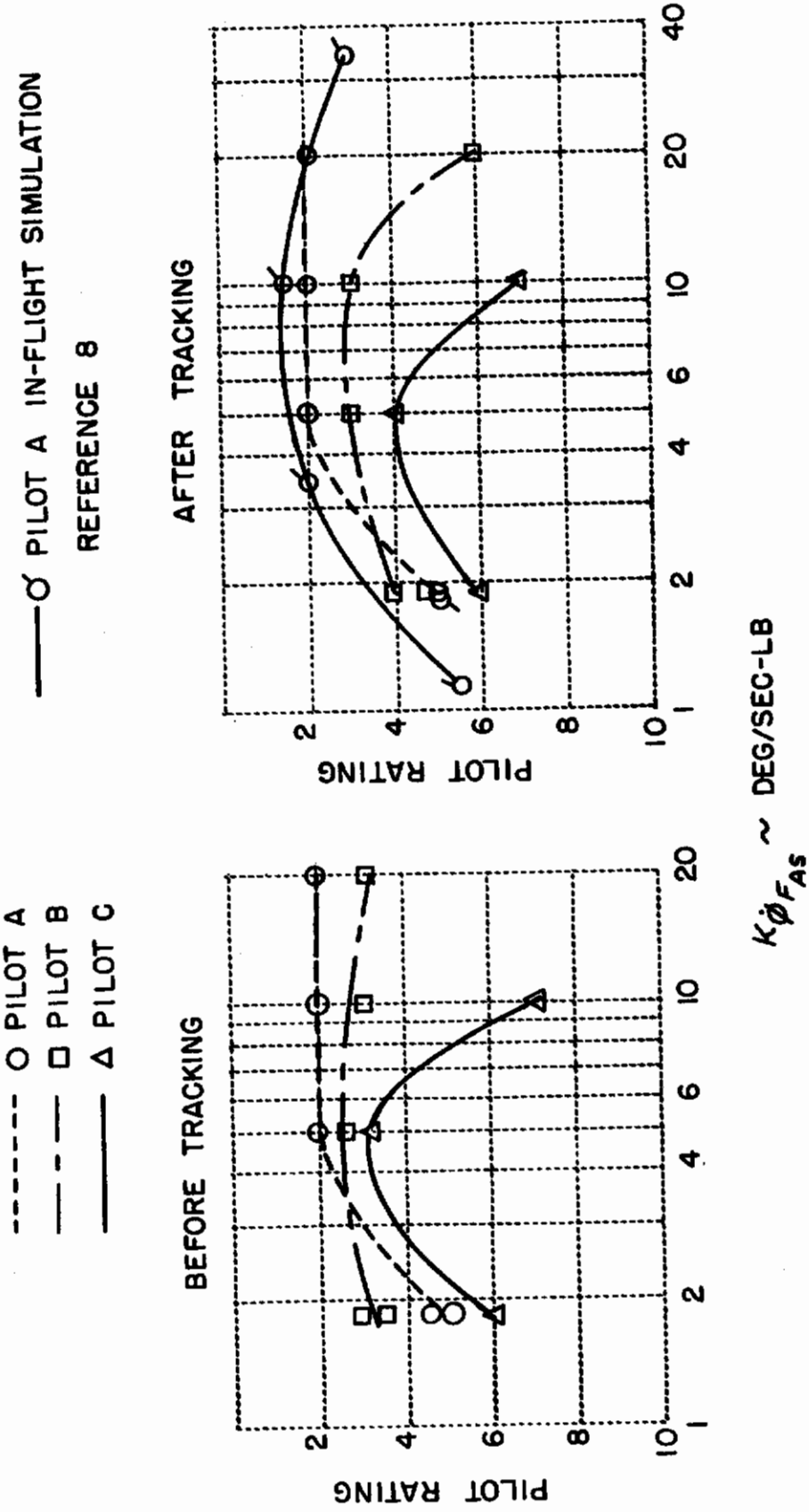

FIGURE 16 PILOT RATING VERSUS GAIN OF ROLL RESPONSE

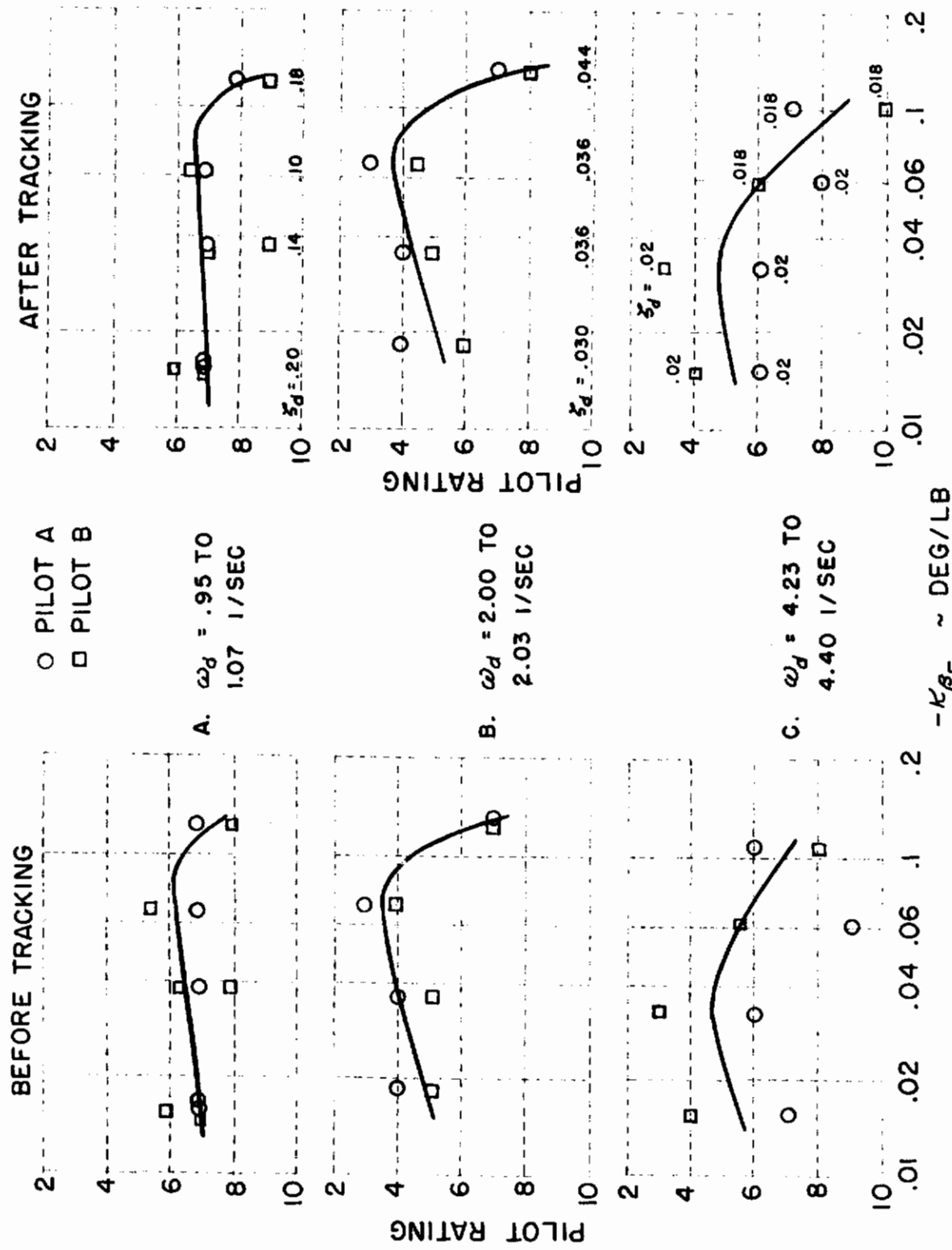

FIGURE 17 PILOT RATING VERSUS GAIN OF β/F_{RP} RESPONSE

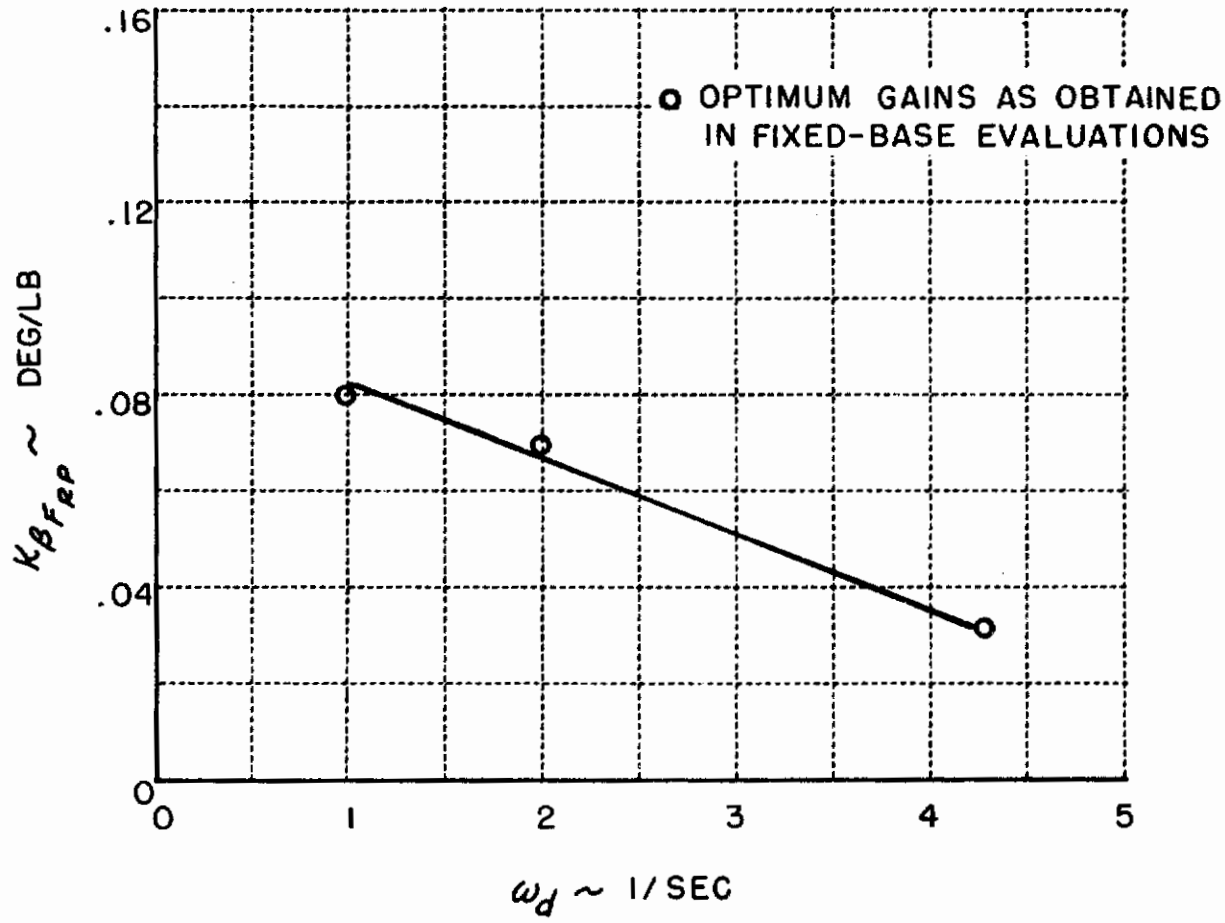

FIGURE 18 SIDESLIP RESPONSE GAIN
VERSUS DUTCH ROLL FREQUENCY

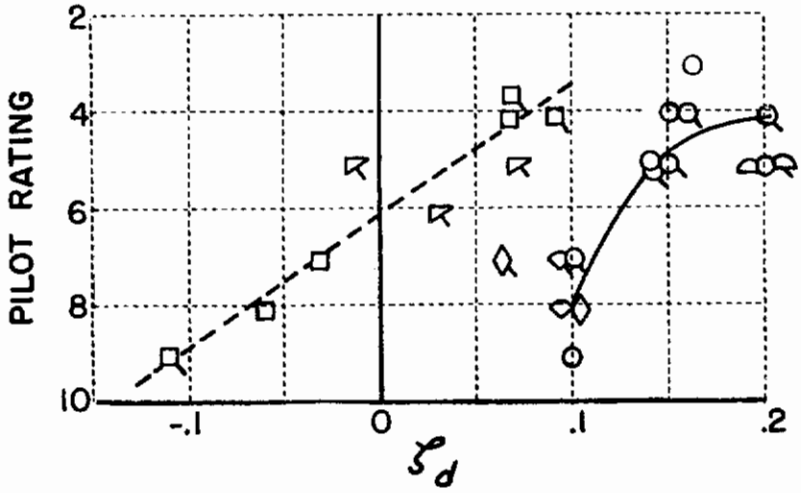

ω_d .95–1.36		
	$\lvert\phi/\beta\rvert$	ω_ϕ/ω_d
○	1.61 – 2.13	1.06 – 1.14
▽	3.00 – 3.81	1.12 – 1.18
□	4.02 – 5.11	1.12 – 1.20
⌓	1.99	.975
◇	3.33 – 3.37	.949 – .957
◇	4.15	.961

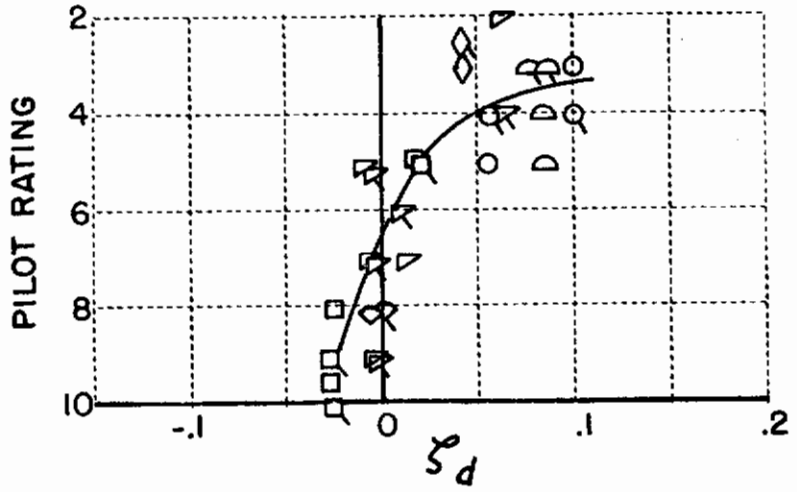

ω_d 1.96–2.27		
	$\lvert\phi/\beta\rvert$	ω_ϕ/ω_d
○	1.11 – 1.13	1.08
▽	2.75 – 3.09	1.16 – 1.18
□	5.10 – 5.42	1.22 – 1.24
⌓	1.20	.98
◇	2.90	.955
◇	5.52	.925

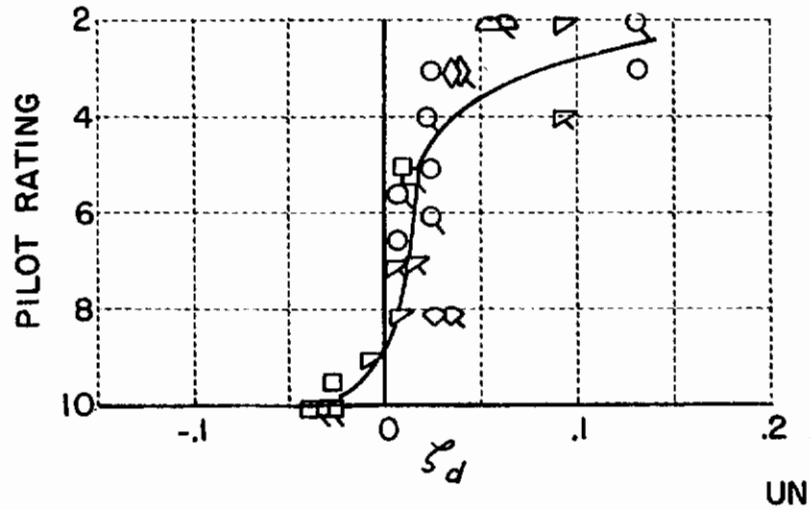

ω_d 4.27–4.52		
	$\lvert\phi/\beta\rvert$	ω_ϕ/ω_d
○	.81 – .83	1.05
▽	2.69 – 2.96	1.13 – 1.14
□	5.01 – 5.54	1.22 – 1.23
⌓	.86	.986
◇	2.77	.963
◇	5.65	.927

NOTE

UNFLAGGED POINTS, PILOT A

FLAGGED POINTS, PILOT B

FIGURE 19 DUTCH ROLL DAMPING VERSUS PILOT RATINGS (BEFORE TRACKING)

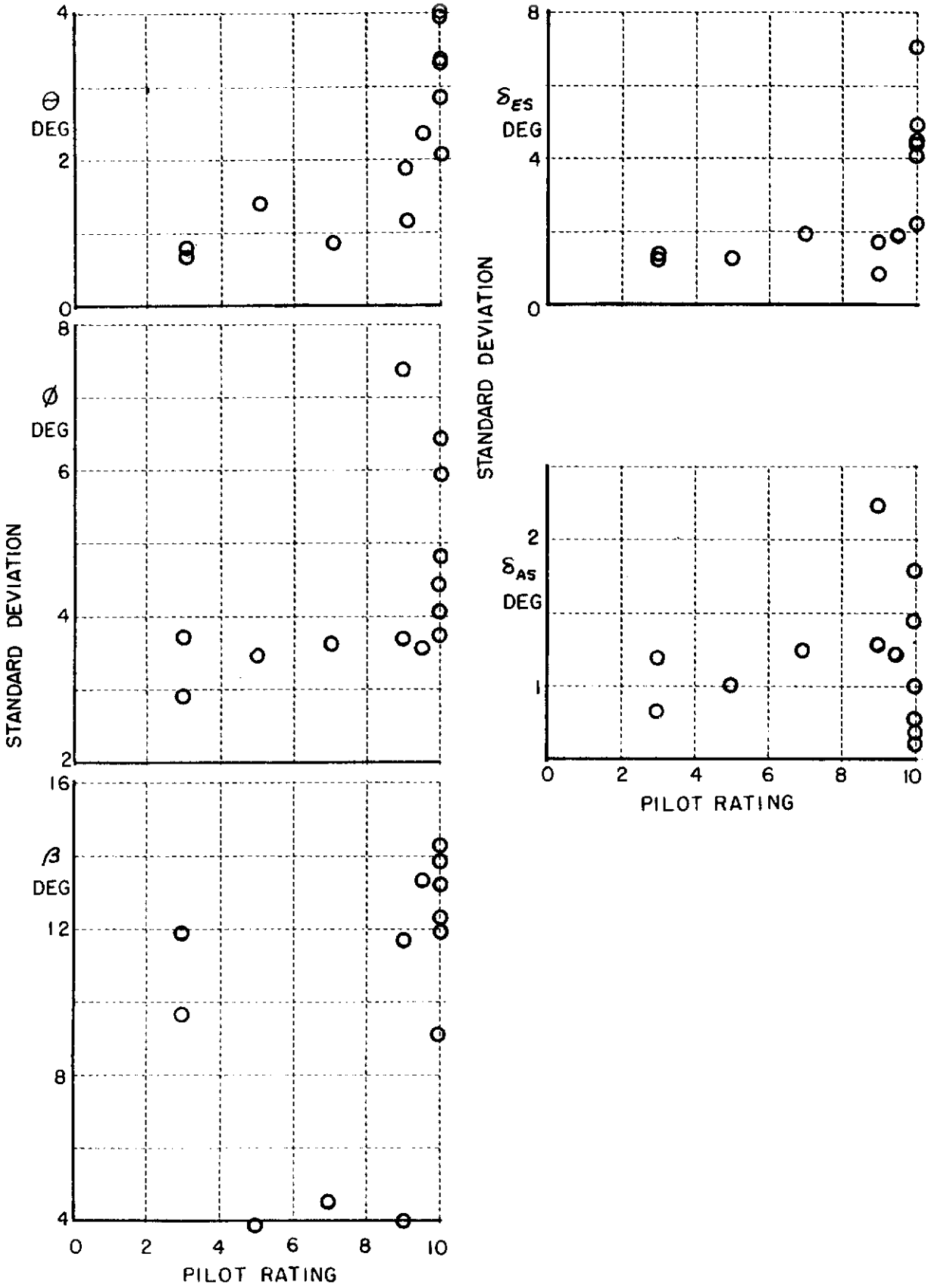

FIGURE 20 STANDARD DEVIATION VERSUS PILOT RATING (LONGITUDINAL EVALUATIONS)

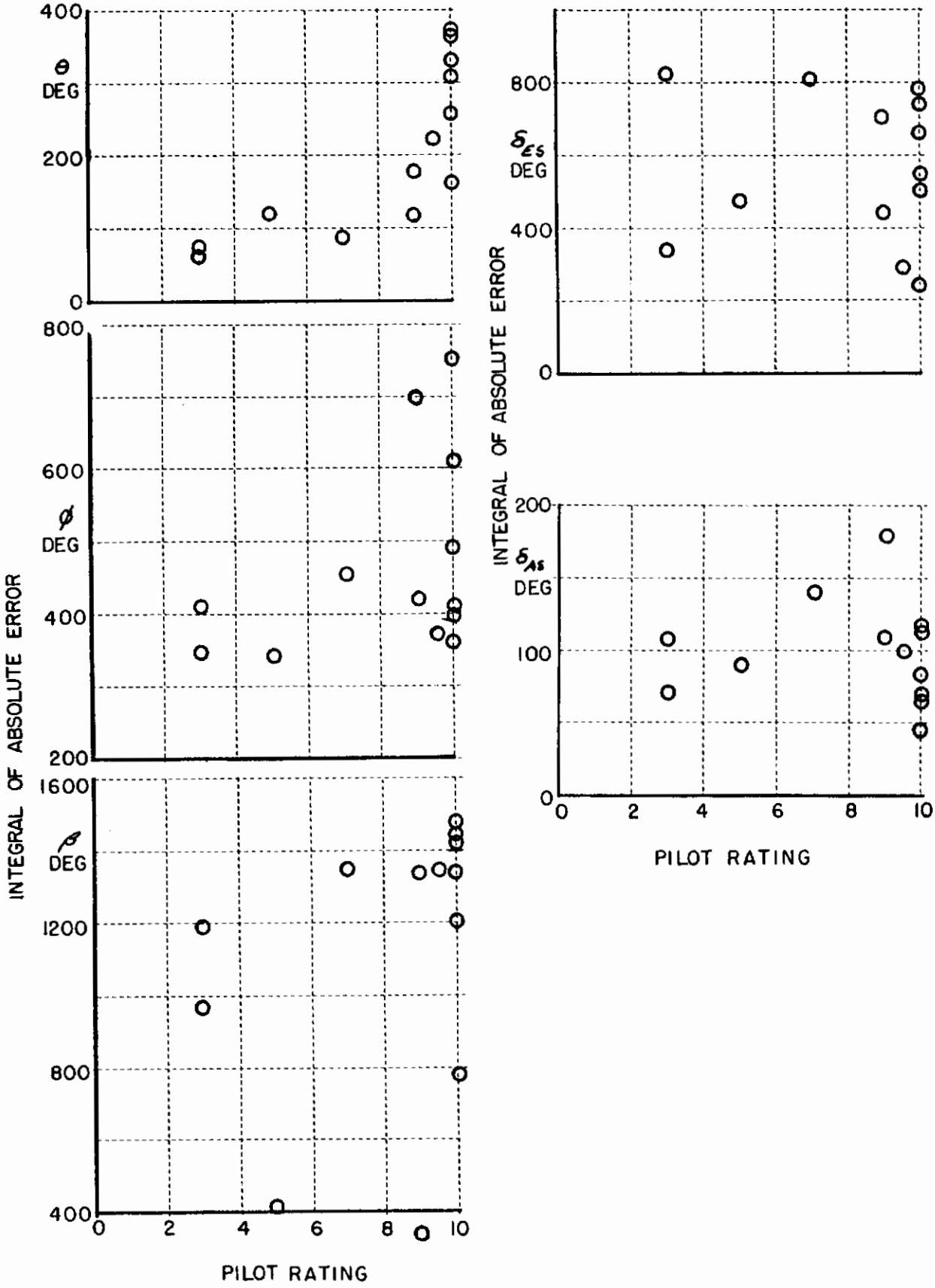

FIGURE 21 INTEGRAL OF ABSOLUTE ERROR VERSUS PILOT RATING (LONGITUDINAL EVALUATIONS)

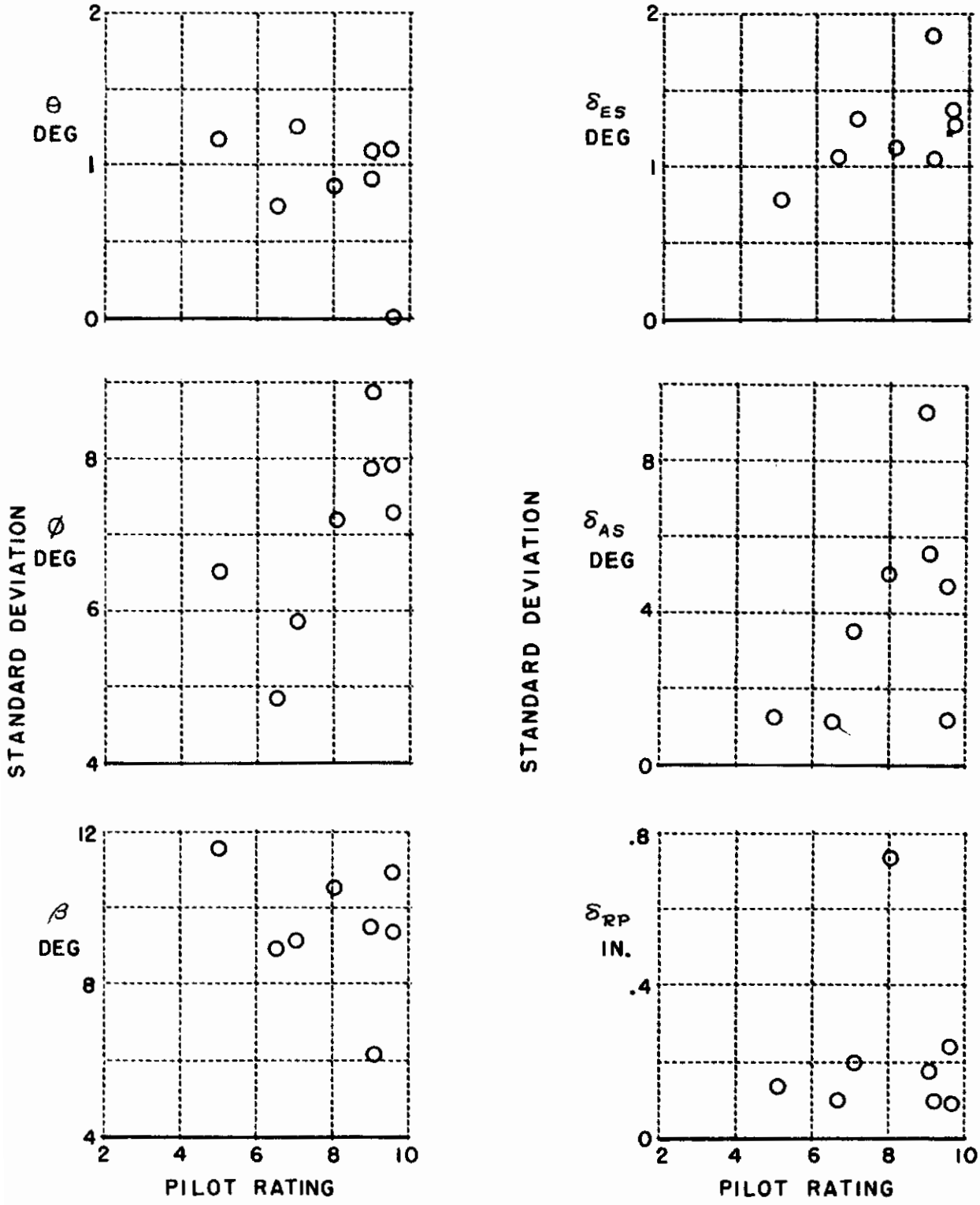

FIGURE 22 STANDARD DEVIATION VERSUS PILOT RATING
(LATERAL-DIRECTIONAL EVALUATIONS)

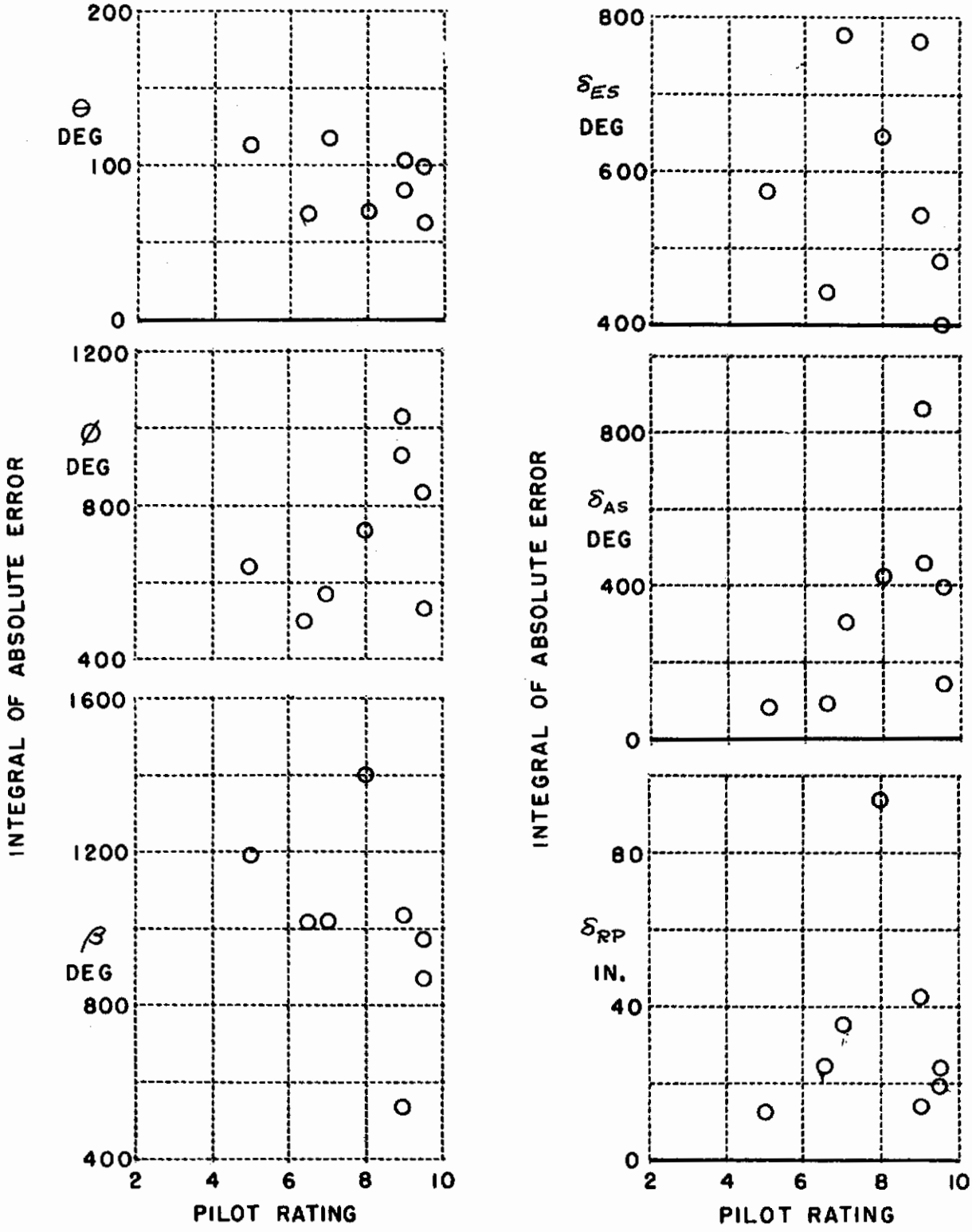

FIGURE 23 INTEGRAL OF ABSOLUTE ERROR VERSUS PILOT RATING (LATERAL-DIRECTIONAL EVALUATIONS)

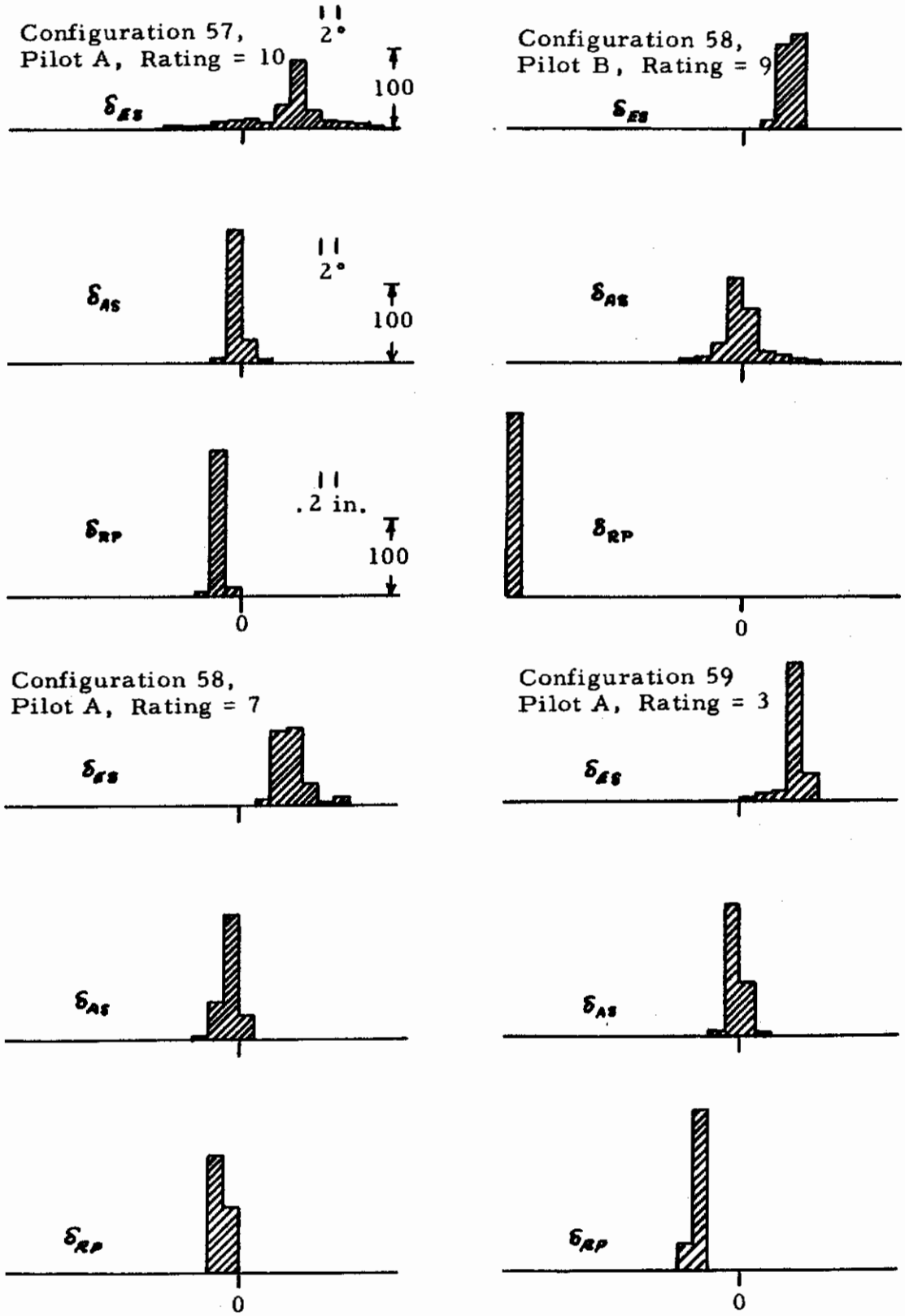

FIGURE 24a DISTRIBUTIONS OF CONTROL INPUTS– LONGITUDINAL EVALUATIONS

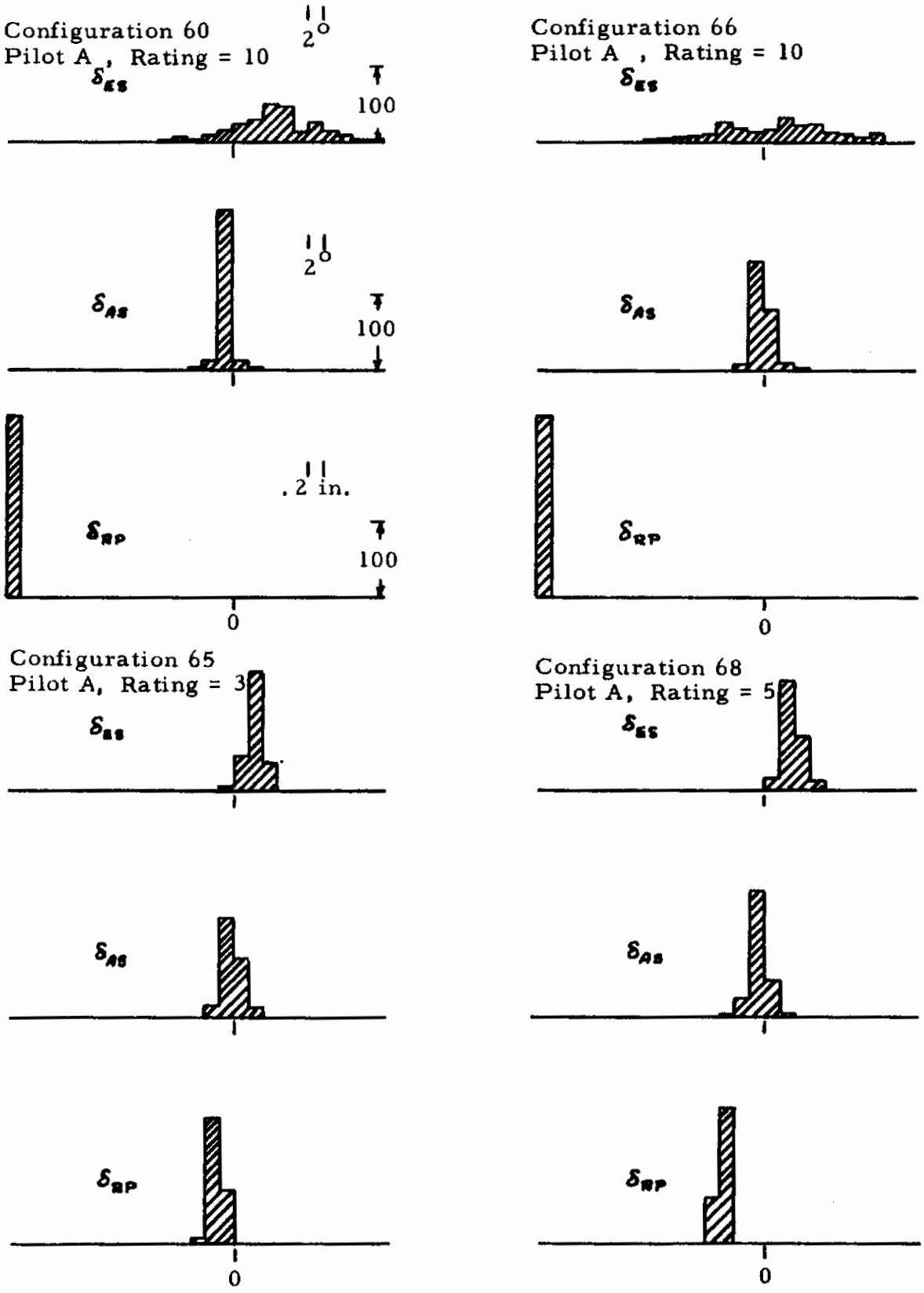

FIGURE 24b DISTRIBUTIONS OF CONTROL INPUTS– LONGITUDINAL EVALUATIONS

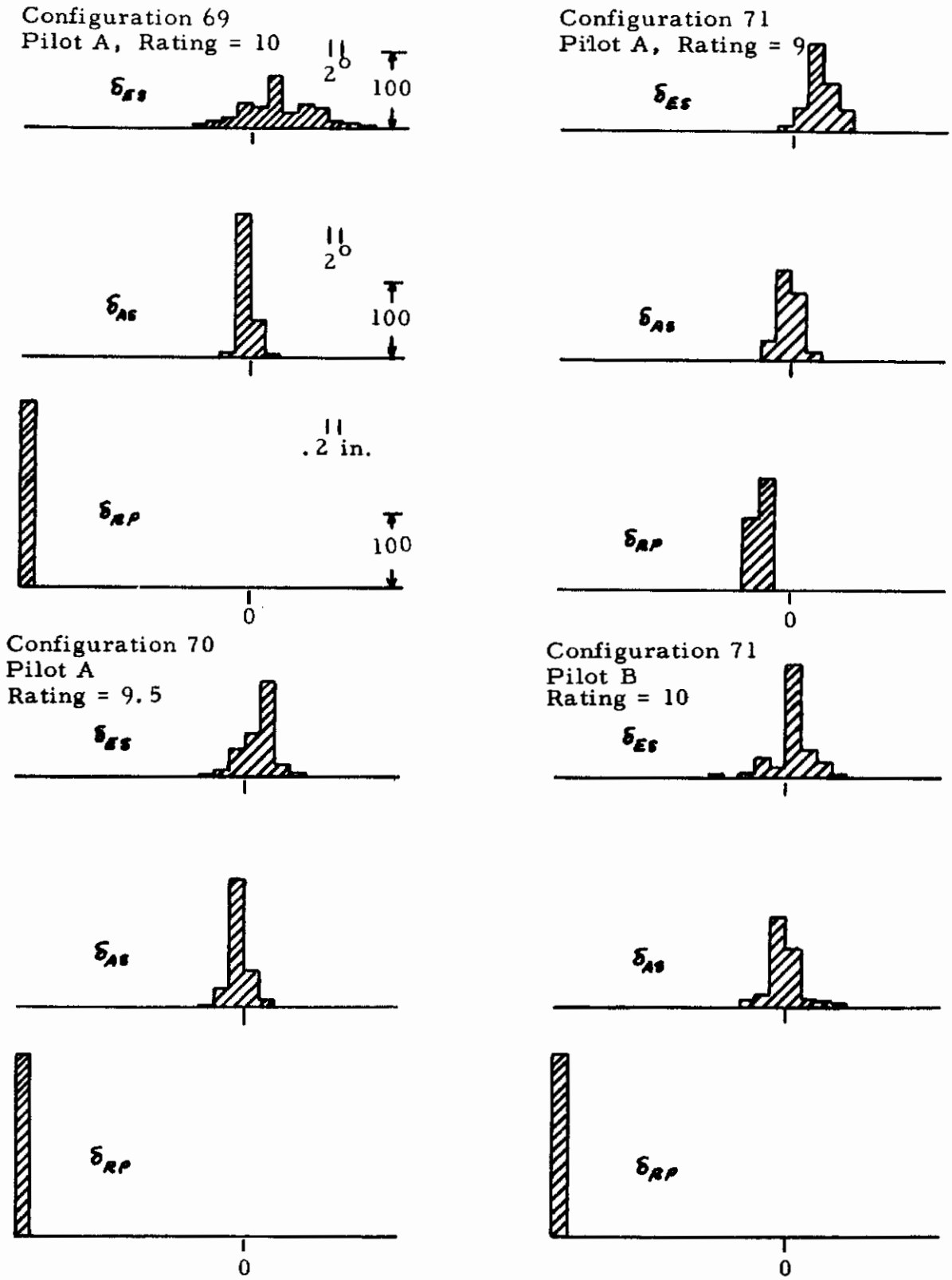

FIGURE 24c DISTRIBUTIONS OF CONTROL INPUTS– LONGITUDINAL EVALUATIONS

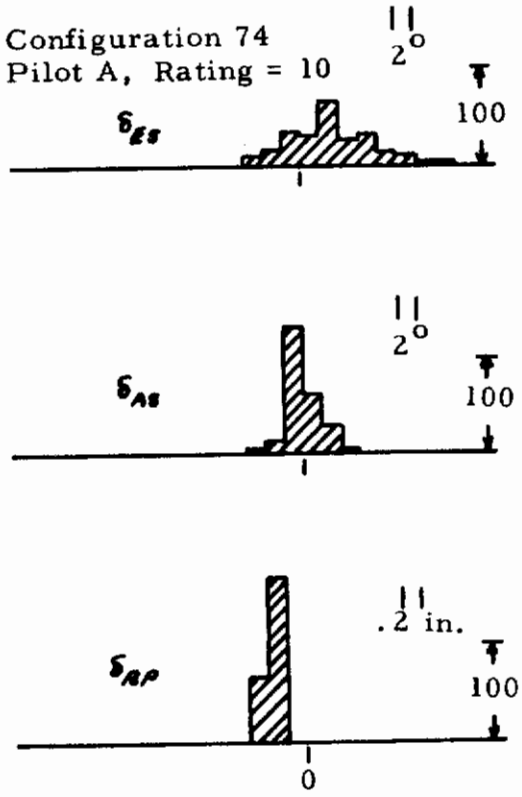

FIGURE 24d DISTRIBUTIONS OF CONTROL INPUTS– LONGITUDINAL EVALUATIONS

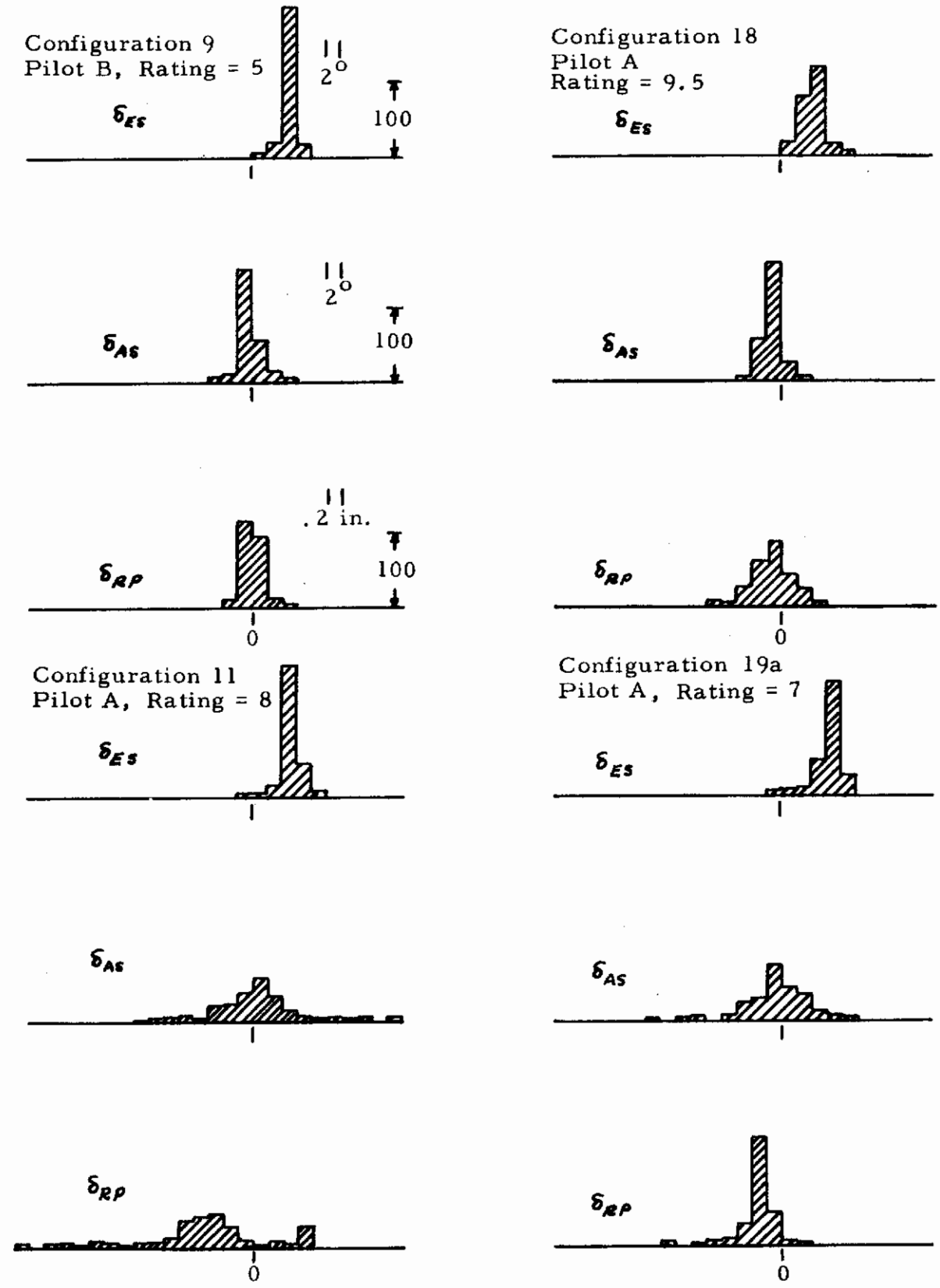

FIGURE 25a DISTRIBUTIONS OF CONTROL INPUTS– LATERAL-DIRECTIONAL EVALUATIONS

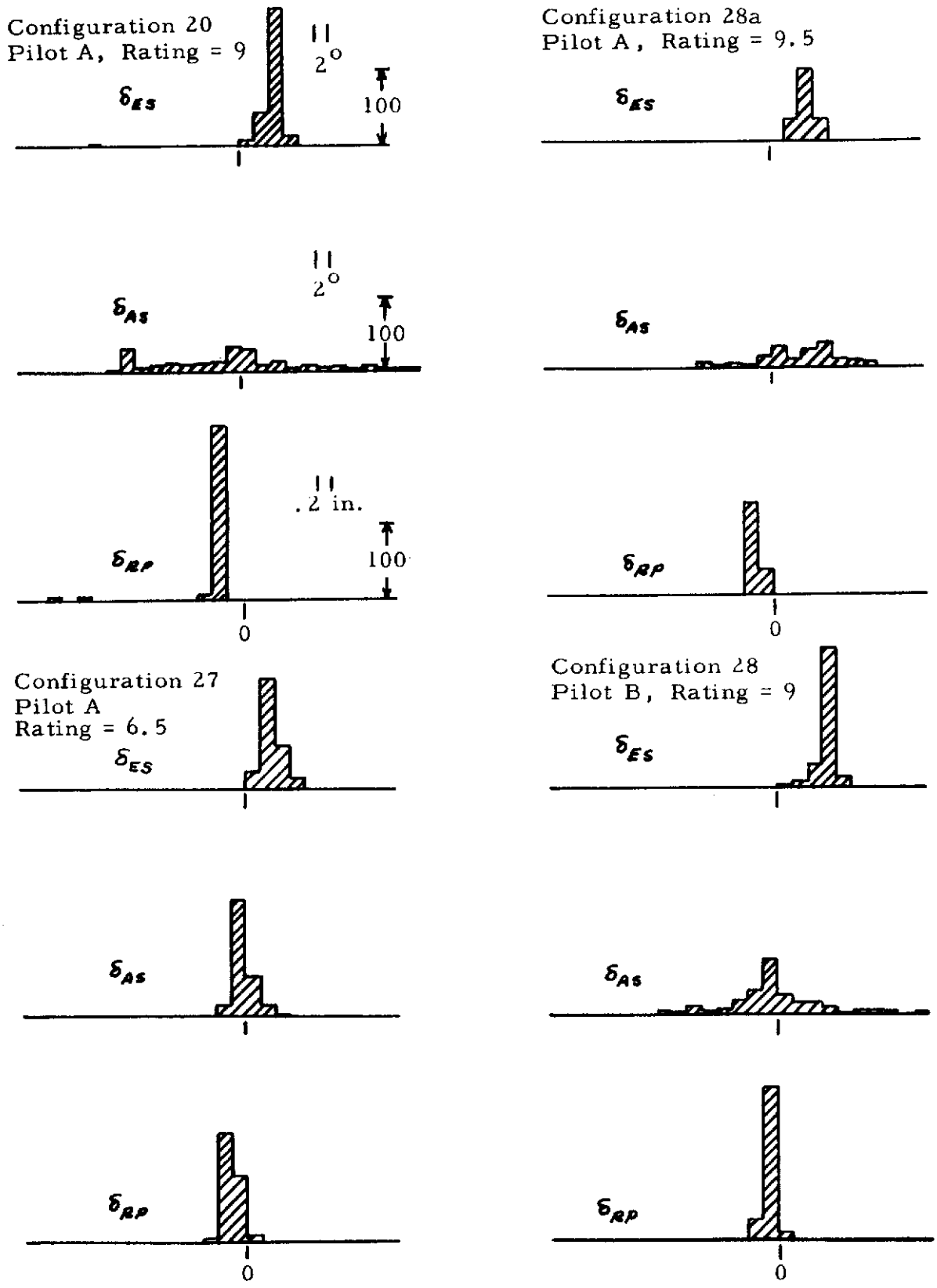

FIGURE 25b DISTRIBUTIONS OF CONTROL INPUTS– LATERAL-DIRECTIONAL EVALUATIONS

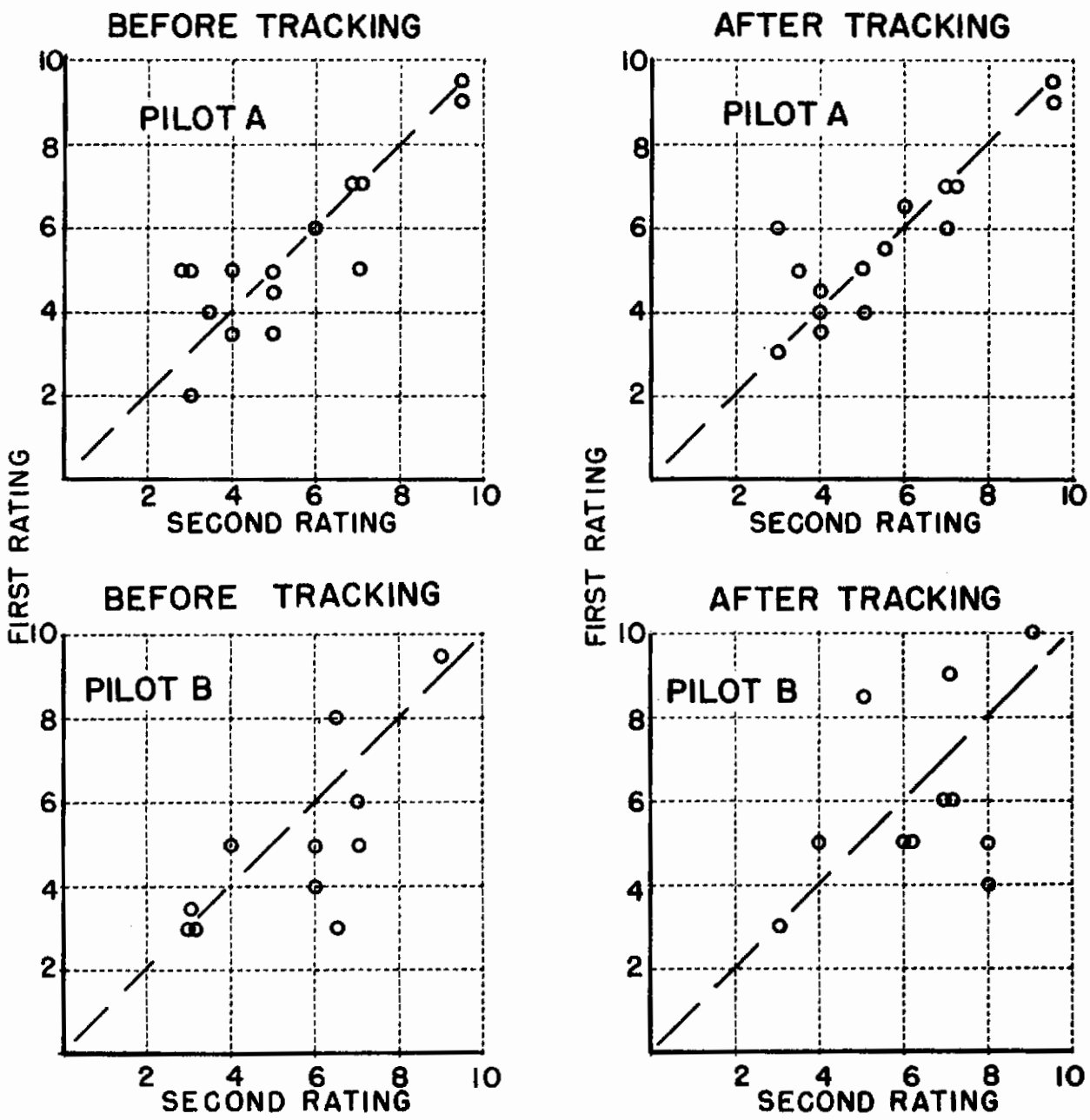

FIGURE 26 INTRAPILOT VARIABILITY
FIXED-BASE SIMULATION

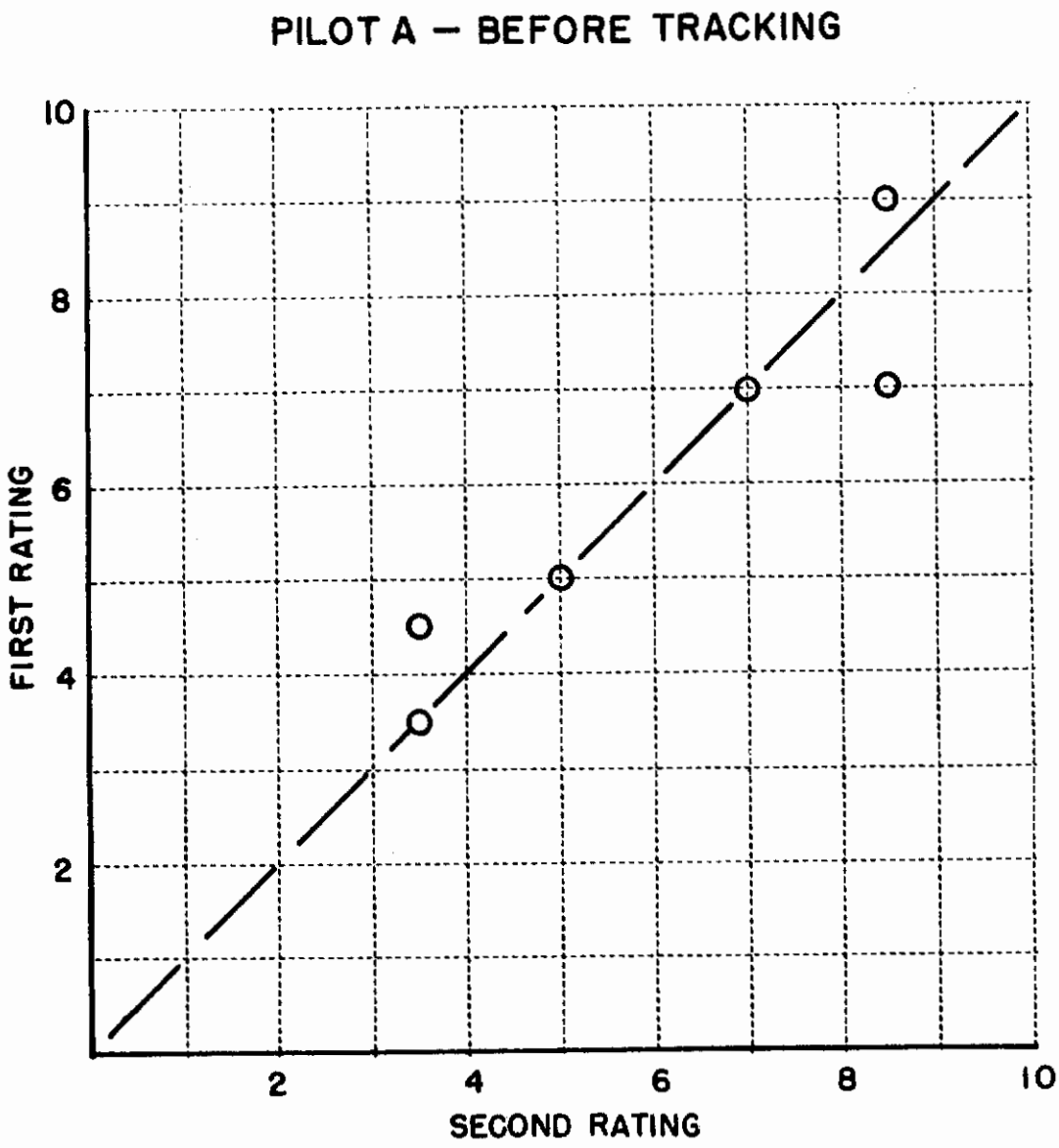

FIGURE 27 INTRAPILOT VARIABILITY
IN-FLIGHT SIMULATION

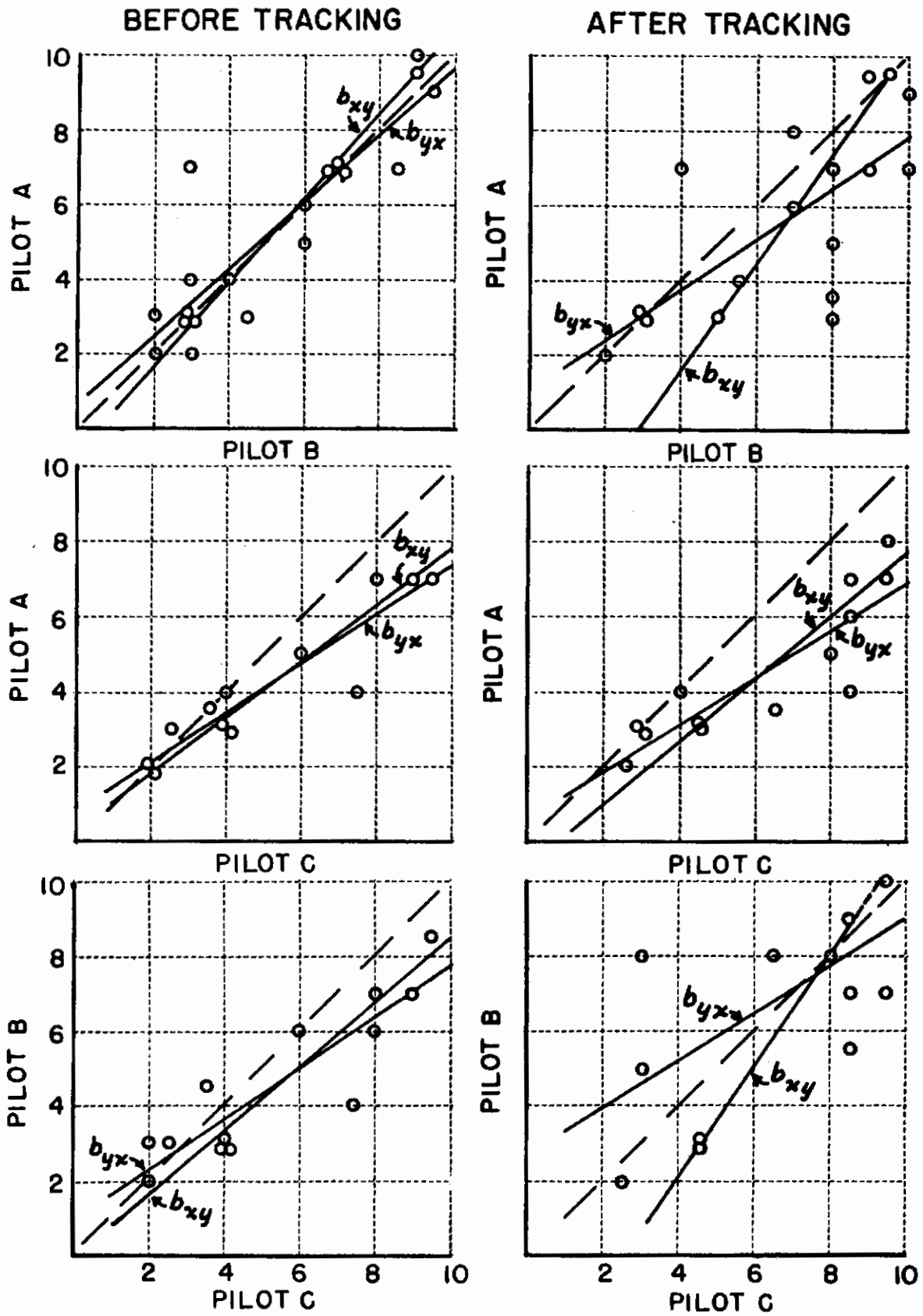

FIGURE 28 INTERPILOT RATING COMPARISONS
LONGITUDINAL EVALUATIONS

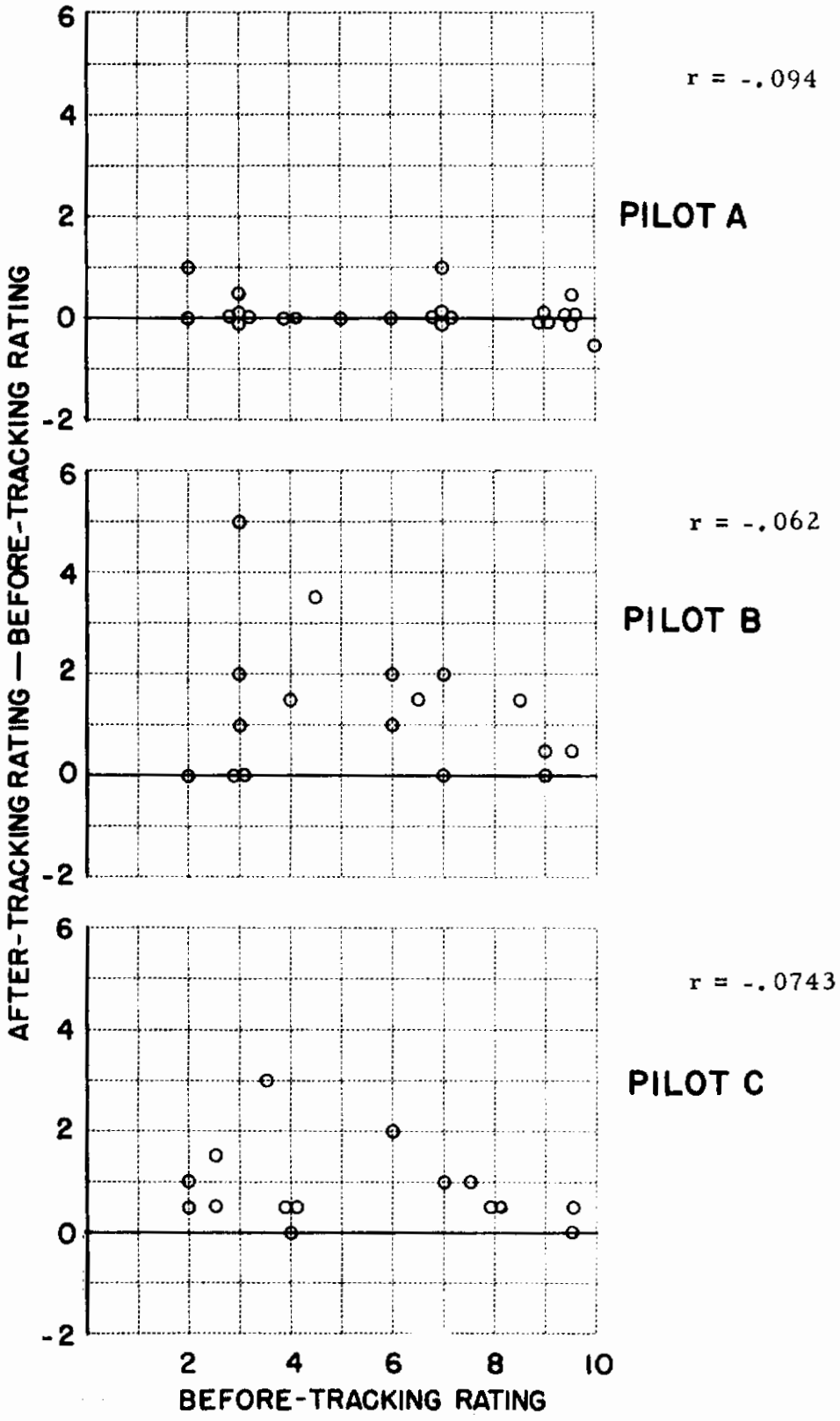

FIGURE 29 (AFTER-BEFORE) TRACKING DIFFERENCES AS FUNCTION OF BEFORE TRACKING RATING LONGITUDINAL EVALUATIONS

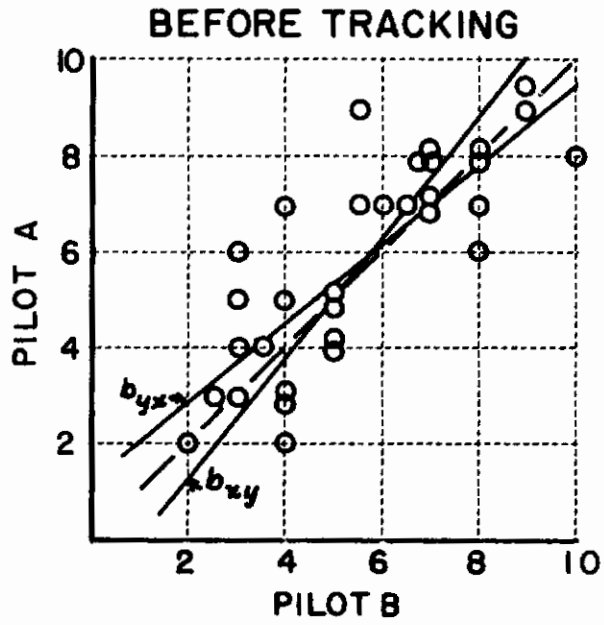

r = .80**

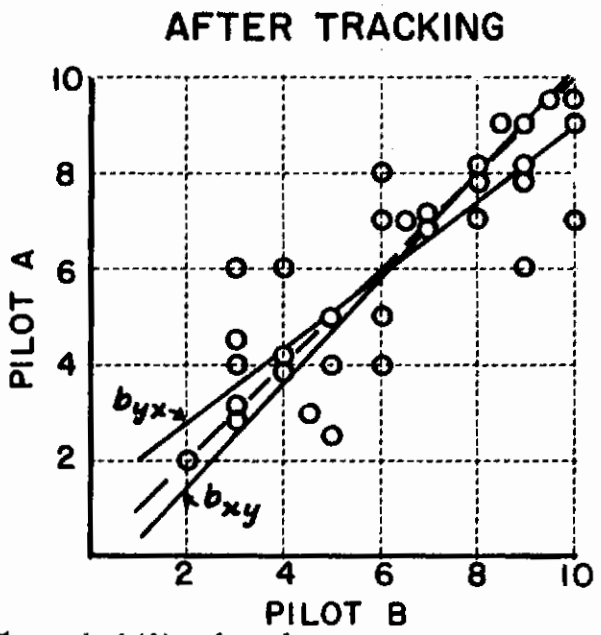

r = .84**

** significant at 1% probability level

FIGURE 30 INTERPILOT RATING COMPARISONS
LATERAL-DIRECTIONAL EVALUATIONS

TABLE I

CONTROL AND DISPLAY ELEMENT CHARACTERISTICS

Side Stick:	Spring Gradient	Equivalent* Second Order Dynamics
Roll	$\frac{F_{AS}}{\delta_{AS}}$ = .317 lb/deg	f_n = 10.3 cps, ζ = .47
Pitch	$\frac{F_{ES}}{\delta_{ES}}$ = 1.0 lb/deg	f_n = 7.95 cps, ζ = .25
F_{AS} applied 3.25 inches above roll controller axis F_{ES} applied 2.35 inches forward of pitch controller axis		
Rudder Pedal		
	$\frac{F_{RP}}{\delta_{RP}}$ = 80 lb/inch	f_n = 5.41 cps, ζ = .63

Control Surface Servos	Equivalent* Second Order Dynamics
Aileron	f_n = 10.6 cps, $\zeta \cong 0.7$
Rudder	f_n = 9.3 cps, $\zeta \cong 0.9$
Elevator	f_n = 10.5 cps, $\zeta \cong 0.75$

Lear Attitude Indicator Cockpit Display	Dynamics
Roll Angle, ϕ	Equivalent* second order: f_n = 3.5 cps, ζ = .56
Sideslip Angle, β	Equivalent* first order: τ = .063. Display sensitivity (lateral needle deflection, positive to right, per incremental sideslip angle) = 0.10 in/deg.
Pitch Angle, θ	Higher order response, not describable by first or second order system. Response time (time to 95% of final value) to step input is 0.2 sec with no overshoot. Display sensitivity (vertical translation of horizon-defining line on sphere per incremental pitch angle) = 0.057 in./deg.

* $\frac{\text{Response}}{\text{Commanded Response}} = \frac{1}{\frac{s^2}{(2\pi f_n)^2} + \frac{2\zeta}{(2\pi f_n)} s + 1}$ or $\frac{1}{\tau s + 1}$

TABLE 2
PILOT COMMENT CARD

PITCH

1. Stick Forces
2. Speed of Response
3. Damping
4. Precision of Control

ROLL

1. Stick Forces
2. Speed of Response
3. Precision of Control

YAW

1. Pedal Forces
2. Stiffness
3. Damping
4. Precision of Control

YAW-ROLL INTERACTION

1. Roll Due to Sideslip
2. Yaw Due to Ailerons

TABLE 3

PILOT'S RATING SCALE

Numerical Rating	Category	Adjective Description Within Category
1	Acceptable	Excellent
2	and	Good
3	Satisfactory	Fair
4	Acceptable	Fair
5	but	Poor
6	Unsatisfactory	Bad
7		Bad
8	Unacceptable	Very Bad
9		Dangerous
10	Unflyable	

That portion of the scale below a rating of 6 was additionally defined to represent the following meanings.

Rating	
7	Bad - Unacceptable for emergency operations if navigation and other systems management operations required.
8	Very Bad - Aircraft controllable, but only with a minimum of cockpit duties.
9	Dangerous - Aircraft just controllable with complete attention.
10	Unflyable.

TABLE 4

PILOT EXPERIENCE

	PILOT		
	A	B	C
TOTAL TIME (HOURS)	2700	2800	5500
JET TIME (HOURS)	600	1000	900
FLIGHT TEST TIME (HOURS)	300	1200	3500
GROUND SIMULATOR TIME (HOURS)	150	300	350
NUMBER OF TYPES FLOWN	20	45	85

TABLE 5a FIXED-BASE EVALUATION – LONGITUDINAL CHARACTERISTICS

CONFIG-URATION	PILOT RATING PILOT A	PILOT B	PILOT C	ω_{sp} 1/sec	ω_{sp}^2 1/sec^2	ζ_{sp}	$2\zeta_{sp}\omega_{sp}$ 1/sec	τ_θ sec	$K'_{\dot\theta_{F_{ES}}}$ deg/sec^3-lb Pilot A	Pilot B	Pilot C	$1/K_{n_{z_{F_{ES}}}}$ lb/g Pilot A	Pilot B	Pilot C	M_α 1/sec^2	$M_{\dot\alpha}$ 1/sec	M_q 1/sec	$M_{\delta_{ES}}$ 1/sec^2 Pilots A & C	Pilot B	L_α 1/sec	$L_{\delta_{ES}}$ 1/sec Pilots A & C	Pilot B	$(n_z/\alpha)_{ss}$ g/rad Pilots A & C	Pilot B
1	4 (4)	3	4 (4)	3.26	10.6	.33	2.15	.843	1.65	1.65	1.65	19.34	19.34	19.34	-9.84	-.30	-.61	1.39	1.39	1.24	-.00745	-.00745	22.53	22.53
2	2 (2)	2 (2.5)	2 (2.5)					.841	5.28	5.28	5.28	6.04	6.04	6.04				4.45	4.45		-.0238	-.0238		
3	3 (3)	2	7 (8)					.842	10.9	10.9	10.9	2.93	2.93	2.93				9.19	9.19		-.0492	-.0492		
3a			2.5 (4)					.842			10.9			2.93				9.19	9.19		-.0492	-.0492		
4	7 (7)	3 (4)						.841	32.4	32.4		.985	.985					27.3	27.3		-.146	-.146		
4a	7 (7)	6.5 (8)						.841	32.4	32.4		.985	.985					27.3	27.3		-.146	-.146		
5	4.5 (5)	3.5 (5)	6 (6)					.840	5.28	8.24	5.28	6.04	3.87	6.04				4.45	6.95		-.0238	-.0372		
5a	5 (5)	3 (4)						.840	5.28	8.24		6.04	3.87											
6	2 (2)	2.5 (3)	3 (4)						5.28	8.24	5.28	6.04	3.87	6.04										
7		3 (3)	7 (7)							8.24	5.28		3.87	6.04										
8	2 (2)	3 (6)							5.28	8.24		6.04	3.87											
9																								
thru																								
56																								
57	10 (10)	10	10	4.65	21.6	-.037	-.34	.825	5.40	8.43	5.40	12.04	7.71	12.04	-23.4	.35	1.33			1.34			23.29	23.29
58	7 (7)	7 (9)	8 (8.5)	4.65	21.6	.020	.19	.830	5.37	8.39	5.37	12.11	7.75	12.11	-22.7	.32	.82			1.33			23.11	23.11
59	3 (3)	3 (3)	4 (4.5)	4.58	21.0	.15	1.39	.822	5.42	8.48	5.42	11.66	7.45	11.66	-20.5	.29	-.35			1.33			23.19	23.19
60	10 (10)	10	10	3.71	13.8	-.12	-.89	.827	5.40	8.43	5.40	7.69	4.93	7.59	-16.1	.40	1.79			1.30			23.33	23.33
61	6 (6)	6 (7)	8 (8.5)	3.77	14.2	.024	.18	.830	5.38	8.39	5.38	7.94	5.09	7.94	-15.2	.33	.78			1.29			23.11	23.11
62	3 (3)	3 (3)	4 (4.5)	3.87	15.0	.17	1.32	.833	5.35	8.36	5.35	8.44	5.40	8.44	-14.6	.23	-.27			1.28			22.85	22.85
63	10 (10)	10	10	2.62	6.90	-.17	-.87	.835	5.34	8.34	5.34	3.89	2.49	3.89	-9.09	.37	1.75			1.25			23.09	23.09
64	7 (7)	8.5 (10)		2.72	7.40	.046	.25	.832	5.36	8.37		4.16	2.66		-8.32	.26	.74			1.25			23.04	23.04
64a			9.5 (9.5)	2.72	7.40	.026	.14	.832			5.36			4.16	-8.32	.37	.74			1.25			23.04	23.04
65	2 (3)	3 (8.5)	2.5 (3)	2.64	6.94	.30	1.59	.833	5.35	8.36	5.35	3.90	2.50	3.90	-6.61	-.08	-.27			1.24			22.90	22.90
65a	2 (3)	3 (5)	2 (3)	2.64	6.94	.30	1.59	.833	5.35	8.36	5.35	3.90	2.50	3.90	-6.61	-.08	-.27			1.24			22.90	22.90
66	10 (10)	10	10	1.73	3.00	-.32	-1.10	.835	5.34	8.35	5.34	1.69	1.08	1.69	-5.43	.35	1.98			1.23			23.11	23.11
67	9.5 (9.5)	10	10	1.79	3.20	0	0	.83	5.36	8.37	5.36	1.80	1.15	1.80	-4.70	.01	1.22			1.23			23.09	23.09
68	5 (5)	6 (8)	6 (8)	1.97	3.90	.25	1.00	.835	5.33	8.32	5.33	2.20	1.41	2.20	-4.17	0	.22			1.22			22.83	22.83
69	10 (10)	10	10		-.50		0	.836	5.32	8.30	5.32				-.94	0	1.20			1.20			22.90	22.90
70	9.5 (9.5)	10	10		-.45		.80	.833	5.34	8.34	5.34				-.08	-.04	.44			1.20			22.89	22.89
71	9 (9)	9.5 (10)	10		-.38		1.62	.837	5.32	8.30	5.32				.75	-.12	-.31			1.19			22.69	22.69
71b	9.5 (9.5)	9 (9)			-.38		1.62	.837	5.32	8.30					.75	-.12	-.31			1.19			22.69	22.69
72	NOT RATED				-4.0		.50	.835	5.33	8.32	5.33				3.20	0	.68			1.18			22.87	22.87

Note: Ratings in parentheses are after the tracking maneuver

NOTE: Ratings in parentheses are those given after the tracking maneuver. The starred (*) ratings of 10 (Unflyable) are assigned based upon the before-tracking rating since the evaluation pilot was either unable to perform the tracking maneuver or else was so certain of the Unflyable rating that he did not wish to waste additional evaluation time on the configuration.

TABLE 5a FIXED-BASE EVALUATION - LONGITUDINAL CHARACTERISTICS (CONTINUED)

CONFIG-URATION	PILOT RATING PILOT A	PILOT B	PILOT C	ω_{sp} 1/sec	ω_{sp}^2 1/sec^2	ζ_{sp}	$2\zeta_{sp}\omega_{sp}$ 1/sec	τ_θ sec	$K'_{\theta_{F_{es}}}$ deg/sec^3-lb Pilot A	Pilot B	Pilot C	$1/K_{n_{z_{F_{es}}}}$ lb/g Pilot A	Pilot B	Pilot C	M_w 1/sec^2	$M_{\dot{w}}$ 1/sec	M_q 1/sec	$M_{\delta_{es}}$ 1/sec^2 Pilots A & C	Pilot B	L_w 1/sec	$L_{\delta_{es}}$ 1/sec Pilots A & C	Pilot B	$(n_z/\alpha)_{ss}$ g/rad Pilots A & C	Pilot B
73	10 (10)	10			-3.20		1.46	.842	5.29	8.26	5.29	--			3.59	.04	-.33	4.45	6.95	1.17	-.0238	-.0372	22.60	22.60
74	10 (10)	10			-3.90		2.58	.835	5.33	8.23	5.33	--			5.47	-.07	-1.34			1.17			22.67	22.67
75	NOT RATED				-10.0		2.0	.835	5.32	8.32	5.32	--			10.99	.01	-.87			1.14			22.72	22.72
76	NOT RATED				-10.0		3.0	.838	5.31	8.30	5.31	--			12.11	0	-1.87			1.13			22.52	22.52
77	10	10			-7.39		3.27	.847	5.28	8.25	5.28	--			10.65	.74	-2.88			1.13			22.25	22.25
78	9 (9)				-.38		1.62	.838	1.66		1.66	--			.75	-.12	-.31	1.39		1.19	-.00745		22.69	
79	9 (9)				-.38		1.62	.837	5.32		5.32	--			.75	-.12	-.31	4,45		1.19	-.0238		22.69	
80	10 (10)				-.38		1.62	.838	10.97		10.97	--			.75	-.12	- 31	9.19		1.19	-.0492		22.69	
81	9.5 (10)				-.38		1.62	.838	32.58		32.58	--			.75	-.12	-.31	27.3		1.19	-.146		22.69	
82	3 (3.5)	4.5 (8)	3,5 (6.5)	1.89	3.58	.26	1.00	.833	1.67	1.67	1.67	6.45	6.45	6.45	-3.85	0	.22	1.39	1.39	1.22	-.00745	-.00745	22.86	22.86
83	4 (4)	4 (5.5)	7.5 (8.5)	1.89	3.58	.26	1.00	.833	5.34	5.34	5.34	2.02	2.02	2.02	-3.85	0	.22	4.45	4.45	1.22	-.0238	-.0238	22.86	22.86
84	7 (8)	7 (7)	9 (9.5)	1.89	3.58	.26	1.00	.834	11.01	11.01	11.01	.979	.979	.979	-3.85	0	.22	9.19	9.19	1.22	-.0492	-.0492	22.86	22.86
85	10 (9.5)	9 (9.5)		1.89	3.58	.26	1.00	.834	32.74	32.74	32.74	.329	.329	.329	-3.85	0	.22	27.3	27.3	1.22	-.146	-.146	22.86	22.86
86	10 (10)			.73	.53	0	0	.840	5.30		5.30	.301		.301	-1.97	0	1.20	4.45		1.20	-.0238		22.79	
86a	10 (10)			.73	.53	0	0	.840	5.30		5.30	.301		.301	-1.97	0	1.20			1.20			22.791	
87	10 (10)				-.36		.11	.990	4.49		4.49	--			-.60	-.05	.95			1.01			19.26	
87a	10 (10)				-.36		.11	.990	4.49		4.49	--			-.60	-.05	.95			1.01			19.26	
88	9.5 (9.5)			1.02	1.12	.074	.15	1.28	3.48		3.48	.969		.969	-1.77	-.06	.70			.79			14.92	
88a	9.5 (9.5)			1.02	1.12	.074	.15	1.28	3.48		3.48	.969		.969	-1.77	-.06	.70			.79			14.92	
89	5 (5.5)			1.45	2.11	.20	.57	.836	5.32		5.32	1.19		1.19	-2.97	-.07	.71			1.21			22.82	
89a	5 (5)			1.45	2.11	.20	.57	.836	5.32		5.32	1.19		1.19	-2.97	-.07	.71			1.21			22.82	
90	6 (6.5)			1.45	2.11	.20	.57	.993	4.48		4.48	1.42		1.42	-2.58	-.01	.46			1.02			19.20	
90a	6 (6)			1.45	2.11	.20	.57	.993	4.48		4.48	1.42		1.42	-2.58	-.01	.46			1.02			19.20	
91	3.5 (4)			1.45	2.11	.20	.57	1.27	3.51		3.51	1.81		1.81	-2.28	.02	.21			.80			15.01	
91a	5 (5)			1.45	2.11	.20	.57	1.27	3.51		3.51	1.81		1.81	-2.28	.02	.21			.80			15.01	
92	5 (5)			2.08	4.33	.18	.76	.838	5.32		5.32	2.45		2.45	-4.60	.24	.22			1.22			22.78	
92a	3 (3.5)			2.08	4.33	.18	.76	.838	5.32		5.32	2.45		2.45	-4.60	.24	.22			1.22			22.78	
93	3.5 (3.5)			2.08	4.33	.18	.76	.995	4.48		4.48	2.91		2.91	-4.30	.30	-.03			1.03			19.17	
93a	4 (4)			2.08	4.33	.18	.76	.995	4.48		4.48	2.91		2.91	-4.30	.30	-.03			1.03			19.17	
94	4 (4)			2.08	4.33	.18	.76	1.274	3.50		3.50	3.72		3.72	-4.10	.34	-.29			.81			14.98	
94a	3.5 (4)			2.08	4.33	.18	.76	1.274	3.50		3.50	3.72		3.72	-4.10	.34	-.29			.81			14.98	

Note: Ratings in parentheses are after the tracking maneuver

NOTE: Ratings in parentheses are those given after the tracking maneuver. The starred (*) ratings of 10 (Unflyable) are assigned based upon the before-tracking rating since the evaluation pilot was either unable to perform the tracking maneuver or else was so certain of the Unflyable rating that he did not wish to waste additional evaluation time on the configuration.

TABLE 5b FIXED-BASE EVALUATION – LATERAL-DIRECTIONAL CHARACTERISTICS

CONF.	PILOT RATING			ω_d	ζ_d	$\lvert\frac{\phi}{\beta}\rvert$	τ_R	$\frac{1}{\tau_s}$	$K_{\dot\phi F_{AS}}$ deg/sec-lb		$K_{\beta F_{RP}}$	$K_{\beta F_{AS}}$	ω_ϕ	ζ_ϕ	$\frac{\omega_\phi}{\omega_d}$	Y_β	$Y_{\delta_{RP}}$	N'_β	$N'_{\dot\beta}$	N'_r	N'_p	$N'_{\delta_{AS}}$ 1/sec²	$N'_{\delta_{RP}}$	L'_β	L'_r	L'_p	$L'_{\delta_{AS}}$ 1/sec²	$L'_{\delta_{RP}}$
	PILOT A	PILOT B	PILOT C	1/sec			sec	1/sec	Pilots A & B	Pilot C	deg/lb	deg/lb	1/sec			1/sec	1/in.-sec	1/sec²	1/sec	1/sec	1/sec	Pilots A & B	1/in.-sec²	1/sec²	1/sec	1/sec	Pilots A & B	1/in.-sec²
1	4 (4)	3	4 (4)	1.97	.083	1.41	.34	≈ 0	10.0	7.25	-.07144		1.95	.083	.99	-.156	-.00504	3.85	0	-.171	-.0525	-.0585	.3992	-10.0	.403	-2.56	8.15	-.3504
2	2 (2)	2 (2.5)	2 (2.5)						10.0	4.90												-.0585					8.15	
3	3 (3)	2	7 (8)						10.0	7.25												-.0585					8.15	
3a			2.5 (4)						10.0	7.25												-.0585					8.15	
4	7 (7)	3 (4)							10.0													-.0585					8.15	
4a	7 (7)	6.5 (8)							10.0													-.0585					8.15	
5	4.5 (5)	3.5 (5)	6 (6)						1.86	1.86												-.0117					1.63	
5a	5 (5)	3 (4)							1.86													-.0117					1.63	
6	2 (2)	2.5 (3)	3 (4)						4.90	4.90												-.0292					4.07	
7		3 (3)	7 (7)						10.0	10.0												-.0585					8.15	
8	2 (2)	3 (6)							20.0													-.117					16.3	
9	4 (4)	5 (5)		1.12	.15	2.06	.40		2.58		-.0570	-.444	1.24	.129	1.11	-.121	-.00134	1.21	-.102	-.317		.312	.1065	-5.03	.813	-2.50	5.73	-.09343
9a	9 (9)	7 (6)		.95	.10	1.96			2.74		-.0776	-.602	1.08	.088	1.14			.853	-.248			.312		-4.78	.813		5.73	
10		5 (6)		1.03	-.015	3.46			1.76		-.0626	-.221	1.22	.040	1.18			1.01	-.469			.155		-8.44	3.25		3.22	
11	8 (8)			1.13	-.060	4.55			1.14		-.0509	-.1093	1.35	.048	1.19			1.23	-.547			.0958		-11.1	6.50		2.06	
11a		5 (5)		1.32	.070	3.81			1.01		-.0399	-.0858	1.48	.137	1.12			1.69	-.253			..0958		-9.29	6.50		2.06	
11b		9 (9.5)		1.14	-.11	4.72			1.14		-.0500	-.1073	1.37	.015	1.20			1.25	-.688			.0958		-11.5	6.50		2.06	
12	3 (3)	4 (4)		1.15	.16	1.61			2.45		-.0555	-.432	1.24	.144	1.08			1.27	-.070			.312		-3.91	.811		5.73	
13		6 (6.5)		1.15	.028	3.00			1.60		-.0526	-.194	1.30	.070	1.13			1.27	-.374			.156		-7.30	3.25		3.22	
14	7 (7)			1.29	-.03	4.61			1.06		-.0408	-.0875	1.48	.061	1.15			1.61	-.515			.0958		-11.2	6.49		2.06	
14a		4 (5)		1.36	.09	4.02			1.00		-.0376	-.0808	1.52	.150	1.12			1.80	-.194			.0958		-9.80	6.49		2.06	
15	5 (4.5)	5 (4)		1.05	.14	2.01			2.63		-.0648	-.507	1.18	.120	1.12			1.05	-.144			.314		-4.86	.806		5.73	
16	4 (4)	3.5 (4)		1.23	.067	5.11			1.77		-.0438	-.158	1.46	.086	1.19			1.46	-.273			.157		-12.4	3.22		3.22	
17	5 (4)	4 (4)		1.36	.20	2.13			.909		-.0395	-.085	1.44	.261	1.06			1.80	+.106			.0964		-5.14	6.45		2.06	
18	9 (9.5)	9 (9.5)		2.00	-.005	2.75			3.26		-.0668	-.282	2.36	.004	1.18	-.160	-.00504	3.95	-.497			.510	.3992	-17.1	.498		5.73	-.3504
19	5 (6)	5 (5)		2.03	-.010	3.01			1.70		-.0645	-.130	2.38	.020	1.17			4.07	-.518			.254		-18.7	1.99		3.22	
19a	7 (7)	7 (8)		2.08	-.004	3.03			1.69		-.0618	-.1493	2.41	.023	1.16			4.27	-.494			.254		-18.8	1.99		3.22	
20	8 (9)	10 (10)		2.23	-.025	5.10			1.19		-.0515	-.0631	2.72	.027	1.22			4.93	-.589			.156		-31.6	3.98		2.06	
21	5 (5)	4 (5)		1.96	.056	1.11			2.24		-.0732	-.312	2.12	.055	1.08			3.79	-.257			.514		-6.81	.493		5.73	
22	7 (8)	6 (6)		2.07	.01	3.09			1.70		-.0622	-.127	2.40	.033	1.16			4.23	-.436			.256		-19.0	1.97		3.22	
23	9.5 (9.5)	9 (10)		2.27	-.026	5.27			1.19		-.0499	-.0618	2.77	.026	1.22			5.10	-.595			.158		-32.4	3.94		2.06	
24	3 (4)	4 (4)		1.97	.10	1.13			2.73		-.0725	-.325	2.13	.091	1.08			3.83	-.083			.535		-6.68	.474		5.73	
25	2 (2.5)	4 (5)		2.09	.068	3.00			1.68		-.0614	-.132	2.42	.073	1.16			4.32	-.193			.267		-17.7	1.90		3.22	
26	5 (6)	5 (9)		2.20	.020	5.42			1.23		-.0528	-.0695	2.73	.054	1.24			4.80	-.433			.164		-32.0	3.79		2.06	
27	6.5 (6.5)	5.5 (5.5)		4.27	.008	.82			2.81		-.0650	-.0961	4.48	.012	1.05	-.311	-.02083	18.2	-.560			.685	1.6505	-15.3	.370		5.73	-1.448
28		7 (9)		4.46	.015	2.69			1.85		-.0578	-.0415	5.05	.024	1.13	-.316		19.8	-.499			.342		-50.0	1.48		3.22	
28a	9 (9.5)			4.46	-.010	2.78			1.86		-.0577	-.0415	5.05	.006	1.13	-.316		19.8	-.722			.342		-51.7	1.48		3.22	

TABLE 5b FIXED-BASE EVALUATION – LATERAL-DIRECTIONAL CHARACTERISTICS (CONTINUED)

CONF.	PILOT RATING			ω_d	ζ_d	$\lvert\frac{\phi}{\beta}\rvert$	τ_R	$\frac{1}{\tau_s}$	$K_{\phi_{F_{AS}}}$ deg/sec-lb		$K_{\beta_{F_{RP}}}$	$K_{\beta_{F_{AS}}}$	ω_ϕ	ζ_ϕ	$\frac{\omega_\phi}{\omega_d}$	Y_β	$Y_{\delta_{RP}}$	N'_β	$N'_{\dot\beta}$	N'_r	N'_p	$N'_{\delta_{AS}}$	$N'_{\delta_{RP}}$	L'_β	L'_r	L'_p	$L'_{\delta_{AS}}$	$L'_{\delta_{RP}}$
	PILOT A	PILOT B	PILOT C	1/sec			sec	1/sec	Pilots A & B	Pilot C	deg/lb	deg/lb	1/sec			1/sec	1/in.-sec	1/sec²	1/sec	1/sec	1/sec	1/sec² Pilots A & B	1/in.-sec²	1/sec²	1/sec	1/sec	1/sec² Pilots A & B	1 / in.-sec²
29	10 (10)	10		4.47	-.040	5.46	.40	≈ 0	1.22		-.0547	-.0238	5.50	-.004	1.23	-.323	-.02083	19.9	-.998	-.317	-.0525	.210	1.6505	-102	2.96	-2.50	2.06	-1.448
30	5 (6)	4 (5)		4.27	.023	.83			2.81		-.0650	-.0975	4.49	.025	1.05	-.311		18.2	-.432			.691		-15.3	.366		5.73	
30a	3 (3)	6 (6)		4.27	.023	.83			2.81		-.0650	-.0975	4.49	.025	1.05	-.311		18.2	-.432			.691		-15.3	.366		5.73	
31	8 (9)	7 (8.5)		4.31	.005	2.93			1.90		-.0614	-.0446	4.91	.017	1.14	-.316		18.5	-.590			.346		-54.0	1.46		3.22	
32	9.5 (9.5)	10		4.52	-.027	5.54			1.21		-.0535	-.0235	5.56	.004	1.23	-.323		20.4	-.844			.212		-102	2.92		2.06	
33	3 (2.5)	2 (2)		4.37	.13	.81			2.79		-.0605	-.0983	4.59	.125	1.05	-.310	-.02050	19.0	+.051	-.775		.723	1.6241	-14.3	.859		5.73	-1.4253
34	2 (2.5)	4 (4.5)		4.33	.090	2.96			1.90		-.0593	-.046	4.94	.095	1.14	-.309		18.6	-.304	-.775		.358		-52.1	3.44		3.22	
35	5 (6)	5 (6)		4.42	.010	5.01			1.19		-.0550	-.0262	5.40	.059	1.22	-.303		19.4	-.990	-.775		.221		-88.3	6.87		2.06	
36	5 (6)	5 (5)		1.13	.20	1.99			2.86		-.0563	+.694	1.10	.217	.975	-.121	-.00134	1.23	+.014	-.317		-.111	.1065	-4.83	.809		9.16	-.09343
37		7 (8)		1.13	.062	3.37			4.13		-.0534	+.976	1.08	.052	.957			1.23	-.298			-.165		-8.17	3.23		13.6	
37a	8 (8)			1.02	.10	3.33			4.06		-.0639	+1.165	.968	.097	.949			.990	-.234			-.165		-8.08	3.23		13.6	
38	8 (8)	7 (8)		1.33	.10	4.15			12.3		-.0388	+2.14	1.28	.080	.961			1.72	-.172			-.504		-10.1	6.47		40.7	
39	5 (4.5)	3 (3)		1.96	.085	1.20			2.88		-.0732	+.303	1.92	.088	.980	-.159	-.00504	3.79	-.142			-.186	.3992	-7.24	.484		9.17	-.3504
39a	4 (4)	3 (3)		1.96	.085	1.20			2.88		-.0732	+.303	1.92	.088	.980	-.159		3.79	-.142			-.186		-7.24	.484		9.17	
40	3 (3)	2.5 (3)		2.08	.042	2.90			3.94		-.0621	+.375	1.99	.038	.955	-.160		4.28	-.302			-.274		-17.5	1.93		13.6	
41	8 (8)	8 (9)		2.22	0	5.52			11.1		-.0519	+.934	2.06	-.024	.925	-.163		4.88	-.480			-.844		-33.3	3.87		40.7	
42	2 (2)	2 (2)		4.23	.058	.86			2.74		-.0664	+.0769	4.17	.059	.986	-.311	-.02083	17.8	-.197	-.376		-.250	1.6505	-15.5	.426		9.15	-1.4484
43	3 (3)	3 (3)		4.43	.038	2.77			4.00		-.0584	+.1003	4.27	.037	.963	-.308		19.6	-.348	-.376		-.371		-50.0	1.70		13.6	
44	8 (9)	8 (9)		4.54	.032	5.65			10.7		-.0530	+.272	4.20	.029	.927	-.302		20.6	-.388	-.376		-1.14		-102	3.41		40.7	
45	7 (8)	8 (9)		1.07	.18	2.42			3.61		-.1219	+1.39	1.00	.205	.939	-.121	-.00269	1.10	-.052	-.317		-.287	.2129	-5.90	1.63		12.9	-.1869
46	7 (7)	5.5 (6.5)		1.03	.10	2.22			3.61		-.0661	+1.49	.967	.105	.939		-.00134	1.01	-.232			-.287	.1065	-5.42	1.63		12.9	-.09343
47	7 (7)	8 (9)		.95	.14	2.24			3.51		-.0381	+1.73	.878	.164	.924		-.000672	.852	-.172			-.287	.05323	-5.47	1.63		12.9	-.04672
47a		6.5 (7)		.95	.14	2.24			3.51		-.0381	+1.73	.878	.164	.924		-.000672	.852	-.172			-.287	.05323	-5.47	1.63		12.9	-.04672
48	7 (7)	6 (6)		1.07	.20	1.74			3.74		-.0158	+1.42	1.02	.215	.955		-.000336	1.10	-.100			-.287	.0266	-4.25	1.63		12.9	-.0234
48a	7 (7)	7 (7)		1.07	.20	1.74			3.74		-.0158	+1.42	1.02	.215	.955		-.000336	1.10	-.100			-.287	.0266	-4.25	1.63		12.9	-.0234
49	7 (7)	7 (8)		2.03	.044	1.67			3.72		-.1309	+.543	1.93	.042	.950	-.159	-.01042	4.07	-.297			-.475	.7752	-10.3	.985		12.9	-.7241
50	3 (3)	4 (4.5)		2.00	.036	1.70			3.70		-.0692	+.558	1.90	.033	.949		-.00504	3.95	-.332			-.475	.3992	-10.5	.985		12.9	-.3504
51	4 (4)	5 (5)		2.03	.036	1.66			3.72		-.0359	+.546	1.93	.032	.950		-.00269	4.07	-.330			-.475	.2129	-10.3	.985		12.9	-.1869
52	4 (4)	5 (6)		2.00	.030	1.61			3.72		-.0185	+.560	1.90	.025	.950		-.00134	3.95	-.356			-.475	.1065	-9.90	.985		12.9	-.09343
53	6 (7)	8 (10)		4.23	.018	1.46			3.80		-.1042	+.154	4.06	.016	.960	-.313	-.0333	17.9	-.478			-.637	2.635	-26.9	.731		12.9	-2.313
54	9 (8)			4.40	.020	1.49			3.81		-.0606	+.144	4.24	.018	.964		-.02083	19.3	-.470			-.637	1.6505	-27.4	.731		12.9	-1.448
54a		5.5 (6)		4.40	.048	1.49			3.81		-.0606	+.144	4.24	.050	.964		-.02083	19.3	-.208			-.637	1.6505	-27.4	.731		12.9	-1.448
55	6 (6)	3 (3)		4.27	.020	1.37			3.82		-.0322	+.152	4.12	.018	.965		-.01042	18.2	-.459			-.637	.8251	-25.2	.731		12.9	-.7241
56	7 (6)	4 (4)		4.31	.020	1.44			3.80		-.0153	+.150	4.15	.018	.962		-.00504	18.5	-.466			-.637	.3992	-26.5	.731		12.9	-.3504
57 thru 94				1.97	.083	1.41	.34		7.40	5.00	-.0714	+.174	1.95	.083	.99	-.156		3.85	0	-.171		-.0585		-10.0	.403	-2.56	8.15	

TABLE 6 IN-FLIGHT EVALUATION - LONGITUDINAL CHARACTERISTICS

Flight Config.	Pilot Rating Pilot A	ω_{sp} 1/sec	ω_{sp}^2 1/sec^2	ζ_{sp}	$2\zeta_{sp}\omega_{sp}$ 1/sec	τ_θ sec	$K'_{\delta_{FES}}$ deg / sec^3-lb	$1/K_{n_{z_{F_{ES}}}}$ lb/g	M_α 1/sec^2	$M_{\dot\alpha}$ 1/sec	M_q 1/sec	$M_{\delta_{ES}}$ 1/sec^2	L_α 1/sec	$L_{\delta_{ES}}$ 1/sec	V ft/sec	IAS knots	$(n_z/\alpha)_{ss}$ g/rad Pilot A
F1	4 (4)	2.20	4.84	.31	1.38	.832	5.05	2.88	-5.14	-.39	.24	4.21	1.23	-.0245	613	250	22.88
F2	9	.447	.200	.25	.22	.814	5.17	.116	-1.71	-.20	1.22	↓	1.24	↓	↓	↓	23.58
F3	8	4.97	24.8	-.010	-.10	.815	5.15	14.5	-26.4	.33	1.15	↓	1.38	↓	↓	↓	23.50
F4	4.5	2.64	6.97	.03	.16	.892	4.72	4.44	-8.15	0	1.01	↓	1.17	↓	↓	↓	21.50
F5	6	1.49	2.22	.23	.70	.888	4.73	1.41	-3.05	-.29	.73	↓	1.14	↓	↓	↓	21.45
F6	9.5	4.79	23.0	-.076	-.73	.888	4.73	14.6	-25.2	.30	1.70	↓	1.27	↓	↓	↓	21.60
F6a	5	1.68	2.82	.25	.84	-	-	-	-	-	-	↓	-	↓	↓	↓	
F7	8 (8)	1.80	3.23	.035	.13	.817	5.14	1.89	-5.03	-.32	1.44	↓	1.25	↓	↓	↓	23.44
F8	4	3.73	13.9	.048	.36	.782	5.38	7.78	-15.4	-.10	1.11	↓	1.37	↓	↓	↓	24.53
F9	9 (9)	.642	.413	.42	.54	.834	5.04	.247	-1.89	-.55	1.22	↓	1.21	↓	↓	↓	22.99
F54	8.5 (9)	-	-.334	-	.51	.787	5.34	-	-1.89	-.45	1.22	↓	1.28	↓	↓	↓	24.33
F10	7 (7)	1.32	1.74	.18	.48	.830	5.07	1.03	-2.63	.01	.73	↓	1.22	↓	↓	↓	23.03
F56	7 (7)	1.31	1.72	.23	.60	.803	5.24	.988	-2.64	-.07	.73	↓	1.26	↓	↓	↓	23.80
F11	4.5 (5)	1.89	3.58	.25	.95	.830	5.07	2.13	-3.88	.04	.24	↓	1.23	↓	↓	↓	23.02
F51	3.5 (3)	1.78	3.17	.24	.85	.828	5.08	1.88	-3.47	.14	.24	↓	1.23	↓	↓	↓	23.06
F12a	9.5 (9.5)	1.04	1.08	.17	.35	.873	4.82	.674	-2.21	-.16	.97	↓	1.16	↓	↓	↓	21.96
F12	7 (8.5)	.527	.278	.59	.62	.950	3.35	.302	-1.31	-.53	.97	3.20	1.06	-.0290	507	205	16.65
F13	3.5 (3.5)	1.34	1.80	.30	.80	.920	3.48	1.88	-2.32	-.16	.47	3.20	1.11	-.0290	↓	↓	17.22
F53	6 (6)	1.40	1.96	.33	.92	.909	7.02	1.02	-2.49	-.27	.47	6.40	1.12	-.0580	↓	↓	17.35
F14	2.5 (2.5)	2.00	4.00	.30	1.20	.970	3.30	4.41	-3.99	-.12	-.01	3.20	1.07	-.0290	↓	↓	16.28
F15	7 (7)	-	-.291	-	.39	1.32	1.44	-	-.85	-.35	.73	1.91	.77	-.0372	398	160	9.45
F55	8.5 (8.5)	-	-.033	-	.26	1.31	2.90	-	-.59	-.22	.73	3.82	.77	-.0744	↓	↓	9.51
F16	5 (5)	1.30	1.69	.24	.62	1.23	3.11	2.52	-1.89	-.01	.24	3.82	.85	-.0744	↓	↓	10.10
F58	5 (4)	1.41	1.99	.26	.73	1.19	1.60	5.77	-2.20	-.09	.24	1.91	.88	-.0372	↓	↓	10.40
F17	3.5 (3.5)	1.91	3.65	.24	.92	1.24	1.53	11.1	-3.44	.19	-.24	1.91	.87	-.0372	↓	↓	9.88
F59	3.5 (3.5)	2.00	4.00	.26	1.04	1.19	1.60	11.6	-3.77	.12	-.25	1.91	.91	-.0372	↓	↓	10.29

NOTE: 1) Pressure altitude, h_p = 25,000 feet

2) Pilot's controls:

a) Two-axis side controller with (δ_{AS}/F_{AS}) = .055 rad/lb or 3.15 deg/lb and (δ_{ES}/F_{ES}) = .0175 rad/lb or 1.0 deg/lb.

b) Rudder pedals with (δ_{RP}/F_{RP}) = .0125 in./lb.

TABLE 7a PERFORMANCE MEASURES - LONGITUDINAL EVALUATIONS

Config.	Pilot	Rating	θ (deg)		ϕ (deg)		β (deg)		δ_{ES} (deg)		δ_{AS} (deg)		$\sqrt{S_{\delta_{ES}}^2 + S_{\delta_{AS}}^2}$
			$\int\|\epsilon\|$	Std. Dev.	$\int\|\epsilon\|$	Std. Dev.	$\int\|\epsilon\|$	Std. Dev.	$\int\|\epsilon\|$	Std. Dev.	$\int\|\epsilon\|$	Std. Dev.	
57	A	10	158.2	2.06	356.8	4.39	773.1	9.01	651.9	4.44	44.3	.598	4.480
58	A	7	85.4	.860	447.8	3.59	1340.5	4.44	803.9	1.89	139.4	1.24	2.260
58	B	9	113.0	1.16	691.4	7.36	333.3	3.90	694.4	.78	175.7	2.23	2.363
59	A	3	61.7	.632	407.8	3.69	964.6	9.73	813.6	1.31	69.4	.82	1.545
60	A	10	310.5	3.30	745.5	5.92	1462.1	14.25	767.7	4.87	81.6	.77	4.930
65	A	3	73.2	.790	343.9	2.88	1190.0	11.8	330.1	1.13	106.6	1.19	1.641
66	A	10	329.4	3.33	395.7	4.04	1412.6	12.25	725.2	6.98	68.0	.986	7.049
68	A	5	120.4	1.40	338.3	3.43	408.2	3.82	463.6	1.24	88.2	.996	1.591
69	A	10	369.4	4.00	488.7	4.77	1195.6	11.9	539.7	4.22	61.9	.698	4.277
70	A	9.5	221.7	2.35	367.4	3.56	1340.1	13.3	281.9	1.94	96.2	1.21	2.286
71	A	9	176.9	1.87	416.0	3.66	1329.6	11.6	438.2	1.74	107.1	1.28	2.160
71	B	10	365.2	3.91	604.1	6.39	1425.7	13.8	235.6	2.20	111.8	1.79	2.842
74	A	10	257.9	2.85	407.5	3.69	1334.4	13.2	499.3	4.04	114.6	1.44	4.289

TABLE 7b PERFORMANCE MEASURES - LATERAL-DIRECTIONAL EVALUATIONS

Config.	Pilot	Rating	θ (deg)		ϕ (deg)		β (deg)		δ_{ES} (deg)		δ_{AS} (deg)		δ_{RP} (in)		$\sqrt{\delta_{ES}^2+\delta_{AS}^2}$
			$\int\lvert\epsilon\rvert$	Std. Dev.	$\int\lvert\epsilon\rvert$	Std. Dev.	$\int\lvert\epsilon\rvert$	Std. Dev.	$\int\lvert\epsilon\rvert$	Std. Dev.	$\int\lvert\epsilon\rvert$	Std. Dev.	$\int\lvert\epsilon\rvert$	Std. Dev.	
9	B	5	111.5	1.14	633.7	6.49	1191.6	11.6	576.0	.783	86.5	1.22	13.2	.141	1.449
11	A	8	70.5	.860	727.9	7.20	1397.9	10.5	645.5	1.13	422.6	5.05	94.1	.742	5.175
18	A	9.5	99.4	1.11	826.8	7.26	967.1	9.33	485.5	1.37	142.8	1.18	24.8	.245	1.808
19a	A	7	117.9	1.24	562.2	5.86	1021.0	9.10	774.5	1.31	307.9	3.58	36.6	.200	3.809
20	A	9	83.0	.89	1030.7	7.85	1035.9	9.45	539.8	1.85	864.1	9.30	43.3	.173	9.460
27	A	6.5	67.9	.704	492.8	4.84	1013.4	8.94	442.6	1.07	95.1	1.18	24.7	.100	1.592
28a	A	9.5	62.2	0	526.9	7.92	866.2	10.9	395.4	1.28	399.4	4.72	19.9	.100	4.890
28	B	9	101.7	1.10	923.3	8.86	538.3	6.11	768.4	1.05	461.6	5.50	14.4	.100	5.599

APPENDIX A
STATISTICAL TESTS AND MEASURES

1. "t" Test of Significance

The "t" test of differences tests the hypothesis that the expected value of the mean of the differences is zero. A value of confidence limits is selected within which the mean of the differences would be expected to occur if the experiment were replicated. The value of "t" for various confidence limits has been calculated, assuming a normal distribution, for various sample sizes and is available in various texts on statistics. If the distribution of the mean of the sample of differences could not include zero (value of "t" greater than that for the selected confidence limits), then there is a significant difference between the paired samples. Confidence limits of 95% are commonly used, although it is generally stated as a 5% probability of error,or "significant at 5% probability level". If a 1% probability error is stated, then a significant difference for 99% confidence limits is indicated. A statement of significance at the 1% probability level implies a "more significant" statement with less probability of error than one at the 5% probability level.

For this particular "t" test of differences,

$$t = \frac{\bar{d}\sqrt{N}}{S_d} \quad , \text{ degrees of freedom} = N - 1 \qquad (1)$$

where

$\bar{d}$ = Mean of the differences
N = Number of comparisons
S_d = Standard deviation of differences

The more general form of the "t" test may be found in References 1 and 2. Tables of the distribution of "t" as a function of degrees of freedom as given in each of these references were used for the analyses in this report.

2. Sample Correlation Coefficient

The sample correlation coefficient is a measure of the dispersion of a sample of data. It may be expressed as follows:

$$r = \frac{\Sigma XY - \frac{(\Sigma X)(\Sigma Y)}{N}}{\sqrt{\left(\Sigma X^2 - \frac{(\Sigma X)^2}{N}\right)\left(\Sigma Y^2 - \frac{(\Sigma Y)^2}{N}\right)}} \qquad (2)$$

where

r = sample correlation coefficient
X = value of one variable
Y = value of second variable
N = number of comparisons

The coefficient, r, may have values from -1.0 to 1.0. If all data points lie precisely upon a straight line of finite slope, r will be 1.0, with the sign depending upon the direction of the slope of this line. A value of zero indicates that one variable cannot be determined to vary with the other due to scatter of the data.

A test of the null hypothesis, the expected value of correlation coefficient = 0, can be made by the "t" test. As presented in Reference 1, this value of t is calculated as follows:

$$t = \frac{r\sqrt{N-2}}{\sqrt{1-r^2}} \quad \text{, degrees of freedom} = N-2$$

Reference 1 (page 174) also presents a table, based upon this calculation of "t", for a range of degrees of freedom at both the 5% and 1% probability levels.

3. Sample Regression Coefficient

The sample regression coefficient is the value of the slope of the line about which the sum of the squares of the deviations of the data points are a minimum ("least squares fit"). This coefficient is normally used when comparing one set of measures with some standard measures. Then, all the error is assumed in the test measures, and a sample regression coefficient relating these test measures to the standard measures may be determined. For the test measure, Y, and the standard measure, X, the sample regression coefficient is defined as:

$$b_{yx} = \frac{\Sigma XY - \frac{\Sigma X \Sigma Y}{N}}{\Sigma X^2 - \frac{(\Sigma X)^2}{N}} \qquad (3)$$

where b_{yx} = sample regression coefficient of Y on X, all error assumed in Y.

N = number of comparisons

For the comparisons of pilot ratings in this report, there is obviously no set of ratings for which the error may be assumed zero. Each set of pilot's ratings contain variability. Therefore, a single regression coefficient can not be presented as relating one set of pilot ratings to another. For purposes of presentation and analysis of the results, both possible coefficients are calculated and both regression lines are indicated on the various figures. The additional sample regression coefficient is defined as:

$$b_{xy} = \frac{\Sigma XY - \frac{\Sigma X \Sigma Y}{N}}{\Sigma Y^2 - \frac{(\Sigma Y)^2}{N}} \qquad (4)$$

where b_{xy} = sample regression coefficient of X on Y, all error assumed in X. Note that this slope is measured from the Y axis rather than the X axis as is the case for b_{yx}.

These coefficients may be tested, via the "t" test, to determine their significant difference from any value of slope, b. The value of "t" is calculated as follows (from Reference 1):

$$t = \frac{b_{yx} - b}{S_{b_{yx}}}, \text{ degrees of freedom} = N - 2 \qquad (5)$$

where $S_{b_{yx}}$ = sample standard deviation of the regression coefficient of Y on X
b = value of slope being tested for.

$$S_{b_{yx}} = \left\{ \frac{\Sigma \left[Y - \frac{\Sigma Y}{N} - b_{yx} \left(X - \frac{\Sigma X}{N} \right) \right]}{(N-2) \left[\Sigma X^2 - \frac{(\Sigma X)^2}{N} \right]} \right\}^{1/2} \qquad (6)$$

For the sample regression coefficient of X on Y,

$$t = \frac{b_{xy} - b}{S_{b_{xy}}}, \text{ degrees of freedom} = N - 2 \qquad (7)$$

$$S_{b_{xy}} = \left\{ \frac{\Sigma \left[X - \frac{\Sigma X}{N} - b_{xy} \left(Y - \frac{\Sigma Y}{N} \right) \right]}{(N-2) \left[\Sigma Y^2 - \frac{(\Sigma Y)^2}{N} \right]} \right\}^{1/2} \qquad (8)$$

There is a direct relationship between the sample regression coefficients and the sample correlation coefficient, r, of section 2 of this appendix. Comparison of equation (2) with equations (3) and (4) of this appendix indicates that:

$$r = \sqrt{b_{yx} \, b_{xy}} \qquad (9)$$

Thus, r is the geometric mean of the two regression coefficients. The nearer the two regression lines approach each other, the closer the correlation coefficient approaches a value of 1.0. As noted after equation (4) above, the

two slopes b_{yx} and b_{xy} are measured from the X and Y axes respectively. Thus, for a value of r = 1.0, the following relation must exist:

$$b_{xy} = \left. \frac{1}{b_{yx}} \right|_{\text{for } r = 1} \tag{10}$$

Or, the two regression lines are each defined by the same line.

APPENDIX B

EQUATIONS OF MOTION AND PERTINENT TRANSFER FUNCTIONS

A. Longitudinal Equations of Motion

1. The longitudinal equations of motion may be written as follows:

$$\left(D_{\hat{u}} + s\right)\hat{u} + \left(D_{\alpha} + D_{\dot{\alpha}}\, s\right)\alpha + \left(\frac{g}{V_o}\cos\gamma_o + D_q\, s\right)\theta = -D_{\delta_e}\,\delta_e$$

$$L_{\hat{u}}\,\hat{u} + \left[L_{\alpha} + \left(L_{\dot{\alpha}} + 1\right)s\right]\alpha + \left[\frac{g}{V_o}\sin\gamma_o + \left(L_q - 1\right)s\right]\theta = -L_{\delta_e}\,\delta_e$$

$$\left(M_{\hat{u}} + M_{\dot{\hat{u}}}\, s\right)\hat{u} + \left(M_{\alpha} + M_{\dot{\alpha}}\, s\right)\alpha + \left(M_q\, s - s^2\right)\theta = -M_{\delta_e}\,\delta_e$$

The above equations are written about orthogonal axes fixed in the airplane with the origin at the center of gravity, the X axis parallel to the resultant velocity vector at t = 0 (i.e., $\theta_o = \gamma_o$), the Z axis downward, and the Y axis out the right wing. Note that:

$$\hat{u} = \frac{1}{V_o}\,u(s)$$

$$\alpha = \alpha(s) = \frac{1}{V_o}\,w(s)$$

$$\theta = \theta(s)$$

$$\delta_e = \delta_e(s)$$

Complete transfer functions for the assumed equations of motion are as follows:

$$\frac{\hat{u}}{\delta_e} = \frac{1}{\Delta_{long}}\left\{\left[-D_{\delta_e}\left(1 + L_{\dot{\alpha}}\right) + L_{\delta_e} D_{\dot{\alpha}}\right]s^3 + \left[D_{\delta_e}\left(L_{\dot{\alpha}}\, M_q - L_{\alpha} + M_q - M_{\dot{\alpha}}\, L_q + M_{\dot{\alpha}}\right)\right.\right.$$
$$+ L_{\delta_e}\left(D_{\alpha} - D_{\dot{\alpha}}\, M_q + M_{\dot{\alpha}}\, D_q\right) + M_{\delta_e}\left(D_{\dot{\alpha}}\, L_q - D_{\dot{\alpha}} - L_{\dot{\alpha}}\, D_q - D_q\right)\Big]s^2$$
$$+\left[D_{\delta_e}\left(L_{\alpha}\, M_q - M_{\alpha}\, L_q + M_{\alpha} - M_{\dot{\alpha}}\,\frac{g}{V_o}\sin\gamma_o\right) + L_{\delta_e}\left(M_{\alpha} D_q - D_{\alpha} M_q - M_{\dot{\alpha}}\,\frac{g}{V_o}\cos\gamma_o\right)\right.$$
$$\left. + M_{\delta_e}\left(D_{\alpha} L_q - D_{\alpha} + D_{\dot{\alpha}}\,\frac{g}{V_o}\sin\gamma_o - L_{\alpha} D_q - L_{\dot{\alpha}}\,\frac{g}{V_o}\cos\gamma_o - \frac{g}{V_o}\cos\gamma_o\right)\right]s$$
$$\left.+\left[-D_{\delta_e}\left(M_{\alpha}\,\frac{g}{V_o}\sin\gamma_o\right) + L_{\delta_e}\left(M_{\alpha}\,\frac{g}{V_o}\cos\gamma_o\right) + M_{\delta_e}\left(-L_{\alpha}\,\frac{g}{V_o}\cos\gamma_o + D_{\alpha}\,\frac{g}{V_o}\sin\gamma_o\right)\right]\right\}$$

$$\frac{\alpha}{\delta_e} = \frac{1}{\Delta_{long}} \left\{ -L_{\delta_e} s^3 + \left[D_{\delta_e} \left(L_{\hat{u}} + M_{\dot{\hat{u}}} L_q - M_{\hat{u}} \right) + L_{\delta_e} \left(-D_{\hat{u}} + M_q - M_{\dot{\hat{u}}} D_q \right) + M_{\delta_e} \left(1 - L_{\dot{q}} \right) \right] s^2 \right.$$
$$+ \left[D_{\delta_e} \left(M_{\hat{u}} L_q - L_{\hat{u}} M_q - M_{\hat{u}} + M_{\dot{\hat{u}}} \frac{g}{V_o} \sin\gamma_o \right) + L_{\delta_e} \left(D_{\hat{u}} M_q - M_{\hat{u}} D_q - M_{\dot{\hat{u}}} \frac{g}{V_o} \cos\gamma_o \right) \right.$$
$$\left. + M_{\delta_e} \left(L_{\hat{u}} D_q - D_{\hat{u}} L_q + D_{\hat{u}} - \frac{g}{V_o} \sin\gamma_o \right) \right] s + \left[D_{\delta_e} \left(M_{\hat{u}} \frac{g}{V_o} \sin\gamma_o \right) + L_{\delta_e} \left(-M_{\hat{u}} \frac{g}{V_o} \cos\gamma_o \right) \right.$$
$$\left. \left. + M_{\delta_e} \left(-D_{\hat{u}} \frac{g}{V_o} \sin\gamma_o + L_{\hat{u}} \frac{g}{V_o} \cos\gamma_o \right) \right] \right\}$$

$$\frac{\theta}{\delta_e} = \frac{1}{\Delta_{long}} \left\{ \left[D_{\delta_e} \left(-M_{\dot{\hat{u}}} - M_{\hat{u}} L_{\dot{\alpha}} \right) + L_{\delta_e} \left(-M_{\dot{\alpha}} + M_{\dot{\hat{u}}} D_{\dot{\alpha}} \right) + M_{\delta_e} \left(1 + L_{\dot{\alpha}} \right) \right] s^2 \right.$$
$$+ \left[D_{\delta_e} \left(L_{\dot{\hat{u}}} M_{\dot{\alpha}} - M_{\hat{u}} L_{\dot{\alpha}} - M_{\hat{u}} - M_{\dot{\hat{u}}} L_\alpha \right) + L_{\delta_e} \left(-M_\alpha - D_{\dot{\hat{u}}} M_{\dot{\alpha}} + M_{\hat{u}} D_{\dot{\alpha}} + M_{\dot{\hat{u}}} D_\alpha \right) \right.$$
$$\left. + M_{\delta_e} \left(D_{\hat{u}} L_{\dot{\alpha}} + D_{\dot{\hat{u}}} + L_\alpha - L_{\dot{\hat{u}}} D_{\dot{\alpha}} \right) \right] s + \left[D_{\delta_e} \left(L_{\hat{u}} M_\alpha - M_{\hat{u}} L_\alpha \right) \right.$$
$$\left. \left. + L_{\delta_e} \left(M_{\dot{\hat{u}}} D_\alpha - D_{\dot{\hat{u}}} M_\alpha \right) + M_{\delta_e} \left(D_{\hat{u}} L_\alpha - L_{\dot{\hat{u}}} D_\alpha \right) \right] \right\}$$

$$\Delta_{long} = \left(1 + L_{\dot{\alpha}} \right) s^4 + \left(D_{\dot{\hat{u}}} L_{\dot{\alpha}} + D_{\hat{u}} + L_\alpha - L_{\dot{\alpha}} M_{\dot{q}} - M_q + M_{\dot{\alpha}} L_q - M_{\dot{\alpha}} - L_{\dot{\hat{u}}} D_{\dot{\alpha}} \right.$$
$$\left. - M_{\dot{\hat{u}}} D_{\dot{\alpha}} L_q + M_{\dot{\hat{u}}} D_{\dot{\alpha}} + M_{\dot{\hat{u}}} L_{\dot{\alpha}} D_q + M_{\hat{u}} D_q \right) s^3 + \left(D_{\dot{\hat{u}}} L_\alpha - D_{\hat{u}} L_{\dot{\alpha}} M_q \right.$$
$$- D_{\dot{\hat{u}}} M_q + D_{\hat{u}} M_{\dot{\alpha}} L_q - D_{\hat{u}} M_{\dot{\alpha}} - L_\alpha M_{\dot{q}} + M_\alpha L_q - M_\alpha + M_{\dot{\alpha}} \frac{g}{V_o} \sin\gamma_o$$
$$- L_{\hat{u}} D_\alpha + L_{\dot{\hat{u}}} D_{\dot{\alpha}} M_q - L_{\dot{\hat{u}}} M_{\dot{\alpha}} D_q - M_{\dot{\hat{u}}} D_{\dot{\alpha}} L_q + M_{\dot{\hat{u}}} D_{\dot{\alpha}} + M_{\dot{\hat{u}}} L_{\dot{\alpha}} D_q$$
$$+ M_{\hat{u}} D_q - M_{\dot{\hat{u}}} D_\alpha L_q + M_{\hat{u}} D_\alpha - M_{\dot{\hat{u}}} D_{\dot{\alpha}} \frac{g}{V_o} \sin\gamma_o + M_{\dot{\hat{u}}} L_\alpha D_q$$
$$\left. + M_{\dot{\hat{u}}} L_{\dot{\alpha}} \frac{g}{V_o} \cos\gamma_o + M_{\hat{u}} \frac{g}{V_o} \cos\gamma_o \right) s^2 + \left(D_{\dot{\hat{u}}} M_\alpha L_q - D_{\hat{u}} L_\alpha M_{\dot{q}} \right.$$
$$- D_{\dot{\hat{u}}} M_\alpha + D_{\hat{u}} M_{\dot{\alpha}} \frac{g}{V_o} \sin\gamma_o + M_\alpha \frac{g}{V_o} \sin\gamma_o + L_{\hat{u}} D_\alpha M_q - L_{\hat{u}} M_\alpha D_q$$
$$- L_{\dot{\hat{u}}} M_{\dot{\alpha}} \frac{g}{V_o} \cos\gamma_o - M_{\dot{\hat{u}}} D_\alpha L_q + M_{\hat{u}} D_\alpha - M_{\dot{\hat{u}}} D_{\dot{\alpha}} \frac{g}{V_o} \sin\gamma_o + M_{\dot{\hat{u}}} L_\alpha D_q$$
$$\left. + M_{\dot{\hat{u}}} L_{\dot{\alpha}} \frac{g}{V_o} \cos\gamma_o + M_{\hat{u}} \frac{g}{V_o} \cos\gamma_o - M_{\hat{u}} D_\alpha \frac{g}{V_o} \sin\gamma_o + M_{\hat{u}} L_\alpha \frac{g}{V_o} \cos\gamma_o \right) s$$
$$+ \left(-L_{\dot{\hat{u}}} M_\alpha \frac{g}{V_o} \cos\gamma_o + D_{\hat{u}} M_\alpha \frac{g}{V_o} \sin\gamma_o - M_{\dot{\hat{u}}} D_\alpha \frac{g}{V_o} \sin\gamma_o + M_{\hat{u}} L_\alpha \frac{g}{V_o} \cos\gamma_o \right)$$

2. Approximate transfer functions may be written as follows for the assumptions that:

$$D_{\dot{\alpha}} = D_q = L_{\dot{\alpha}} = L_q = 0 \text{ and } \gamma_o = 0$$

$$\frac{\hat{u}}{\delta_e} = \frac{1}{\Delta_{long}}\left\{-D_{\delta_e}s^3 + \left[-D_{\delta_e}\left(L_\alpha - M_q - M_{\dot{\alpha}}\right) + L_{\delta_e}D_\alpha\right]s^2 + \left[D_{\delta_e}\left(L_\alpha M_q + M_\alpha\right) + L_{\delta_e}\left(-D_\alpha M_q + M_{\dot{\alpha}}\frac{g}{V_o}\right) + M_{\delta_e}\left(-D_\alpha - \frac{g}{V_o}\right)\right]s + \left[L_{\delta_e}M_\alpha\frac{g}{V_o} - M_{\delta_e}L_\alpha\frac{g}{V_o}\right]\right\}$$

$$\frac{\alpha}{\delta_e} = \frac{1}{\Delta_{long}}\left\{-L_{\delta_e}s^3 + \left[D_{\delta_e}\left(L_{\hat{u}} - M_{\hat{u}}\right) + L_{\delta_e}\left(-D_{\hat{u}} + M_q\right) + M_{\delta_e}\right]s^2 + \left[D_{\delta_e}\left(-M_{\hat{u}} - L_{\hat{u}}M_q\right) + L_{\delta_e}\left(D_{\hat{u}}M_q + M_{\hat{u}}\frac{g}{V_o}\right) + M_{\delta_e}\left(D_{\hat{u}}\right)\right]s + \left[-L_{\delta_e}M_{\hat{u}}\frac{g}{V_o} + M_{\delta_e}\left(L_{\hat{u}}\frac{g}{V_o}\right)\right]\right\}$$

$$\frac{\theta}{\delta_e} = \frac{1}{\Delta_{long}}\left\{\left[-D_{\delta_e}M_{\hat{u}} - L_{\delta_e}M_{\dot{\alpha}} + M_{\delta_e}\right]s^2 + \left[D_{\delta_e}\left(L_{\hat{u}}M_{\dot{\alpha}} - M_{\hat{u}} - M_{\hat{u}}L_\alpha\right) + L_{\delta_e}\left(-M_\alpha - D_{\hat{u}}M_{\dot{\alpha}} + M_{\hat{u}}D_\alpha\right) + M_{\delta_e}\left(D_{\hat{u}} + L_\alpha\right)\right]s + \left[D_{\delta_e}\left(L_{\hat{u}}M_\alpha - M_{\hat{u}}L_\alpha\right) + L_{\delta_e}\left(M_{\hat{u}}D_\alpha - D_{\hat{u}}M_\alpha\right) + M_{\delta_e}\left(D_{\hat{u}}L_\alpha - L_{\hat{u}}D_\alpha\right)\right]\right\}$$

$$\Delta_{long} = s^4 + \left(D_{\hat{u}} + L_\alpha - M_q - M_{\dot{\alpha}}\right)s^3 + \left(D_{\hat{u}}L_\alpha - D_{\hat{u}}M_q - D_{\hat{u}}M_{\dot{\alpha}} - L_\alpha M_q - M_\alpha - L_{\hat{u}}D_\alpha + M_{\hat{u}}D_\alpha + M_{\hat{u}}\frac{g}{V_o}\right)s^2 + \left(-D_{\hat{u}}M_\alpha - D_{\hat{u}}L_\alpha M_q + L_{\hat{u}}D_\alpha M_q - L_{\hat{u}}M_{\dot{\alpha}}\frac{g}{V_o} + M_{\hat{u}}D_\alpha + M_{\hat{u}}\frac{g}{V_o} + M_{\hat{u}}L_\alpha\frac{g}{V_o}\right)s + \left(-L_{\hat{u}}M_\alpha\frac{g}{V_o} + M_{\hat{u}}L_\alpha\frac{g}{V_o}\right)$$

3. Further simplification is often possible when:

$$D_{\delta_e} = M_{\hat{u}} = 0$$

in addition to the above assumptions that:

$$D_{\dot{\alpha}} = D_q = L_{\dot{\alpha}} = L_q = 0 \text{ and } \gamma_o = 0$$

The transfer functions then take the following forms:

$$\frac{\hat{u}}{\delta_e} = \frac{1}{\Delta_{long}} \left\{ L_{\delta_e} D_{\dot{\alpha}} s^2 + \left[L_{\delta_e} \left(-D_{\dot{\alpha}} M_q + M_{\dot{\alpha}} \frac{g}{V_o} \right) + M_{\delta_e} \left(-D_\alpha - \frac{g}{V_o} \right) \right] s + \left[L_{\delta_e} M_\alpha \frac{g}{V_o} - M_{\delta_e} L_\alpha \frac{g}{V_o} \right] \right\}$$

$$\frac{\alpha}{\delta_e} = \frac{1}{\Delta_{long}} \left\{ -L_{\delta_e} s^3 + \left[L_{\delta_e} \left(-D_{\hat{u}} + M_q \right) + M_{\delta_e} \right] s^2 + \left[L_{\delta_e} D_{\hat{u}} M_q + M_{\delta_e} D_{\hat{u}} \right] s + \left[-L_{\delta_e} M_{\hat{u}} \frac{g}{V_o} + M_{\delta_e} L_{\hat{u}} \frac{g}{V_o} \right] \right\}$$

$$\frac{\theta}{\delta_e} = \frac{1}{\Delta_{long}} \left\{ \left[-L_{\delta_e} M_{\dot{\alpha}} + M_{\delta_e} \right] s^2 + \left[L_{\delta_e} \left(-M_\alpha - D_{\hat{u}} M_{\dot{\alpha}} \right) + M_{\delta_e} \left(D_{\hat{u}} + L_\alpha \right) \right] s + \left[L_{\delta_e} \left(M_{\hat{u}} D_\alpha - D_{\hat{u}} M_\alpha \right) + M_{\delta_e} \left(D_{\hat{u}} L_\alpha - L_{\hat{u}} D_\alpha \right) \right] \right\}$$

$$\Delta_{long} = s^4 + \left(D_{\hat{u}} + L_\alpha - M_q - M_{\dot{\alpha}} \right) s^3 + \left(D_{\hat{u}} L_\alpha - D_{\hat{u}} M_q - D_{\hat{u}} M_{\dot{\alpha}} - L_\alpha M_q - M_\alpha - L_{\hat{u}} D_{\dot{\alpha}} \right) s^2 + \left(-D_{\hat{u}} M_{\dot{\alpha}} - D_{\hat{u}} L_\alpha M_q + L_{\hat{u}} D_{\dot{\alpha}} M_q - L_{\hat{u}} M_{\dot{\alpha}} \frac{g}{V_o} + M_{\hat{u}} D_\alpha + M_{\hat{u}} \frac{g}{V_o} \right) s + \left(-L_{\hat{u}} M_\alpha \frac{g}{V_o} + M_{\hat{u}} L_\alpha \frac{g}{V_o} \right)$$

In factored form, the transfer functions may be written:

$$\frac{\hat{u}}{\delta_e} = \frac{1}{\Delta_{long}} \left\{ A_{\hat{u}} \left(s + \frac{1}{T_{\hat{u}_1}} \right) \left(s + \frac{1}{T_{\hat{u}_2}} \right) \right\}$$

$$\frac{\alpha}{\delta_e} = \frac{1}{\Delta_{long}} \left\{ A_\alpha \left(s + \frac{1}{T_\alpha} \right) \left(s^2 + 2 \zeta_\alpha \omega_\alpha s + \omega_\alpha^2 \right) \right\}$$

$$\frac{\theta}{\delta_e} = \frac{1}{\Delta_{long}} \left\{ A_\theta \left(s + \frac{1}{T_{\theta_1}} \right) \left(s + \frac{1}{T_{\theta_2}} \right) \right\}$$

$$\Delta_{long} = \left(s^2 + 2 \zeta_p \omega_p s + \omega_p^2 \right) \left(s^2 + 2 \zeta_{sp} \omega_{sp} s + \omega_{sp}^2 \right)$$

4. If constant speed is assumed (i.e., $\Omega = 0$), the conventional longitudinal short period approximations are obtained:

$$\frac{\alpha}{\delta_e} = \frac{-L_{\delta_e} s + \left(M_{\delta_e} + L_{\delta_e} M_q\right)}{s^2 + \left(L_\alpha - M_q - M_{\dot{\alpha}}\right) s + \left(-L_\alpha M_q - M_\alpha\right)}$$

$$\frac{\theta}{\delta_e} = \frac{\left(M_{\delta_e} - L_{\delta_e} M_{\dot{\alpha}}\right) s + \left(-L_{\delta_e} M_\alpha + M_{\delta_e} L_\alpha\right)}{s\left[s^2 + \left(L_\alpha - M_q - M_{\dot{\alpha}}\right) s + \left(-L_\alpha M_q - M_\alpha\right)\right]}$$

In factored form, these transfer functions are usually written:

$$\frac{\alpha}{\delta_e} = \frac{K_{\alpha_{\delta_e}} \left(\tau_\alpha s + 1\right)}{\frac{s^2}{\omega_{sp}^2} + \frac{2\zeta_{sp}}{\omega_{sp}} s + 1}$$

$$\frac{\theta}{\delta_e} = \frac{K_{\theta_{\delta_e}} \left(\tau_\theta s + 1\right)}{s\left(\frac{s^2}{\omega_{sp}^2} + \frac{2\zeta_{sp}}{\omega_{sp}} s + 1\right)}$$

However, when ω_{sp}^2 approaches zero as in this report, it is more convenient to use the form:

$$\frac{\alpha}{\delta_e} = \frac{K'_{\alpha_{\delta_e}} \left(\tau_\alpha s + 1\right)}{s^2 + 2\zeta_{sp}\omega_{sp} s + \omega_{sp}^2}$$

$$\frac{\theta}{\delta_e} = \frac{K'_{\theta_{\delta_e}} \left(\tau_\theta s + 1\right)}{s\left(s^2 + 2\zeta_{sp}\omega_{sp} s + \omega_{sp}^2\right)}$$

Where

$$\omega_{sp}^2 = -L_\alpha M_q - M_\alpha$$

$$2\zeta_{sp}\omega_{sp} = L_\alpha - M_q - M_{\dot{\alpha}}$$

$$K'_{\alpha_{\delta_e}} = M_{\delta_e} + L_{\delta_e} M_q$$

$$= \omega_{sp}^2 K_{\alpha_{\delta_e}}$$

$$K'_{\dot\theta_{\delta_e}} = -L_{\delta_e} M_\alpha + M_{\delta_e} L_\alpha$$
$$= \omega_{sp}^2 \, K_{\dot\theta_{\delta_e}}$$

$$\tau_\alpha = \frac{-L_{\delta_e}}{M_{\delta_e} + L_{\delta_e} M_q}$$

$$\tau_\theta = \frac{M_{\delta_e} - L_{\delta_e} M_{\dot\alpha}}{-L_{\delta_e} M_\alpha + M_{\delta_e} L_\alpha}$$

5. In simulation experiments which utilize variable stability airplanes, it is pertinent to relate the control effectiveness stability derivatives and transfer function gains to the pilot's cockpit control. This is done by multiplying the control surface derivatives and gains by the "gear ratio", δ_e / δ_{ES}:

$$D_{\delta_{ES}} = \frac{\delta_e}{\delta_{ES}} D_{\delta_e}$$

$$L_{\delta_{ES}} = \frac{\delta_e}{\delta_{ES}} L_{\delta_e}$$

$$M_{\delta_{ES}} = \frac{\delta_e}{\delta_{ES}} M_{\delta_e}$$

$$K'_{\alpha_{\delta_{ES}}} = \frac{\delta_e}{\delta_{ES}} K'_{\alpha_{\delta_e}}$$

$$K'_{\dot\theta_{\delta_{ES}}} = \frac{\delta_e}{\delta_{ES}} K'_{\dot\theta_{\delta_e}}$$

Similarly, the transfer function gains may be related to the pilot's applied stick force, F_{ES}, by multiplying by the control feel gradient, δ_{ES}/F_{ES}:

$$K'_{\alpha_{F_{ES}}} = \frac{\delta_{ES}}{F_{ES}} K'_{\alpha_{\delta_{ES}}}$$

$$K'_{\dot\theta_{F_{ES}}} = \frac{\delta_{ES}}{F_{ES}} K'_{\dot\theta_{\delta_{ES}}}$$

B. Lateral-Directional Equations of Motion

1. The lateral-directional equations of motion may be written as follows (from References 4 and 8):

$$\left(Y_\beta - s\right)\beta - r + \left(\frac{g}{V_o} + \alpha_o\, s\right)\phi = -Y_{\delta_{AS}}\,\delta_{AS} - Y_{\delta_{RP}}\,\delta_{RP} \tag{1}$$

$$\left(N'_\beta + N'_{\dot\beta}\, s\right)\beta + \left(N'_r - s\right) r + N'_p\, s\,\phi = -N'_{\delta_{AS}}\,\delta_{AS} - N'_{\delta_{RP}}\,\delta_{RP} \tag{2}$$

$$\left(L'_\beta + L'_{\dot\beta}\, s\right)\beta + L'_r\, r + \left(L'_p\, s - s^2\right)\phi = -L'_{\delta_{AS}}\,\delta_{AS} - L'_{\delta_{RP}}\,\delta_{RP} \tag{3}$$

Complete transfer functions of pertinent aircraft responses to control inputs are as follows:

$$\begin{aligned}\frac{\beta}{\delta_{AS}} = \frac{1}{\Delta}\Big\{ & Y_{\delta_{AS}}\, s^3 + \left[-N'_{\delta_{AS}} + \alpha_o\, L'_{\delta_{AS}} - Y_{\delta_{AS}}\left(L'_p + N'_r\right)\right] s^2 \\ & + \left[N'_{\delta_{AS}}\, L'_p - L'_{\delta_{AS}}\, N'_p + \alpha_o\left(N'_{\delta_{AS}}\, L'_r - L'_{\delta_{AS}}\, N'_r\right)\right. \\ & \left. + \left(g/V_o\right) L'_{\delta_{AS}} - Y_{\delta_{AS}}\left(N'_p\, L'_r - N'_r\, L'_p\right)\right] s \\ & + g/V_o\left[N'_{\delta_{AS}}\, L'_r - L'_{\delta_{AS}}\, N'_r\right]\Big\}\end{aligned} \tag{4}$$

$$\begin{aligned}\frac{r}{\delta_{AS}} = \frac{1}{\Delta}\Big\{ & \left[N'_{\delta_{AS}} + Y_{\delta_{AS}} N'_{\dot\beta}\right] s^3 + \left[L'_{\delta_{AS}}\, N'_p - N'_{\delta_{AS}}\left(L'_p + Y_\beta\right)\right. \\ & \left. + \alpha_o\left(L'_{\delta_{AS}}\, N'_{\dot\beta} - N'_{\delta_{AS}}\, L'_{\dot\beta}\right) + Y_{\delta_{AS}}\left(N'_p\, L'_{\dot\beta} - N'_{\dot\beta}\, L'_p + N'_\beta\right)\right] s^2 \\ & + \left[Y_\beta\left(N'_{\delta_{AS}}\, L'_p - L'_{\delta_{AS}}\, N'_p\right) + \alpha_o\left(L'_{\delta_{AS}}\, N'_\beta - N'_{\delta_{AS}}\, L'_\beta\right)\right. \\ & + g/V_o\left(L'_{\delta_{AS}}\, N'_{\dot\beta} - N'_{\delta_{AS}}\, L'_{\dot\beta}\right) + Y_{\delta_{AS}}\left(N'_p\, L'_\beta - N'_{\dot\beta}\, L'_p\right)\Big] s \\ & \left. + g/V_o\left[L'_{\delta_{AS}}\, N'_\beta - N'_{\delta_{AS}}\, L'_\beta\right]\right\}\end{aligned} \tag{5}$$

$$\frac{\phi}{\delta_{AS}} = \frac{1}{\Delta}\left\{\left[L'_{\delta_{AS}} + Y_{\delta_{AS}} L'_{\dot\beta}\right] s^2 + \left[N'_{\delta_{AS}}\left(L'_r - L'_{\dot\beta}\right) - L'_{\delta_{AS}}\left(N'_r - N'_{\dot\beta} + Y_\beta\right)\right.\right.$$
$$\left. + Y_{\delta_{AS}}\left(N'_{\dot\beta} L'_r + L'_\beta - N'_r L'_{\dot\beta}\right)\right] s$$
$$\left. + \left[L'_{\delta_{AS}}\left(N'_\beta + Y_\beta N'_r\right) - N'_{\delta_{AS}}\left(L'_\beta + Y_\beta L'_r\right) + Y_{\delta_{AS}}\left(N'_{\dot\beta} L'_r - N'_r L'_{\dot\beta}\right)\right]\right\} \tag{6}$$

$$\frac{\beta}{\delta_{RP}} = \frac{1}{\Delta}\left\{Y_{\delta_{RP}} s^3 + \left[-N'_{\delta_{RP}} - Y_{\delta_{RP}}\left(L'_p + N'_r\right) + \alpha_0 L'_{\delta_{RP}}\right] s^2\right.$$
$$+\left[N'_{\delta_{RP}} L'_p - L'_{\delta_{RP}} N'_p - Y_{\delta_{RP}}\left(N'_p L'_r - N'_r L'_p\right)\right.$$
$$\left. + \alpha_0\left(N'_{\delta_{RP}} L'_r - L'_{\delta_{RP}} N'_r\right) + \frac{g}{V_0} L'_{\delta_{RP}}\right] s$$
$$\left. + g/V_0\left[N'_{\delta_{RP}} L'_r - L'_{\delta_{RP}} N'_r\right]\right\} \tag{7}$$

$$\frac{r}{\delta_{RP}} = \frac{1}{\Delta}\left\{\left[N'_{\delta_{RP}} + Y_{\delta_{RP}} N'_{\dot\beta}\right] s^3 + \left[L'_{\delta_{RP}} N'_p - N'_{\delta_{RP}}\left(L'_p + Y_\beta\right)\right.\right.$$
$$\left. + \alpha_0\left(L'_{\delta_{RP}} N'_{\dot\beta} - N'_{\delta_{RP}} L'_{\dot\beta}\right) + Y_{\delta_{RP}}\left(N'_p L'_{\dot\beta} - N'_{\dot\beta} L_p + N'_\beta\right)\right] s^2$$
$$+\left[Y_\beta\left(N'_{\delta_{RP}} L'_p - L'_{\delta_{RP}} N'_p\right) + \alpha_0\left(L'_{\delta_{RP}} N'_\beta - N'_{\delta_{RP}} L'_\beta\right)\right.$$
$$\left. + g/V_0\left(L'_{\delta_{RP}} N'_{\dot\beta} - N'_{\delta_{RP}} L'_{\dot\beta}\right) + Y_{\delta_{RP}}\left(N'_p L'_\beta - N'_\beta L'_p\right)\right] s$$
$$\left. + g/V_0\left[L'_{\delta_{RP}} N'_\beta - N'_{\delta_{RP}} L'_\beta\right]\right\} \tag{8}$$

$$\frac{\phi}{\delta_{RP}} = \frac{1}{\Delta}\left\{\left[L'_{\delta_{RP}} + Y_{\delta_{RP}} L'_{\dot\beta}\right] s^2 + \left[N'_{\delta_{RP}}\left(L'_r - L'_{\dot\beta}\right) - L'_{\delta_{RP}}\left(N'_r - N'_{\dot\beta} + Y_\beta\right)\right.\right.$$
$$\left. + Y_{\delta_{RP}}\left(N'_{\dot\beta} L'_r + L'_\beta - N'_r L'_{\dot\beta}\right)\right] s + \left[L'_{\delta_{RP}}\left(N'_\beta + Y_\beta N'_r\right)\right.$$
$$\left. \left. - N'_{\delta_{RP}}\left(L'_\beta + Y_\beta L'_r\right) + Y_{\delta_{RP}}\left(N'_\beta L'_r - N'_r L'_\beta\right)\right]\right\} \tag{9}$$

$$\Delta = s^4 + \left[N'_{\dot\beta} - L'_p - N'_r - Y_\beta - \alpha_o L'_{\dot\beta}\right] s^3$$
$$+ \left[N'_\beta + N'_r L'_p - N'_p L'_r - N'_{\dot\beta} L'_p + N'_p L'_{\dot\beta} + Y_\beta \left(L'_p + N'_r\right) + \alpha_o \left(N'_r L'_{\dot\beta} - N'_{\dot\beta} L'_r - L'_\beta\right)\right.$$
$$\left. - \frac{g}{V_o} L'_{\dot\beta}\right] s^2 + \left[N'_p L'_\beta - N'_\beta L'_p + Y_\beta \left(N'_p L'_r - N'_r L'_p\right) + \alpha_o \left(N'_r L'_\beta - N'_\beta L'_r\right)\right.$$
$$\left. + g/V_o \left(N'_r L'_{\dot\beta} - N'_{\dot\beta} L'_r - L'_\beta\right)\right] s + \left[g/V_o \left(N'_r L'_\beta - N'_\beta L'_r\right)\right] \qquad (10)$$

2. a. For the assumptions of (1) no spiral motion as approximated by setting $g/V_o = 0$, (2) $\alpha_o = 0$, and (3) $Y_{\delta_{AS}} = 0$, the above transfer functions reduce to the following:

$$\frac{\beta}{\delta_{AS}} = \frac{1}{\Delta}\left\{-N'_{\delta_{AS}} s^2 + \left(N'_{\delta_{AS}} L'_p - L'_{\delta_{AS}} N'_p\right) s\right\} \qquad (11)$$

$$\frac{r}{\delta_{AS}} = \frac{1}{\Delta}\left\{N'_{\delta_{AS}} s^3 + \left[L'_{\delta_{AS}} N'_p - N'_{\delta_{AS}} \left(L'_p + Y_\beta\right)\right] s^2 + Y_\beta \left(N'_{\delta_{AS}} L'_p - L'_{\delta_{AS}} N'_p\right) s\right\} \qquad (12)$$

$$\frac{\phi}{\delta_{AS}} = \frac{1}{\Delta}\left\{L'_{\delta_{AS}} s^2 + \left[N'_{\delta_{AS}} \left(L'_r - L'_{\dot\beta}\right) - L'_{\delta_{AS}} \left(N'_r - N'_{\dot\beta} + Y_\beta\right)\right] s\right.$$
$$\left. + \left[L'_{\delta_{AS}} \left(N'_\beta + Y_\beta N'_r\right) - N'_{\delta_{AS}} \left(L'_\beta + Y_\beta L'_r\right)\right]\right\} \qquad (13)$$

$$\frac{\beta}{\delta_{RP}} = \frac{1}{\Delta}\left\{Y_{\delta_{RP}} s^3 - \left[N'_{\delta_{RP}} + Y_{\delta_{RP}} \left(L'_p + N'_r\right)\right] s^2\right.$$
$$\left. + \left[N'_{\delta_{RP}} L'_p - L'_{\delta_{RP}} N'_p - Y_{\delta_{RP}} \left(N'_p L'_r - N'_r L'_p\right)\right] s\right\} \qquad (14)$$

$$\frac{r}{\delta_{RP}} = \frac{1}{\Delta}\left\{\left[N'_{\delta_{RP}} + Y_{\delta_{RP}} N'_{\dot\beta}\right] s^3 + \left[L'_{\delta_{RP}} N'_p - N'_{\delta_{RP}} \left(L'_p + Y_\beta\right)\right.\right.$$
$$\left. + Y_{\delta_{RP}} \left(N'_p L'_{\dot\beta} - N'_{\dot\beta} L'_p + N'_\beta\right)\right] s^2 + \left[Y_\beta \left(N'_{\delta_{RP}} L'_p - L'_{\delta_{RP}} N'_p\right)\right.$$
$$\left.\left. + Y_{\delta_{RP}} \left(N'_p L'_\beta - N'_\beta L'_p\right)\right] s\right\} \qquad (15)$$

$$\frac{\phi}{\delta_{RP}} = \frac{1}{\Delta}\left\{\left[L'_{\delta_{RP}} + Y_{\delta_{RP}} L'_{\dot\beta}\right]s^2 + \left[N'_{\delta_{RP}}\left(L'_r - L'_{\dot\beta}\right) - L'_{\delta_{RP}}\left(N'_r - N'_{\dot\beta} + Y_\beta\right)\right.\right.$$
$$\left. + Y_{\delta_{RP}}\left(N'_{\dot\beta} L'_r - N'_r L'_{\dot\beta} + L_\beta\right)\right]s + \left[L'_{\delta_{RP}}\left(N'_\beta + Y_\beta N'_r\right) - N'_{\delta_{RP}}\left(L'_\beta + Y_\beta L'_r\right)\right.$$
$$\left.\left. + Y_{\delta_{RP}}\left(N'_\beta L'_r - N'_r L'_\beta\right)\right]\right\} \tag{16}$$

$$\Delta = s^4 + \left[N'_{\dot\beta} - L'_p - N'_r - Y_\beta\right]s^3 + \left[N'_\beta + N'_r L'_p - N'_p L'_r - N'_{\dot\beta} L'_p + N'_p L'_{\dot\beta} + Y_\beta\left(L'_p + N'_r\right)\right]s^2$$
$$+ \left[N'_p L'_\beta - N'_\beta L'_p + Y_\beta\left(N'_p L'_r - N'_r L'_p\right)\right]s \tag{17}$$

Transfer functions (11) through (16) may be written as follows:

$$\frac{\beta}{\delta_{AS}} = \frac{K_{\beta_{\delta_{AS}}}\left(\tau_{\beta_A} s + 1\right)}{\left(\tau_R s + 1\right)\left(\frac{s^2}{\omega_d^2} + \frac{2\zeta_d}{\omega_d} s + 1\right)} \tag{18}$$

$$\frac{r}{\delta_{AS}} = \frac{K_{r_{\delta_{AS}}}\left(\frac{s^2}{\omega_{r_A}^2} + \frac{2\zeta_{r_A}}{\omega_{r_A}} s + 1\right)}{\left(\tau_R s + 1\right)\left(\frac{s^2}{\omega_d^2} + \frac{2\zeta_d}{\omega_d} s + 1\right)} \tag{19}$$

$$\frac{\phi}{\delta_{AS}} = \frac{K_{\phi_{\delta_{AS}}}\left(\frac{s^2}{\omega_{\phi_A}^2} + \frac{2\zeta_{\phi_A}}{\omega_{\phi_A}} s + 1\right)}{s\left(\tau_R s + 1\right)\left(\frac{s^2}{\omega_d^2} + \frac{2\zeta_d}{\omega_d} s + 1\right)} \tag{20}$$

$$\frac{\beta}{\delta_{RP}} = \frac{K_{\beta_{\delta_{RP}}}\left(\frac{s^2}{\omega_{\beta_R}^2} + \frac{2\zeta_{\beta_R}}{\omega_{\beta_R}} s + 1\right)}{\left(\tau_R s + 1\right)\left(\frac{s^2}{\omega_d^2} + \frac{2\zeta_d}{\omega_d} s + 1\right)} \tag{21}$$

$$\frac{r}{\delta_{RP}} = \frac{K_{r\delta_{RP}}\left(\frac{s^2}{\omega_{r_R}^2} + \frac{2\zeta_{r_R}}{\omega_{r_R}}s + 1\right)}{\left(\tau_R s + 1\right)\left(\frac{s^2}{\omega_d^2} + \frac{2\zeta_d}{\omega_d}s + 1\right)} \tag{22}$$

$$\frac{\phi}{\delta_{RP}} = \frac{K_{\phi\delta_{RP}}\left(\frac{s^2}{\omega_{\phi_R}^2} + \frac{2\zeta_{\phi_R}}{\omega_{\phi_R}}s + 1\right)}{s\left(\tau_R s + 1\right)\left(\frac{s^2}{\omega_d^2} + \frac{2\zeta_d}{\omega_d}s + 1\right)} \tag{23}$$

where:

$$* \; K_{\beta\delta_{AS}} = \frac{N'_{\delta_{AS}} L'_p - L'_{\delta_{AS}} N'_p}{N'_p L'_\beta - N'_\beta L'_p + Y_\beta\left(N'_p L'_r - N'_r L'_p\right)} \tag{24}$$

$$* \; K_{r\delta_{AS}} = \frac{Y_\beta\left(N'_{\delta_{AS}} L'_p - L'_{\delta_{AS}} N'_p\right)}{N'_p L'_\beta - N'_\beta L'_p + Y_\beta\left(N'_p L'_r - N'_r L'_p\right)} \tag{25}$$

$$* \; K_{\dot\phi\delta_{AS}} = \frac{L'_{\delta_{AS}}\left(N'_\beta + Y_\beta N'_r\right) - N'_{\delta_{AS}}\left(L'_\beta + Y_\beta L'_r\right)}{N'_p L'_\beta - N'_\beta L'_p + Y_\beta\left(N'_p L'_r - N'_r L'_p\right)} \tag{26}$$

$$* \; K_{\beta\delta_{RP}} = \frac{N'_{\delta_{RP}} L'_p - L'_{\delta_{RP}} N'_p - Y_{\delta_{RP}}\left(N'_p L'_r - N'_r L'_p\right)}{N'_p L'_\beta - N'_\beta L'_p + Y_\beta\left(N'_p L'_r - N'_r L'_p\right)} \tag{27}$$

$$* \; K_{r\delta_{RP}} = \frac{Y_\beta\left(N'_{\delta_{RP}} L'_p - L'_{\delta_{RP}} N'_p\right) + Y_{\delta_{RP}}\left(N'_p L'_\beta - N'_\beta L'_p\right)}{N'_p L'_\beta - N'_\beta L'_p + Y_\beta\left(N'_p L'_r - N'_r L'_p\right)} \tag{28}$$

$$* \; K_{\dot\phi\delta_{RP}} = \frac{L'_{\delta_{RP}}\left(N'_\beta + Y_\beta N'_r\right) - N'_{\delta_{RP}}\left(L'_\beta + Y_\beta L'_r\right) + Y_{\delta_{RP}}\left(N'_\beta L'_r - N'_r L'_\beta\right)}{N'_p L'_\beta - N'_\beta L'_p + Y_\beta\left(N'_p L'_r - N'_r L'_p\right)} \tag{29}$$

---

* In this report the gains of these transfer functions are given with respect to pilot applied force. Expressed in terms of applied force, the gains are as follows:

$$K_{(\;)F_{AS}} = K_{(\;)\delta_{AS}}\frac{\delta_{AS}}{F_{AS}} \qquad K_{(\;)F_{RP}} = K_{(\;)\delta_{RP}}\frac{\delta_{RP}}{F_{RP}}$$

$$\tau_{\beta_A} = \frac{-N'_{\delta_{AS}}}{N'_{\delta_{AS}} L'_p - L'_{\delta_{AS}} N'_p} = \frac{-1}{L'_p - \frac{L'_{\delta_{AS}}}{N'_{\delta_{AS}}} N'_p} \tag{30}$$

$$\omega_{r_A}^2 = \frac{Y_\beta \left(N'_{\delta_{AS}} L'_p - L'_{\delta_{AS}} N'_p\right)}{N'_{\delta_{AS}}} = Y_\beta \left(L'_p - \frac{L'_{\delta_{AS}}}{N'_{\delta_{AS}}} N'_p\right) \tag{31}$$

$$2\zeta_{r_A}\omega_{r_A} = \frac{\left[L'_{\delta_{AS}} N'_p - N'_{\delta_{AS}} \left(L'_p + Y_\beta\right)\right]}{N'_{\delta_{AS}}} = \frac{L'_{\delta_{AS}}}{N'_{\delta_{AS}}} N'_p - \left(L'_p + Y_\beta\right) \tag{32}$$

$$\omega_{\phi_A}^2 = \frac{L'_{\delta_{AS}} \left(N'_\beta + Y_\beta N'_r\right) - N'_{\delta_{AS}} \left(L'_\beta + Y_\beta L'_r\right)}{L'_{\delta_{AS}}} = N'_\beta + Y_\beta N'_r - \frac{N'_{\delta_{AS}}}{L'_{\delta_{AS}}} \left(L'_\beta + Y_\beta L'_r\right) \tag{33}$$

$$2\zeta_{\phi_A}\omega_{\phi_A} = \frac{\left[N'_{\delta_{AS}} \left(L'_r - L'_{\dot\beta}\right) - L'_{\delta_{AS}} \left(N'_r - N'_{\dot\beta} + Y_\beta\right)\right]}{L'_{\delta_{AS}}} = \frac{N'_{\delta_{AS}}}{L'_{\delta_{AS}}} \left(L'_r - L'_{\dot\beta}\right) - \left(N'_r - N'_{\dot\beta} + Y_\beta\right) \tag{34}$$

$$\omega_{\beta_R}^2 = \frac{N'_{\delta_{RP}} L'_p - L'_{\delta_{RP}} N'_p - Y_{\delta_{RP}} \left(N'_p L'_r - N'_r L'_p\right)}{Y_{\delta_{RP}}} = \frac{N'_{\delta_{RP}} L'_p - L'_{\delta_{RP}} N'_p}{Y_{\delta_{RP}}} - \left(N'_p L'_r - N'_r L'_p\right) \tag{35}$$

$$2\zeta_{\beta_R}\omega_{\beta_R} = \frac{\left[-N'_{\delta_{RP}} - Y_{\delta_{RP}} \left(L'_p + N'_r\right)\right]}{Y_{\delta_{RP}}} = -\frac{N'_{\delta_{RP}}}{Y_{\delta_{RP}}} - \left(L'_p + N'_r\right) \tag{36}$$

$$\omega_{r_R}^2 = \frac{Y_\beta \left(N'_{\delta_{RP}} L'_p - L'_{\delta_{RP}} N'_p\right) + Y_{\delta_{RP}} \left(N'_p L'_\beta - N'_\beta L'_p\right)}{N'_{\delta_{RP}} + Y_{\delta_{RP}} N'_{\dot\beta}} \tag{37}$$

$$2\zeta_{r_R}\omega_{r_R} = \frac{\left[L'_{\delta_{RP}} N'_p - N'_{\delta_{RP}} \left(L'_p + Y_\beta\right) + Y_{\delta_{RP}} \left(N'_p L'_{\dot\beta} - N'_{\dot\beta} L'_p + N'_\beta\right)\right]}{N'_{\delta_{RP}} + Y_{\delta_{RP}} N'_{\dot\beta}} \tag{38}$$

$$\omega_{\phi_R}^2 = \frac{L'_{\delta_{RP}} \left(N'_\beta + Y_\beta N'_r\right) - N'_{\delta_{RP}} \left(L'_\beta + Y_\beta L'_r\right) + Y_{\delta_{RP}} \left(N'_\beta L'_r - N'_r L'_\beta\right)}{L'_{\delta_{RP}} + Y_{\delta_{RP}} L'_{\dot\beta}} \tag{39}$$

$$2\zeta_{\phi_R}\omega_{\phi_R} = \frac{\left[N'_{\delta_{RP}}\left(L'_r - L'_{\dot\beta}\right) - L'_{\delta_{RP}}\left(N'_r - N'_{\dot\beta} + Y_\beta\right) + Y_{\delta_{RP}}\left(N'_{\dot\beta}L'_r - N'_r L'_{\dot\beta} + L_\beta\right)\right]}{L'_{\delta_{RP}} + Y_{\delta_{RP}}L'_{\dot\beta}} \tag{40}$$

b. For the additional assumption that

$$\tau_R = -\frac{1}{L'_p} \tag{41}$$

then:

$$\omega_d^2 = \frac{N'_p L'_\beta - N'_\beta L'_p + Y_\beta\left(N'_p L'_r - N'_r L'_p\right)}{-L'_p} \tag{42}$$

$$2\zeta_d\omega_d = N'_{\dot\beta} - N'_r - Y_\beta \tag{43}$$

C. From Equations 33 and 42 (for $g/V_o = \alpha_o = Y_{\delta_{AS}} = 0$ and $\tau_R = -1/L'_p$)

$$\frac{\omega_{\phi_A}^2}{\omega_d^2} = \frac{N'_\beta + Y_\beta N'_r - \frac{N'_{\delta_{AS}}}{L'_{\delta_{AS}}}\left(L'_\beta + Y_\beta L'_r\right)}{N'_\beta + Y_\beta N'_r - \frac{N'_p}{L'_p}\left(L'_\beta + Y_\beta L'_r\right)} \tag{44}$$

For $Y_\beta = N'_p = 0$, Equation 44 reduces to

$$\frac{\omega_{\phi_A}^2}{\omega_d^2} = 1 - \frac{N'_{\delta_{AS}}}{L'_{\delta_{AS}}}\,\frac{L'_\beta}{N'_\beta} \tag{45}$$

D. An expression for the parameter ϕ/β may be obtained by setting Equations 2 and 3 to zero and solving for ϕ/β :

$$\frac{\phi}{\beta} = \frac{-L'_{\dot\beta}s^2 + \left(L'_{\dot\beta}N'_r - L'_\beta - L'_r N'_{\dot\beta}\right)s + N'_r L'_\beta - L'_r N'_\beta}{-s^3 + \left(N'_r + L'_p\right)s^2 - \left(L'_p N'_r - L'_r N'_p\right)s} \tag{46}$$

The magnitude of this parameter is obtained by substituting in Equation 46

$$s = -\zeta_d\omega_d \pm i\,\omega_d\sqrt{1-\zeta_d^2} \tag{47}$$

Assuming $L'_{\dot\beta} = 0$ and $|L_r N'_{\dot\beta}| \ll |L'_\beta|$, Equation 46 reduces to:

$$\frac{\phi}{\beta} \cong \frac{L'_\beta s - \left(N'_r L'_\beta - L'_r N'_\beta\right)}{s^3 - \left(N'_r + L'_p\right)s^2 + \left(L'_p N'_r - L'_r N'_p\right)s} \tag{48}$$

If $|L'_r N'_p| \ll |L'_p N'_r|$, the denominator of Equation (48) may be factored:

$$\frac{\phi}{\beta} \cong \frac{L'_\beta \left(s - N'_r + L'_r \; N'_\beta / L'_\beta\right)}{s\,(s - N'_r)(s - L'_p)} \tag{49}$$

If $\left| L'_r \frac{N'_\beta}{L'_\beta} \right| \ll |N'_r|$, the approximate expression for ϕ/β becomes:

$$\frac{\phi}{\beta} \cong \frac{L'_\beta}{s(s - L'_p)} \tag{50}$$

If ζ_d is very small, $\omega_d^2 \cong N'_\beta$, and $\tau_R \cong -\frac{1}{L'_p}$, it can be shown that:

$$\left| \frac{\phi}{\beta} \right| \cong \frac{L'_\beta / N'_\beta}{\sqrt{1 + \frac{1}{\omega_d^2 \tau_R^2}}} \tag{51}$$